“The effect of natural genetic variation at *Ppd-H1* on the regulation of pre-anthesis development in barley (*Hordeum vulgare* L.) in response to the photoperiod”

Inaugural-Dissertation

zur

Erlangung des Doktorgrades

der Mathematisch-Naturwissenschaftlichen Fakultät

der Universität zu Köln

vorgelegt von

Benedikt Digel geb. Drosse

aus Köln

Köln, Oktober 2014

Die vorliegende Arbeit wurde am Max-Planck-Institut für Pflanzenzüchtungsforschung in Köln in der Abteilung für Entwicklungsbiologie der Pflanzen (Direktor: Prof. Dr. George Coupland) angefertigt.

Berichterstatter:	Prof. Dr. George Coupland
	Prof. Dr. Ute Höcker
Prüfungsvorsitzender:	Prof. Dr. Ulf-Ingo Flügge
Tag der mündlichen Prüfung:	14. Oktober 2014

Table of Contents

Abstract

The timing of reproductive development determines spike architecture and thus yield in temperate grasses such as barley (*Hordeum vulgare* L.). Reproductive development in barley is controlled by the photoperiod response gene *Ppd-H1* which accelerates flowering time under long-day (LD) conditions. A natural mutation in *Ppd-H1* prevalent in spring barley causes a reduced photoperiod response, and thus, late flowering under LD. However, it is not very well understood how LD and *Ppd-H1* control pre-anthesis development, and thus spike architecture and yield in barley.

This work reports about morphological and molecular changes in the leaf and at the shoot apex of barley in response to the photoperiod and genetic variation at *Ppd-H1*. Expression variation in the leaf and main shoot apices (MSA) were analyzed using RNA-sequencing and qRT-PCR in the three spring barley cultivars Scarlett, Bowman and Triumph and derived introgression lines. The spring barley lines were characterized by the natural mutation in *Ppd-H1*, whereas the derived introgression lines carry the photoperiod responsive, dominant wild type *Ppd-H1* allele introduced from wild or winter barley.

LD and the dominant *Ppd-H1* allele accelerated all phases of shoot apex development, but had the strongest effect on inflorescence maturation. Photoperiod-shift experiments revealed that the duration of the vegetative and early reproductive phase determined the number of spikelet primordia and seeds per spike. Whereas in *Arabidopsis* a few long days are sufficient for floral commitment, in barley flowering only occurred under continuous LD exposure. Short-day (SD) did not prevent floral transition, but impaired inflorescence development and caused the abortion of the main shoot inflorescence. Consequently, long photoperiods and the dominant *Ppd-H1* allele reduced the number of spikelet primordia, but promoted spikelet fertility and ensured main shoot survival.

In the absence of a complete barley genome reference sequence, we generated a barley reference sequence for improved analysis of a shoot apex specific transcriptome from the vegetative and early reproductive phases. Genes differentially regulated during development or in response to day length and variation at *Ppd-H1* were classified into 31 co-expression clusters, and characterized by enriched Gene Ontology terms, thus providing a valuable resource for future studies on shoot apex development in barley.

LD and the dominant *Ppd-H1* allele caused an up-regulation of the barley orthologs of *Flowering Locus T*, *HvFT1* in the leaf and *HvFT2* in the MSA. Both genes were co-regulated with genes involved in nutrient transport and flower fertility, suggesting that improved nutrient mobilization under LD was

important to maintain inflorescence development. LD and the dominant *Ppd-H1* allele up-regulated the expression of the three *AP1/FUL-like* MADS box transcription factors, *HvVRN1*, *HvBM3* and *HvBM8* and floral homeotic genes homologous to *APETALA3*, *PISTILATA*, *SEPALLATA1* and *3* of *Arabidopsis*. Floral development was thus strongly LD dependent. Contrastingly, floral transition correlated with the day-length and *Ppd-H1* independent down-regulation of the *SHORT VEGETATIVE PHASE-like* (*SVP-like*) genes *HvBM1*, *HvBM10* and *HvVRT2* and a *Ppd-H1* independent up-regulation of *HvSOC1-1* in the MSA. Thus, expression of *SVP-like* genes and *HvSOC1-1* in the MSA seemed to be independent of *HvFT1* and *HvFT2* expression levels in barley. These results point to differences in the regulation of the floral transition in *Arabidopsis*, where *SOC1* and *SVP* are regulated by FT.

In summary, our results demonstrate that LD and *Ppd-H1* control the number and maturation of floral primordia presumably by up-regulating *FT-like* genes and improving nutrient mobilization in the leaf and MSA. The study thus lays the foundation to understanding the genetic and molecular control of pre-anthesis development and yield structure in temperate cereals.

Zusammenfassung

Der zeitliche Ablauf der reproduktiven Entwicklung bestimmt die Ährenstruktur und somit den Ertrag in Nutzgräsern der gemäßigten Zone wie zum Beispiel von Gerste (*Hordeum vulgare* L.). Unter Langtag (LT) Bedingungen beschleunigt das Photoperiode abhängige *Ppd-H1* Gen die Blüte von Gerste. Eine natürliche Mutation in *Ppd-H1*, wie sie vor allem in Sommergerste vorkommt, führt zu einer abgeschwächten Reaktion auf die Photoperiode und verzögert die Blüte im LT. Über die genetische Regulation, wie LT und *Ppd-H1* die Entwicklung bis zur Blüte (Prä-Anthese Entwicklung) in Gerste steuern und somit die Ährenarchitektur und den Ertrag beeinflussen, ist jedoch nur wenig bekannt.

Die vorliegende Arbeit beschreibt die morphologischen und molekularen Veränderungen in Blättern und am Sprossapex während der Prä-Anthese Entwicklung von Gerste, sowie deren Abhängigkeit von der Photoperiode und genetischer Variation in *Ppd-H1*. Hierzu wurden in den drei Sommergersten Scarlett, Bowman und Triumph und in von diesen abstammenden *Ppd-H1* Introgressionslinien Genexpressionsanalysen mittels RNA-Sequenzierung und qRT-PCR in Blättern und am Hauptsprossapex (HSA) durchgeführt. Die Sommergersten tragen die zuvor beschriebene natürliche Mutation in *Ppd-H1* und die Introgressionslinien das dominante und Photoperiode sensitive *Ppd-H1* Allel aus Wild- bzw. Wintergerste.

LT und das dominante *Ppd-H1* Allel beschleunigten alle Entwicklungsphasesn des HSA, besonders jedoch die Infloreszenzentwicklung. Transferexperimente zwischen LT und Kurztag (KT) zeigten, dass die Dauer der vegetativen und frühen reproduktiven Phase die Anzahl der Blütchen und Körner pro Ähre bestimmt. Im Gegensatz zu *Arabidopsis*, der zu einer vollständigen Blühinduktion wenige Tage mit langer Photoperiode ausreichen, benötigte Gerste LT Bedingungen während der gesamten Prä-Anthese Entwicklung zur Produktion fertiler Blüten. Zwar fand die Transition von vegetativem zu reproduktivem Wachstum (Blühtransition) auch unter KT statt, die kurze Photoperiode beeinträchtigte jedoch die Infloreszenzentwicklung und führte zu einem frühzeitigen Absterben des HSA. Somit verringerten LT und das dominante *Ppd-H1* Allel zwar die Anzahl der induzierten Blütenprimordien, ermöglichten aber die Fortentwicklung der Hauptsprossinfloreszenz und förderten die Blütenfertilität.

Aufgrund einer nur unvollständigen Gerstengenomsequenz stellten wir für die Analyse des Sprossapikaltranskriptoms während der vegetativen und frühen reproduktiven Phase eine spezifische Referenzsequenz zusammen. Gene, die zwischen verschiedenen Entwicklungsstadien des HSA, Photoperioden oder aufgrund genetischer Variation an *Ppd-H1* differentiell reguliert waren, wurden in 31 Co-Expressionscluster eingeteilt und mit Hilfe von Gene Ontology Annotationen charakterisiert.

Die so identifizierten Gencluster stellen ein wertvolles Hilfsmittel für zukünftige Analysen der Sprossapexentwicklung in Gerste dar.

Im Detail, führten LT und das dominante *Ppd-H1* Allel zu einer erhöhten Expression von *HvFT1* und *HvFT2,* die beide Orthologe des *FLOWERING LOCUS T* (*FT*) Gens in *Arabidopsis* darstellen. Die Co-Regulation von *HvFT1* und *HvFT2* mit Genen des Nährstofftransports und der Blütenentwicklung deutete darauf hin, dass möglicherweise eine erhöhte Nährstoffverfügbarkeit zur Aufrechterhaltung der Infloreszenzentwicklung unter LT beigetragen haben könnte. Die starke LT Abhängigkeit der Infloreszenzentwicklung zeigte sich außerdem an einer LT und *Ppd-H1* abhängige Induktion der drei *AP1/FUL-like* MADS-box Transkriptionsfaktoren *HvVRN1*, *HvBM3* und *HvBM8* sowie von Homologen der homöotischen Blütenentwicklungsgene *APETALA3*, *PISTILATA* und *SEPALLATA1* und *3* aus *Arabidopsis*. Im Gegensatz hierzu, korrelierte die Blühtransition mit einer Photoperiode und *Ppd-H1* unabhängigen Repression der *SHORT VEGETATIVE PHASE-like* (*SVP-like*) Gene *HvBM1*, *HvBM1*, *HvVRT2* und einer *Ppd-H1* unabhängigen Induktion von *HvSOC1-1* im Sprossapex. Die Expression von *SVP-like* Genen und *HvSOC1-1* am Sprossapex war daher unabhängig von der *HvFT1* und *HvFT2* Expression in Gerste, was auf Unterschiede zu der FT abhängigen Regulation von *SVP* und *SOC1* in *Arabidopsis* hindeutet.

Zusammenfassend zeigen die Ergebnisse, dass LT und *Ppd-H1* die Anzahl und Entwicklung von Blütenprimordien möglicherweise durch die Induktion von *FT-like* Genen und einer gesteigerten Nährstoffverfügbarkeit in Blättern und am Sprossapex regulieren. Wir präsentieren somit erste grundlegende Ergebnisse, die zum weiteren Verständnis der genetischen Regulation der Prä-Anthese Entwicklung und somit der Ertragsstruktur von Getreiden der gemäßigten Zone beitragen können.

1 Introduction

Cereals are the most important staple crops produced for animal feed and human consumption. Wheat and barley are among the top four cereal crop species with a yearly production of ca. 713 Mt and 145 Mt, respectively, harvested from an arable land of 268 Mha worldwide in 2013 (FAO 2014). Improving yield of the small grain cereals barley and wheat requires the plant phenology to match the constraints of the targeted environment. Thus, the control of flowering time, as the time from germination to anthesis, has been identified as a key adaptive trait in breeding programs to maximize crop yields.

1.1 Phenology of reproductive development in barley

Barley is a facultative long-day (LD) plant and flowering time is controlled in response to environmental cues, primarily by photoperiod, ambient temperature and vernalization. In some barley genotypes short-day (SD) accelerates flowering time in a similar way as cold treatment, and was therefore referred to as short-day vernalization (Roberts *et al.* 1988). Unlike ambient temperature, photoperiod and vernalization have a predominant impact on the developmental rate only during certain parts of the pre-flowering period (Slafer and Rawson 1994, Gonzáles *et al.* 2002, Whitechurch *et al.* 2007), thus, different phenological phases of pre-anthesis development differ in their sensitivity to distinct environmental cues.

Pre-anthesis development in temperate cereals has been divided into three phases based on morphological changes of the shoot apex: the vegetative phase, the early reproductive phase and the late reproductive phase (Fig. 1, Slafer and Rawson 1994, Gonzáles 2002, Garcia del Moral *et al.* 2002), previously described as pre-inductive, inductive and post-inductive phase by Ellis *et al.* (1988). During the vegetative phase, the crop initiates leaves until floral initiation, which is generally estimated as the formation of the first spikelet primordia, visible as double ridges at the shoot apex of the main shoot. In the subsequent early reproductive phase, the spikelets are differentiated until the initiation of the terminal spikelet in wheat. Finally, during the late reproductive phase, the stem internodes elongate, the spikelet primordia reach their maximum number at awn primordium stage in barley, and then mature. During this process some florets degenerate while others reach the fertile stage at anthesis. A quantitative scale for barley development based on the morphogenesis of the shoot apex and carpels has been introduced by Waddington *et al.* (1983). Hereafter, developmental stages of the shoot apex will be referred to as Waddington stages (W).

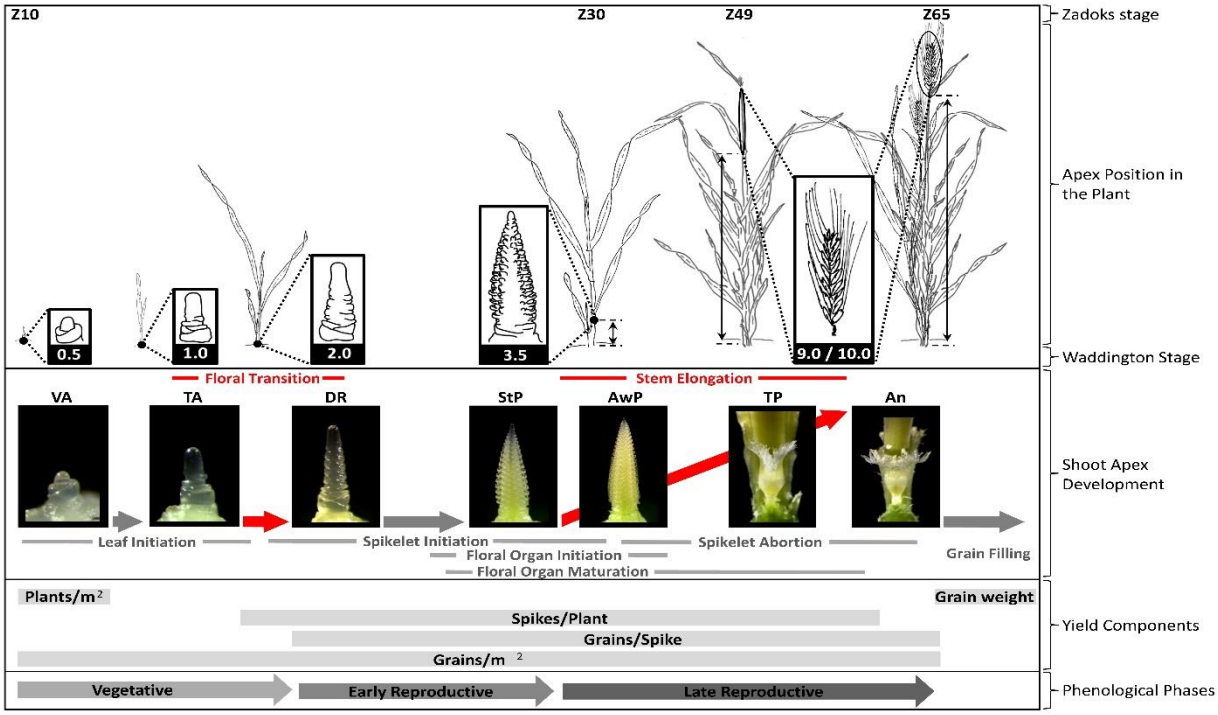

Figure 1: Yield component traits, as determined during distinct phenological phases of barley. Selected macroscopic stages of barley development are shown referring to the Zadoks scale (Zadoks *et al.* 1974). Z10: time of emergence; Z30: beginning of stem elongation; Z49: first awns visible outside the leaf sheath (also: "tipping", Alqudah and Schnurbusch 2014); Z65: beginning of anthesis. Developmental stage of the shoot apex and inflorescence at each macroscopic stage are demonstrated in sketches and photos and the Waddington stage is reported below the sketch (Waddington *et al.* 1983). VA: vegetative shoot apex; TA: transition apex; DR: double ridge stage; StP: stamen primordium stage; AwP: awn primordium stage; TP: tipping; An: anthesis. Photos at TP and An represent the stigma of the most advanced spikelet of the main shoot spike. Developmental processes at the shoot apex, yield component traits and phenological phases are presented in the boxes below. Durations of the developmental processes/ phases are represented by the bar length in relation to the developmental stages of the apex. The figure is adapted from Slafer and Rawson 1994, García del Moral *et al.* 2002, Borrás-Gelonch 2013 (thesis).

Vernalization affects flowering time, predominantly by reducing the duration of the vegetative phase (Griffiths *et al.* 1985, Roberts *et al.* 1988), although minor effects of vernalization were also reported on the subsequent phases (Gonzáles 2002). In contrast, long photoperiods had minor effects on the duration of the vegetative phase, but strongly accelerated the late reproductive phase of inflorescence development (Roberts *et al.* 1988, Miralles and Richards 2000). Analyses of wheat development under artificially manipulated photoperiods have shown that the stem elongation phase was the most sensitive to changes in photoperiod (Slafer *et al.* 2001). Thus, the timing and duration of the different developmental phases vary independently and are determined genetically in response to the environment (González *et al.* 2003, Whitechurch *et al.* 2007).

1.2 Flowering time as determinant of yield

Flowering time integrates the durations of pre-anthesis phases and depends on a timely coordination of morphological changes at the shoot apex, formation of the spike, and plant growth, e.g. stem elongation. During the maximum stem and spike growth phase floret primordia are aborted, which has been attributed to the competition between spike and stem for limited assimilates (Fig. 1, Gonzáles *et*

al. 2003, Ghiglione *et al.* 2008, Gonzáles *et al.* 2011). Consequently, the duration of stem elongation has been associated with the number of fertile florets (Miralles and Richards 2000, Gonzáles *et al.* 2003, Slafer 2003), which is correlated to the spike dry weight at anthesis and sets the final number of grains, the most important component of cereal yield (Reynolds *et al.* 2009). Slafer *et al.* (2001) hypothesized, that increasing the duration of stem elongation phase would result in a higher number of fertile florets as an alternative to improving wheat yield potential. However, they further suggested that manipulating the length of different developmental phases should be achieved without affecting the total time to flowering, but specifically by changing the partitioning between individual pre-anthesis phases before and after the onset of stem elongation. Thus, a better understanding of the physiological and genetic basis of flowering time, including possible signaling in response to different environmental cues, such as photoperiod and temperature may permit floret abortion to be minimized for a more optimal source-sink balance.

1.3 Variation in flowering time and adaptation

Genetic variation in the vernalization and photoperiod pathways was crucial for the successful expansion of barley cultivation from the Fertile Crescent to temperate climates. Vernalization requirement and response are characterized by the temporal separation between the plant's exposure to cold in winter and the onset of flowering in spring and a renewed vernalization requirement for flowering in subsequent generations. This vernalization requirement prevents flowering during winter for the protection of the floral organs from cold. After exposure to cold and completed vernalization, photoperiod sensitivity induces flowering in response to increasing day length.

Barley is characterized by two major growth types: winter and spring. Winter growth types are defined here as genotypes which show accelerated flowering after vernalization, a prolonged exposure to cold temperature. In contrast, spring barley does not respond to vernalization. However, there exists a continuous gradation regarding spring and winter growth habits from typical spring to extreme winter (vernalization requirement) (Enomoto 1929, within Saisho *et al.* 2011). Wild barley *H. vulgare* ssp. *spontaneum*, the progenitor of cultivated barley originated in the Fertile Crescent and is still a widespread species found over the Eastern Mediterranean basin and Western Asiatic countries. Wild barley is classified as having a winter growth habit and early flowering under LD, indicating that the winter growth habit is ancestral in barley (Saisho *et al.* 2011). In Mediterranean areas and the Near East, cultivated barley is generally sown in autumn and typically displays a winter growth habit, responds to vernalization, but may also flower eventually in the absence of vernalization. However, there exists large variation in growth habit between and within landrace populations from the Fertile Crescent (Weltzien 1988, 1989). The distribution of winter and spring type genotypes in the Fertile

Crescent coincides with the increasingly continental weather patterns from west and south to east, and depends on the use of barley for sheep grazing in some areas. The spring growth type is thus more common in coastal areas and southern parts of the Fertile Crescent where winter temperatures are mild, but cultivars with and without vernalization response occupy similar cultivation areas (Yasuda *et al.* 1993, Saisho *et al.* 2011). Winter growth types have been selected and improved for cold resistance for cultivation in northern latitudes (Cockram *et al.* 2007). Spring growth types have been selected and bred for sowing in spring and a reduced photoperiod response for late flowering in summer. Late flowering in temperate environments with a long growing season allows cereal crops to exploit an extended vegetative period for resource storage. A further expansion of barley cultivation to northern areas with cold winters and short summers required the selection of early flowering in spring grown barley. This led to the selection of early flowering genotypes which do not respond to the photoperiod or vernalization, and are characterized by the presence of the so called "*earliness per se*" (*eps*) or "*early maturity*" (*eam*) genes. Scandinavian breeding programs used different mutagenic treatments to generate early maturing barley mutants in spring barley backgrounds which produce a day neutral phenotype with rapid flowering under SD or LD conditions (Lundvquist 2009). For example, the *eam8* mutation on chromosome 1HL generated by mutagenic treatment and detected in natural lines was successfully introduced into breeding lines and released as cultivars adapted to Scandinavian cultivation areas. Derived cultivars (Mari) were also used in breeding programs to breed for early flowering and adaptation to terminal drought in Mediterranean areas (Lundqvist *et al.* 2009).

1.4 Flowering time genes and floral pathways in barley

The genetic control of flowering time in response to photoperiod and vernalization has been extensively studied in *Arabidopsis thaliana*, henceforth referred to as *Arabidopsis*, which is like barley and wheat a facultative long-day plant and grows as a summer and winter annual. Flowering time genes and pathways as revealed in *Arabidopsis* show a high degree of conservation across plant species. Orthologs of a large number of *Arabidopsis* flowering time genes, notably from the photoperiod response pathway, have been detected in the cereals (Cockram *et al.* 2007, Distelfeld *et al.* 2009, Higgins *et al.* 2010). However, major flowering time genes in barley and wheat have been identified using natural genetic diversity and QTL mapping (Turner *et al.* 2005, Yan *et al.* 2003), rather than homology to *Arabidopsis* flowering time genes. Nevertheless, information from *Arabidopsis* has supported the functional characterization of barley flowering time regulators and assignment to floral pathways. Major regulators of flowering time in barley are the photoperiod response gene *Ppd-H1*, and the vernalization responsive genes *Vrn-H1*, *Vrn-H2* and *Vrn-H3* (Turner *et al.* 2005, Yan *et al.* 2003, 2004, 2006). Figure 2 provides an overview on barley flowering time genes and their connectivity

within the flowering time pathway. Figure 3 indicates map positions of major flowering time genes and QTL. Allelic variation and functional interactions between the genes are discussed below.

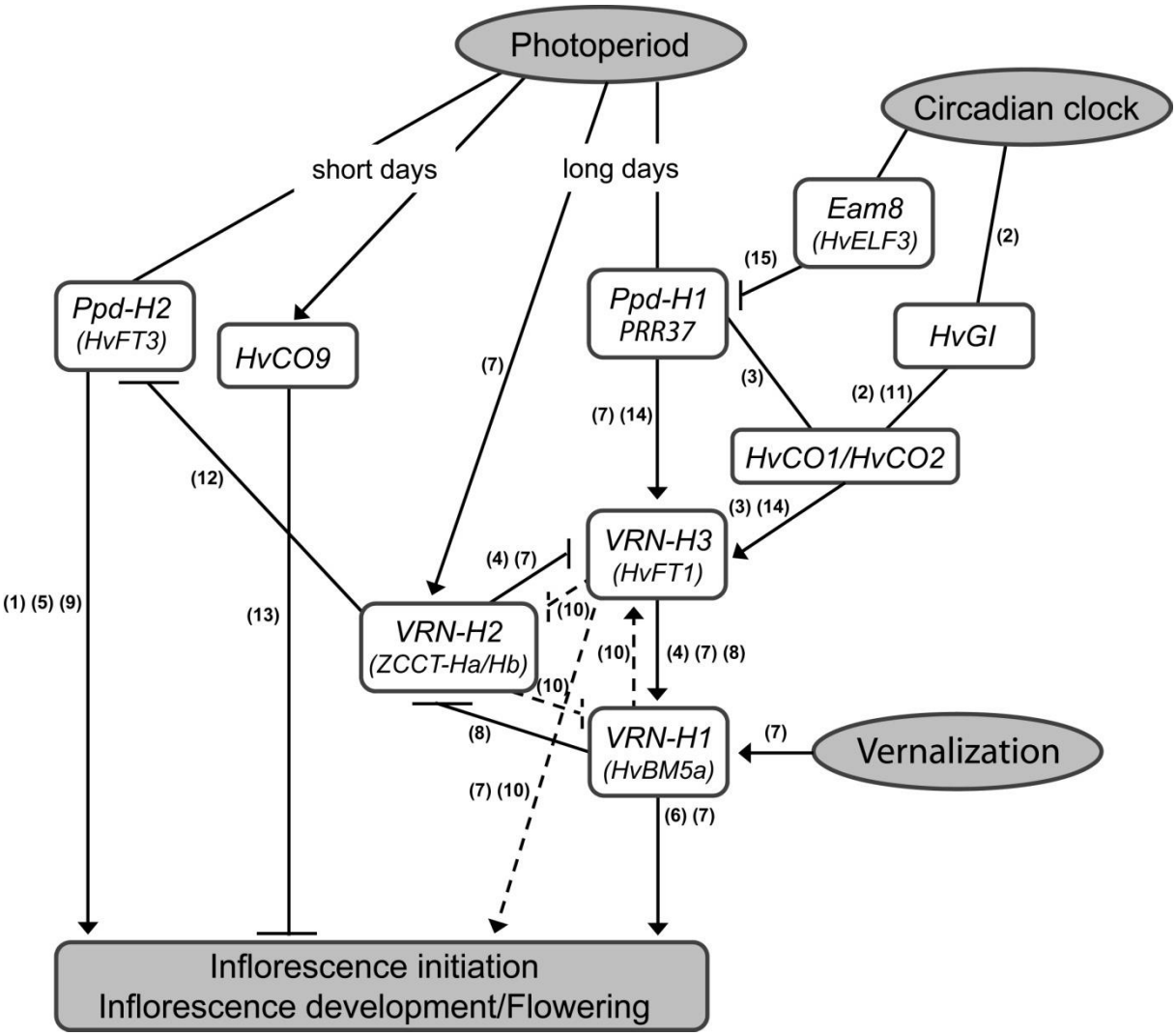

Figure 2: Flowering time model in barley. The interactions between photoperiod and vernalization pathways are shown. Numbers in brackets indicate literature in which experimental evidences support this model, dashed lines indicate alternative models of gene interactions; (1) Laurie *et al.* 1995; (2) Dunford *et al.* 2005; (3) Turner *et al.* 2005; (4) Yan *et al.* 2006; (5) Faure *et al.* 2007; (6) Shitsukawa *et al.* 2007; (7) Hemming *et al.* 2008; (8) Li and Dubcovsky 2008; (9) Kikuchi *et al.* 2009; (10) Shimada *et al.* 2009; (11) Hong *et al.* 2010; (12) Casao *et al.* 2011; (13) Kikuchi *et al.* 2011; (14) Campoli *et al.* 2012a; (15) Faure *et al.* 2012.

1.4.1 Photoperiod pathway

The acquisition of day length neutrality was crucial for the "green revolution" and the development of superior wheat cultivars (Borlaug 1983). Photoperiod insensitivity is widespread in the world's wheat varieties and predominates in regions where spring wheat is grown as a crop over the winter (short-day) period and where autumn sown winter wheat needs to mature in the following year before the onset of high summer temperatures (Law 1987, Law and Worland 1997, Worland and Snape 2001). A mutation in the regulatory region of the photoperiod response factor *Ppd-D1* was identified as causative for day length-neutrality in wheat (Beales *et al.* 2007). Recent studies have shown that

functional variation at *Ppd-D1a*, *Ppd-A1a* or *Ppd-B1a* in tetraploid and hexaploid wheat are associated with deletions in the promoter of the gene or differences in copy number which all result in an up-regulation of the *Ppd1* homeologous genes (Wilhelm *et al.* 2009, Shaw *et al.* 2012, Diaz *et al.* 2012). In barley, the homeologous photoperiod response gene *Ppd-H1* maps to the short arm of chromosome 2H and is considered the key gene in determining flowering time under LD conditions. *Ppd-H1* is a member of the pseudo-response regulator (PRR) family, orthologous to the circadian clock gene *PRR7* in *Arabidopsis*. The dominant *Ppd-H1* allele causes early flowering under LD and is prevalent in (Mediterranean) winter and wild barley. Mutations in the conserved CCT-domain or the sixth exon of the gene were associated with the late flowering under inductive long photoperiods, and these mutations have been selected in Northern European spring barley genotypes (Turner *et al.* 2005, Jones *et al.* 2008). Turner *et al.* (2005) have shown that barley genotypes with a dominant *Ppd-H1* allele are characterized by elevated expression of *Vrn-H3/HvFT1*. Similarly, increased expression of *Ppd1* in wheat up-regulated the *TaFT* homoeologous genes in a genome-independent manner (Shaw *et al.* 2012). *TaFT* and *Vrn-H3* map to the short arm of the homoeologous chromosome group 7 and encode a RAF kinase inhibitor like protein with homology to the protein of the *Arabidopsis* gene *Flowering locus T* (*FT*). Polymorphisms in the first intron of *Vrn-H3* have been associated with winter or spring growth habit, where the spring allele shows a higher expression level (Yan *et al.* 2006). In *Arabidopsis*, FT is the mobile florigen hormone which moves as a protein from the leaves through the phloem to the shoot apical meristem where it induces the switch from vegetative to reproductive growth (Corbesier *et al.* 2007). Tamaki *et al.* (2007) have shown that also in rice the protein encoded by *Hd3a*, orthologous to FT, moves from the leaf to the shoot apical meristem and induces flowering.

The prominent role of PPD1 in the control of photoperiod sensitivity in wheat and barley suggests that the circadian clock plays an important role in the control of flowering in cereals. Circadian clocks synchronize biological processes with the diurnal cycle, using molecular mechanisms that include interlocked transcriptional feedback loops. In *Arabidopsis*, the circadian clock is composed of three negative feedback loops: (a) the inhibition of evening complex (EC) genes *EARLY FLOWERING 3* (*ELF3*), *EARLY FLOWERING 4* (*ELF4*) and *LUX ARRHYTHMO* (*LUX*, also known as *PHYTOCLOCK1*) by the rise of *CIRCADIAN CLOCK ASSOCIATED1* (*CCA1*) and *LATE ELONGATED HYPOCOTYL* (*LHY*) late at night, (b) the inhibition of *PRR* genes by the EC early at night, and (c) the inhibition of *LHY/CCA1* by *TIMING OF CAB EXPRESSION1* (*TOC1*) in the morning (Huang *et al.* 2012, Pokhilko *et al.* 2012). In addition, the evening expressed *GIGANTEA* (*GI*) protein was modeled as a negative regulator of the EC, which in turn inhibits *TOC1* expression (Pokhilko *et al.*, 2012). Campoli and colleagues (2012b) have shown that circadian clock genes are structurally conserved in barley compared to *Arabidopsis* and their circadian expression patterns suggested conserved functions. However, phylogenetic analyses revealed that duplications/deletions of clock genes occurred throughout the evolution of eudicots and monocots.

For instance the *PRR* genes duplicated independently in monocots and eudicots, and only one homolog of the two paralogous *Arabidopsis* clock genes *LHY/CCA1* is found in monocots (Takata *et al.* 2010, Campoli *et al.* 2012b). In this context it is interesting to note that natural variation at *PPD1* in barley and wheat are major determinants of photoperiod sensitivity (Turner *et al.* 2005, Beales *et al.* 2007), while natural variation at *PRR* genes in *Arabidopsis* did not have a strong effect on flowering time (Ehrenreich *et al.* 2009). In barley, day length neutrality has not been widely used in breeding programs, but natural and induced *early maturity* (*eam*) mutants have been used to breed for early flowering spring barley (Lundqvist 2009). Recently, the gene underlying the *eam8* locus on chromosome 1H was identified as *HvELF3*, orthologous to the *Arabidopsis* clock gene *ELF3* (Faure *et al.* 2012, Zakhrabekova *et al.* 2012). Faure and colleagues (2012) showed that under non-inductive SD conditions, the mutation at *HvElf3* causes an up-regulation of *Ppd-H1* and consequently an activation of the downstream photoperiodic pathway. In *Arabidopsis*, ELF3 physically associates with the promoter of *PRR9* to repress its transcription suggesting that transcriptional targets of ELF3 are partly conserved between *Arabidopsis* and barley (Dixon et al. 2011, Herrero *et al.* 2012). The molecular and phenotypic effects of the mutation in *HvElf3* were thus similar to the effects of mutation in the promoter of *Ppd-D1a*; both mutations cause an up-regulation of *PPD1* and photoperiod insensitivity.

The circadian clock also controls expression of output genes from the flowering time pathway. In *Arabidopsis*, *FT* expression is triggered by the photoperiod response gene *CONSTANS* (*CO*) (Samach *et al.* 2000). *CO* is regulated at the transcriptional level by several genes that are part of the circadian clock or are under circadian clock control, so that *CO* mRNA accumulates at the end of a long day. At the protein level CO is regulated by the cryptochromes Cry1 and Cry2, the phytochromes PhyA, PhyB, and the ubiquitin ligase CONSTITUTIVE PHOTOMORPHOGENIC 1 (COP1) that respectively stabilize CO in light or de-stabilize CO in darkness (Jang *et al.* 2008). As *CO* transcription occurs before dusk in LD but after dusk in SD, CO protein only accumulates and mediates transcription of *FT* under LD (Turck *et al.* 2008).

In barley, nine orthologs of the *AtCO* gene have been isolated, with *HvCO1* and *HvCO2* showing the highest similarity to the *Arabidopsis CO* gene, while *HvCO1* is the positional ortholog of *Hd1*, a major determinant of photoperiod sensitivity in rice (Griffith *et al.* 2003, Higgins *et al.* 2010). Turner *et al.* (2005) suggested that the mutation in *Ppd-H1* of spring barley delayed flowering time by shifting the diurnal expression peaks of *HvCO1* and *HvCO2* mRNA into the dark phase, so that the protein is not synthesized and *Vrn-H3*/*HvFT1* not expressed. Campoli *et al.* (2012a) have recently confirmed that *HvCO1* induces flowering in barley, over-expression of *HvCO1* up-regulated *HvFT1* and accelerated flowering under LD and SD conditions. However, analysis of a mapping population segregating for over-

expression of *HvCO1* and functional variation at *Ppd-H1* showed that *Ppd-H1* induced *HvFT1* expression downstream or independent of *HvCO1* transcription (Campoli *et al.* 2012a).

In *Arabidopsis*, *CO* transcription is controlled by the clock protein GI (Fowler *et al.* 1999). In barley, functional conservation of the single ortholog *HvGI* has not yet been demonstrated (Dunford *et al.* 2005). However, in rice over-expression of *OsGI* induced expression of *Hd1*, the rice ortholog of *CO* in *Arabidopsis* (Hayama *et al.* 2003). In addition, heterologous expression of the *Brachypodium dystachion* GIGANTEA protein in a GI-deficient *Arabidopsis* mutant rescued the late flowering phenotype, suggesting that the role of GI is conserved in the *Triticeae* species (Hong *et al.* 2010).

In barley, five different *FT*-like genes were detected, *HvFT1*, *HvFT2*, *HvFT3*, *HvFT4* and *HvFT5* (Faure *et al.* 2007), of which only *HvFT1* (*Vrn-H3*) has been identified as a flowering promoter (Kikuchi *et al.* 2009). However, *HvFT3* has been recently proposed as a candidate gene for the photoperiod response gene *Ppd-H2* which maps to the long arm of chromosome 1H (Faure *et al.* 2007, Kikuchi *et al.* 2009). So far, two major functional variants of *HvFT3* are known (Casao *et al.* 2011a, 2011b, Cuesta-Marcos *et al.* 2008a). The dominant functional allele is prevalent in Southern European barley germplasm and causes faster flowering under SD conditions when vernalization is not fully satisfied (Casao *et al.* 2011b). A partial deletion of the gene results in a recessive non-functional allele that is common in winter barley (Kikuchi *et al.* 2009, Faure *et al.* 2007). Expression of both, *HvFT1* and *HvFT3* is repressed by *Vrn-H2* and thus also controlled by the vernalization pathway (Yan *et al.* 2006, Casao *et al.* 2011a).

1.4.2 Vernalization pathway

Vernalization response in barley is primarily controlled by genetic variation at *Vrn-H1* and *Vrn-H2*. *Vrn-H1*, located on the long arm of chromosome 5H, encodes a MADS-box transcription factor with high similarity to the *Arabidopsis* meristem identity genes *APETALA1*, *CAULIFLOWER*, and *FRUITFUL* (Yan *et al.* 2003). The recessive winter allele at *Vrn-H1* is only expressed after exposure to cold. Insertions or deletions in the first intron of *Vrn-H1* in spring barley cause up-regulation of the gene independently of vernalization (Hemming *et al.* 2009). Hemming *et al.* (2009) identified regions within the first intron of *Vrn-H1* associated with the repression of the gene in non-vernalized plants. These regions, however, are not required for induction of *Vrn-H1* by cold (Hemming *et al.* 2009). Expression of *Vrn-H1* is important for the transition to reproductive growth. The *Triticum monococcum* mutant *mvp* (*maintained vegetative phase*), which carries a deletion of the *VRN1* locus, never transitioned from the vegetative to the reproductive phase (Shitsukawa *et al.* 2007). Although a deletion of additional flowering time genes, e.g. PHYTOCHROME C, were linked to the deletion of the *VRN1* locus in the *mvp* mutant (Distelfeld *et al.* 2010), Shimada *et al.* (2009) described that in wheat, the up-regulation of *VRN1* under LD was followed by the accumulation of *VRN3 (TaFT)* transcripts, while *TaFT* was not

expressed in the *mvp* mutant of einkorn wheat. Consequently, the authors suggested that *VRN1* is upstream of *VRN3* (*FT*) and up-regulates *VRN3* expression under LD conditions. Additionally, Diaz *et al.* (2012) have demonstrated that as for *PPD1*, copy number variation of *VRN1* correlated with the expression level and vernalization requirement. However, most recently, Chen *et al.* (2012) reported that *VRN1* is only indirectly required for the induction of *TaFT* in wheat, by repressing the *TaFT*-repressor *VRN2* upon vernalization. However, *VRN1* was not required for the induction of *TaFT1* and flowering in the absence of *VRN2*.

In barley, *Vrn-H1* down-regulates expression of *Vrn-H2*, which is only expressed under LD conditions. The *Vrn-H2* region on chromosome 4HL includes one truncated and two full sequence ZCCT (Zinc finger and CCT domain) genes, *ZCCT-Ha*, *ZCCT-Hb*, *ZCCT-Hc* with no clear orthologs in *Arabidopsis* (Yan *et al.* 2004). In photoperiod-sensitive winter barley, *Vrn-H2* represses *Vrn-H3* (*HvFT1*) to counteract the *Ppd-H1* dependent long-day induction of *Vrn-H3* prior to winter. *Vrn-H2* expression is maintained at high levels, prior to vernalization and down-regulated by *Vrn-H1* during exposure to cold. Up-regulation of *Vrn-H1* during vernalization and consequent down-regulation of *Vrn-H2* promotes inflorescence meristem identity at the shoot apex and accelerates inflorescence initiation. Down-regulation of *Vrn-H2* transcript levels in the leaves facilitates the up-regulation of *Vrn-H3* under LDs mediated by *Ppd-H1* and possibly by *HvCO1* (Yan *et al.* 2006, Hemming *et al.* 2008, Campoli *et al.* 2012a). High levels of *Vrn-H3* in turn up-regulate *Vrn-H1*. Li and Dubcovsky (2008) have shown that wheat *VRN3* induces *VRN1* transcription via the interaction with FDL2 (FD-LIKE2) and argue that *VRN3* is the integrator of low temperature and long daylength responses.

Kikuchi *et al.* (2011) have recently shown that *HvCO9*, which belongs to the same grass specific *CO*-like subfamily of the flowering repressors *Vrn-H2* in barley and *Ghd7* in rice (Xue *et al.* 2008), delays flowering under non-inductive SD conditions, possibly by down-regulating *HvFT1*. In the *Triticeae*, the chromosomal region on 4H containing the *Vrn2* locus has originated from a duplication of a chromosomal region on chromosome 1 carrying the *HvCO9* locus (Cockram *et al.* 2010). The *Vrn2* locus may thus be derived from a targeted duplication of *HvCO9* to the homeologous region after the divergence of *Triticeae* (Kikuchi *et al.* 2011). It is interesting that grass species have developed systems for flowering repression that are different from those of *Arabidopsis*. Despite homology between *Arabidopsis* and cereal flowering time genes, gene duplication may have favoured functional diversification of flowering time pathways. Functional comparison of cereal and *Arabidopsis CO* and *FT* families, for example, demonstrates that their connectivity within the flowering pathways has been modified; and they can be regulated by different external and internal factors.

1.5 QTL for flowering time in barley

Functional variation at *Ppd-H1*, *Ppd-H2*, *Vrn-H1*, *Vrn-H2* and *Vrn-H3* has been consistently identified in QTL studies using crosses between elite winter and spring barley genotypes (Laurie *et al.* 1995, Sameri *et al.* 2011). However, QTL studies within winter barley germplasm, primarily in Mediterranean barley including wild barley (*H. spontaneum*) and barley landraces have revealed additional major flowering time loci. Figure 3 shows consensus QTL for flowering time in barley and indicates candidate genes or potentially allelic mutants which map close to these QTL. A selection of the consensus QTL and possible candidate genes are discussed below.

In crosses involving wild barley or Mediterranean landrace genotypes, QTL for flowering time are consistently detected close to the *Eam6* locus at the centromeric region of chromosome 2H (Marquez-Cedillo *et al.* 2001, Pillen *et al.* 2004, von Korff *et al.* 2008, Wang *et al.* 2010). This locus has major effects on flowering time in autumn sown field trials in Mediterranean and Australian environments and has been associated with variation in the duration of the basic vegetative period (Boyd *et al.* 2003, Cuesta-Marcos *et al.* 2008a, b). *Eam6* on chromosome 2H was identified as an ortholog of *Antirrhinum CENTRORADIALIS* (*HvCEN*), homeologous to *Arabidopsis TFL1*. *TFL1* is an *FT*-like gene, but unlike *FT* encodes a repressor of flowering. Comadran *et al.* (2012) showed that natural variation at *HvCEN* contributed to the adaptation of barley to higher latitudes with cool and wet summers and thus extended growing seasons. Genetic variation for flowering time control was also identified at the *FLT-2L* locus on the long arm of chromosome arm 2H (Teulat *et al.* 2001, Ivandic *et al.* 2002, Boyd *et al.* 2003, Baum *et al.* 2003, Pillen *et al.* 2003, 2004, von Korff *et al.* 2006, 2008, 2010, Eleuch *et al.* 2008, Borràs-Gelonch *et al.* 2010). The locus, which also affected plant height and rachis internode length, was fine mapped to a region which included *HvAP2*, a gene encoding an AP2 domain protein, with sequence similarity to the wheat domestication gene *Q* located on chromosome 5A and conferring a similar phenotype to the barley *Flt-2L* mutation (Chen A *et al.* 2009). A number of crosses involving elite and exotic germplasm also revealed genetic variation for flowering time at the long arm of chromosome 3H (Laurie *et al.* 1995, Bezant *et al.* 1996, Boyd *et al.* 2003, Baum *et al.* 2003, Szücs *et al.* 2006, Cuesta-Marcos *et al.* 2008a). Early flowering at this locus was caused by the exotic allele and was correlated with increased plant height and reduced yield under favourable conditions, but increased yield under marginal rain-fed conditions (von Korff *et al.* 2006, von Korff *et al.* 2008). This QTL coincides with the *sdw1/denso* locus which reduces growth and has been selected in elite barley to reduce lodging and optimize yield under favourable conditions. *Ga20-oxidase*, a gene involved in the synthesis of gibberellin has been recently proposed as a potential candidate for this locus (Jia *et al.* 2009).

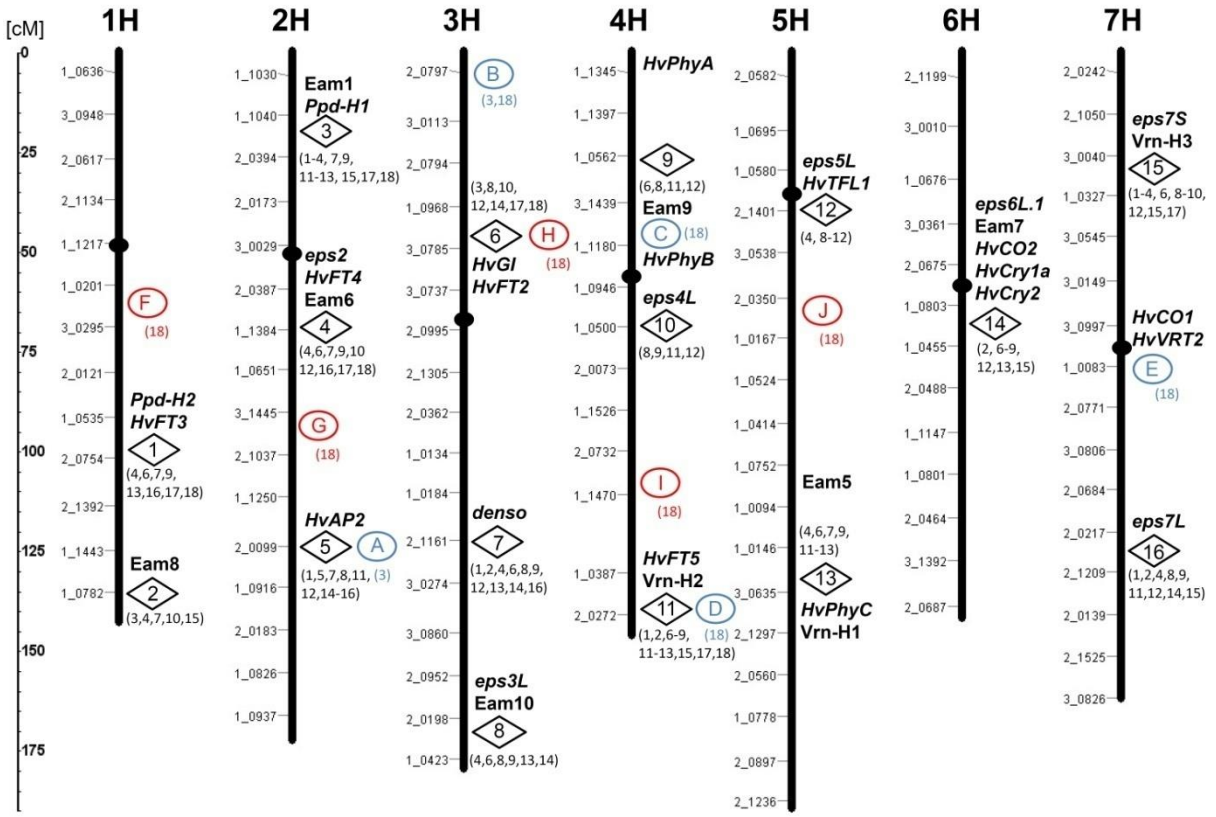

Figure 3: Consensus map of flowering time QTL positions in barley. Positions of QTL and flowering time candidate genes were projected onto the Barley OPA 2011 consensus map of Muñoz-Amatriaín *et al.* (2011). Markers to the left of the chromosomes represent POPA SNP markers. Numbers in diamond shaped boxes to the right of the chromosomes summarize approximate positions for flowering time QTL identified in at least four independent studies. QTL identified for individual pre-anthesis phases in Borrás-Gelonch *et al.* 2010 and 2012 are indicated as circles: QTL for vegetative and early reproductive phase in blue (A-E) and QTL for stem elongation phase in red (F-J). Positions of centromeres are indicated as black filled ovals. References for candidate genes are reported in the text. Publications corresponding to QTL positions are indicated with indices. 1: Baum *et al.* 2003; 2: Bezant *et al.* 1996; 3: Borrás-Gelonch *et al.* 2010; 4: Boyd *et al.* 2003; 5: Chen A *et al.* 2009; 6: Cuesta-Marcos *et al.* 2008a; 7: Cuesta-Marcos *et al.* 2008b; 8: Ivandic *et al.* 2002; 9: Laurie *et al.* 1995; 10: Márquez-Cedillo *et al.* 2001; 11: Pillen *et al.* 2003; 12: Pillen *et al.* 2004; 13: Szücs *et al.* 2006; 14: Teulat *et al.* 2001; 15: von Korff *et al.* 2006; 16: von Korff *et al.* 2008; 17: Wang *et al.* 2010, 18: Borrás-Gelonch *et al.* 2012.

QTL for flowering time at the centromeric region of chromosome 6H also coincided with QTL for plant height and yield, where the wild barley alleles reduced time to flowering, plant height and yield under favourable conditions (Laurie *et al.* 1995, Bezant *et al.* 1996, Ivandic *et al.* 2002, Pillen *et al.* 2004, Korff *et al.* 2006, Cuesta-Marcos *et al.* 2008a, b). The blue/UV-A light cryptochrome photoreceptors Cry1a and Cry2, which regulate plant growth and development (Quail 2002), map to the centromeric region of 6H (Szücs *et al.* 2006). Furthermore, the same region of 6H harbours the *eam7* mutation which determines photoperiod insensitivity and early flowering under LD conditions (Stracke and Börner 1998). QTL studies for agronomic traits suggest that flowering time is strongly correlated with plant height and yield. However, very little is known about direct or indirect effects of individual flowering time genes and QTL on plant architecture and yield structure. Genetic dissection of individual pre-

anthesis phases may thus allow further characterizing pleiotropic effects of individual flowering time genes on plant architecture and yield components.

1.6 Pleiotropic effects of flowering time genes

Studies in rice and tomato have already demonstrated that flowering time genes have pleiotropic effects on a number of traits including inflorescence architecture and grain yield. In rice, *Ghd7* encoding a CCT domain protein, acts as a regulator of flowering time, panicle size and seed number (Xue *et al.* 2008). In tomato, the loss-of-function allele of *SINGLE FLOWER TRUSS* (*SFT*) increases the total number of inflorescences, flowers and fruits per plant. This gene was shown to increase yield up to 60% if in heterozygous state, providing one of the first example of overdominance in heterosis for yield (Krieger *et al.* 2010). Although major cereal genes have been identified which affect the time from germination to flowering/anthesis, little information exists about genes and molecular changes in the leaf and in the meristem that determine the initiation and duration of the different developmental phases (Shitsukawa *et al.* 2007, Chen Y *et al.* 2009, González *et al.* 2005, Borrás-Gelonch 2012a, 2012b). In wheat, expression of *VRN1* is important for the transition to a reproductive meristem (Shitsukawa *et al.* 2007). However, Chen Y *et al.* (2009) found that variation in stem elongation and inflorescence development mapped close to *Vrn-H1* in a barley mapping population, suggesting that this gene also affects later developmental phases. Variation in the duration of the vegetative phase was also ascribed to *eam* or *eps* loci. Lewis *et al.* (2008) found that variation at the *eps-A1* locus affected transition to the reproductive stage and formation of a terminal spikelet, but not inflorescence development in wheat. These differences were paralleled by a significant decrease in the number of spikelets per spike, in both greenhouse and field experiments. In contrast, variation at the photoperiod response gene *Ppd-H1* and over-expression of *HvCO1* primarily affected the stem elongation phase and inflorescence development (Campoli *et al.* 2012a). However, studies in wheat have shown that variation at *Ppd-D1* affected all phases of pre-anthesis development (González *et al.* 2005). The authors also showed that lengthening the late reproductive phase of stem elongation in wheat, increased spike weight and the number of fertile florets at anthesis. These studies demonstrate that flowering time genes have an indirect effect on yield potential by fine-tuning flowering time for an optimal adaptation to different environments. In addition to this indirect effect, flowering time genes have a more direct impact on yield by affecting basic developmental processes and thus individual grain yield components.

1.7 Thesis aims

As described above, a better understanding of the genetic basis of pre-anthesis development may contribute to unravelling the genetic basis of inflorescence architectures and thus yield in cereals. However, previous studies investigated the genetic regulation of individual pre-anthesis phases by QTL analyses (Borrás-Gelonch *et al.* 2012a, 2012b) or focused on a limited number of candidate genes (Gonzáles *et al.* 2005, Trevaskis *et al.* 2007a, Shitsukawa *et al.* 2007). To the best of our knowledge, no efforts have been undertaken in wheat or barley so far to identify genes specifically acting at the shoot apex to regulate pre-anthesis development on a genome wide scale.

Thus, in the present study, we were aiming at a detailed description of morphological and transcriptional changes in leaves and at the shoot apex during the leaf and spikelet initiation phase. Using RNA-sequencing and qRT-PCR, we intended to identify molecular changes in the shoot apex and leaf and correlate these to morphological changes at the main shoot apex. Our investigations on the genetic regulation of pre-anthesis development followed three major objectives:

1) We aimed to characterize the effects of the photoperiod and variation at *Ppd-H1* on different phases of shoot apex development, i.e. the floral transition, development and maturation of floret primordia and thus spikelet fertility and seed set.

2) Although barley requires long photoperiods for completion of the flowering process, floral transition and early stages of inflorescence development are also reached by plants under short photoperiods. By investigating the transcriptomes of shoot apices at defined developmental stages of SD and LD grown plants, we were aiming at the identification of central regulators of the floral transition and early inflorescence development independent of the photoperiod in barley.

3) *Ppd-H1* has been described to promote the floral transition and inflorescence development in barley through induction of *HvFT1* expression in leaves in response to long photoperiods (Turner *et al.* 2005, Campoli *et al.* 2012b). However, little is known about the genes acting downstream of *Ppd-H1*/ *HvFT1* in leaves and at the shoot apex to promote reproductive development of barley. Thus, by making use of natural genetic variation at *Ppd-H1*, we intended to identify candidate genes acting as part of the photoperiod and *Ppd-H1* dependent flowering pathway in leaves and shoot apices.

2 Results

We investigated photoperiod and *Ppd-H1*-dependent and photoperiod-independent morphological and molecular changes during barley MSA development. For this purpose, we studied MSA and leaf development in three pairs of spring barley and derived introgression lines, Scarlett/S42-IL107, Bowman/BW281 and Triumph/Triumph-IL all differing for the natural mutation in *Ppd-H1.* Whole transcriptome changes in MSA and leaves of Scarlett and S42-IL107 were examined under SDs and LDs. In order to confirm developmental and *Ppd-H1* dependent effects observed in the whole transcriptome analysis, expression of selected candidate genes was verified in MSA and leaves of all three pairs of introgression lines.

2.1 Morphological analysis of barley lines with allelic variation at *Ppd-H1*

2.1.1 Introgression of *Ppd-H1* in spring barley background results in an acceleration of all phases of pre-anthesis development

When plants were grown under LDs, heading date of the main shoot spike was recorded for Bowman at 39 days after germination (DAG), for Scarlett at 46 DAG and Triumph at 60 DAG (Fig. 5A). The introgression lines with the dominant *Ppd-H1* allele exhibited a faster floral transition and reproductive development. BW281 headed at 23 DAG, S42-IL107 at 27 DAG and Triumph-IL at 35 DAG and thus 16, 19 and 25 days earlier than the respective recurrent parents carrying the natural mutation at *ppd-H1*. Under LDs, the MSA of all genotypes showed a biphasic pattern of development. LDs and the introgression of *Ppd-H1* caused only a moderate acceleration of the vegetative phase and early reproductive development until the beginning of internode elongation, but a strong acceleration of inflorescence development until heading (Fig. 4B, Suppl. Tab. S1). The acceleration of early plant development in the introgression lines was also reflected by the lower final number of leaves emerged from the main culm (Fig. 5B). Under SDs, the MSA developed at a constant rate and was not affected by genetic variation at *Ppd-H1* (Fig. 4B, Suppl. Tab. S1). However, none of the investigated genotypes flowered from the main shoot under SDs, as the main shoot inflorescence was aborted before anthesis during the time of stem elongation (W4.0-W6.0).

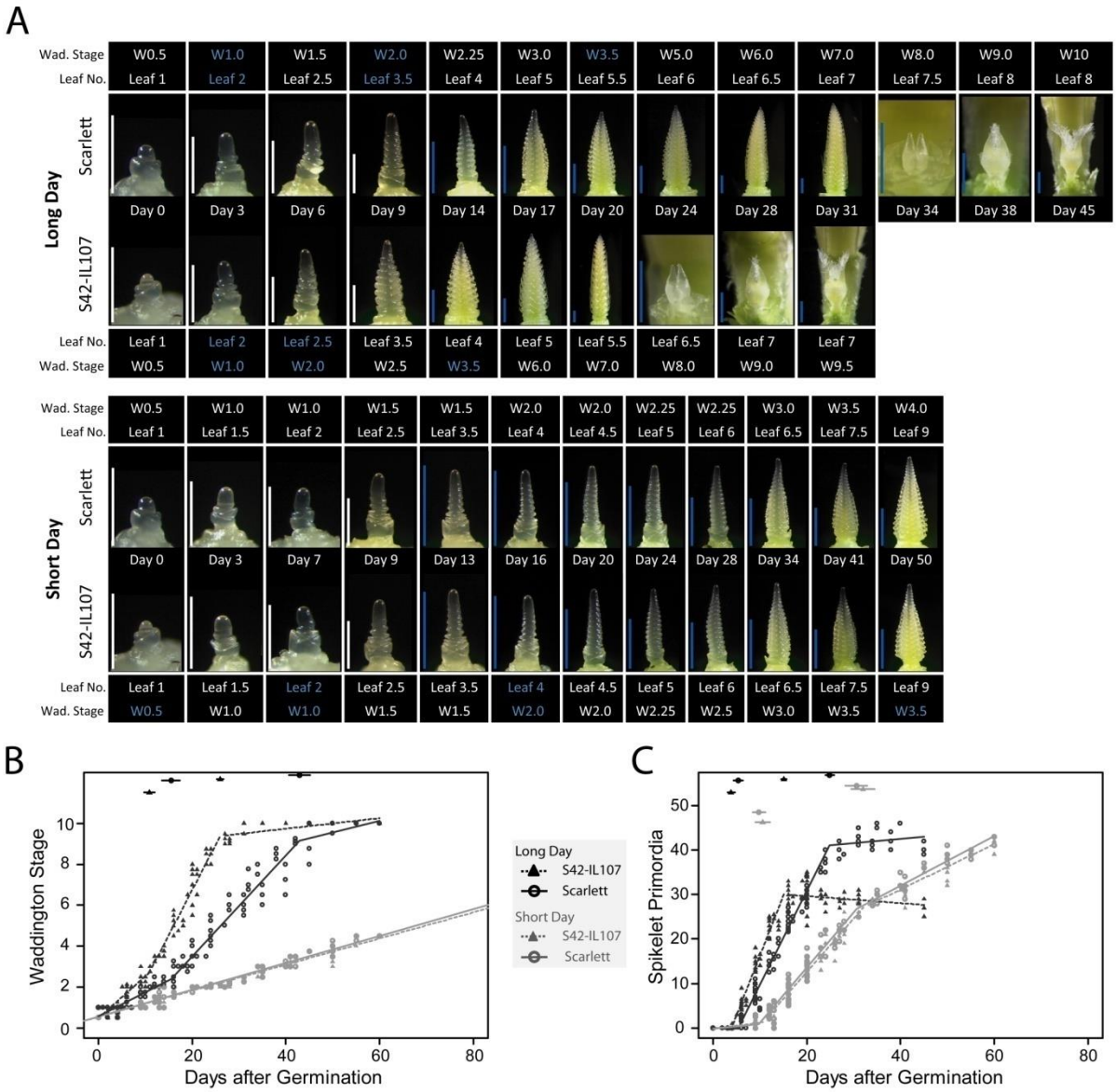

Figure 4: Developmental phenotypes of barley main shoot apices
(A) Development of the main shoot apex of Scarlett and S42-IL107. Developmental stage of the apex (W: Waddington stage) and number of leaves emerged from the main shoot are reported. Plants were grown under short-day conditions (SD) or transferred to long photoperiods (LD) seven days after germination (Day 0). Blue labels indicate stages, at which leaf and apex samples were harvested for transcriptome profiling using RNA-sequencing. White bars (500µm), blue bars (1mm). Broken line regression analyses are shown for **(B)** shoot apex development and **(C)** spikelet primordia appearance on main shoot inflorescences of plants germinated and grown under SD or LD. Positions of regression line breakpoints and their 95% confidence intervals (95%-CI) are indicated above each chart. Slopes of individual segments of the composite regression lines representing the rate of apex development and spikelet primodia induction with their 95%-CIs are presented in Suppl. Tab. S1.

Further, we tested if the faster maturation of the MSA in the introgression lines was associated with an increased global activity of the shoot apical meristem. For this purpose, we determined the rate of spikelet primordia emergence at the MSA in Scarlett and S42-IL107 (Fig. 4C). The rate of spikelet primordia emergence was increased in both genotypes under LDs as compared to SDs. S42-IL107 showed an earlier induction of the first spikelet primordia under LDs, and the rate of spikelet primordia emergence was increased with 2.7 as compared to Scarlett with 2.1 spikelet primordia per day (Suppl.

Tab. S1). Variation at *Ppd-H1* affected the longevity of the inflorescence meristem (IM), as the period of spikelet primordia induction was prolonged in the presence of the mutated *ppd-H1* allele, e.g. until W4.0 in S42-IL107 and until W6.0 in Scarlett. However, the number of spikelet primordia at W3.5 corresponded to the number of fully developed spikelets per spike at flowering, suggesting that spikelet primordia emerged after W3.5 did not develop into fertile flowers (Fig. 5C). Because the duration of the early developmental phase was longer in the presence of a mutated *ppd-H1* allele, the number of spikelet primordia at stamen primordium stage (W3.5), the number of final spikelets and seeds per spike was increased in Scarlett, Bowman and Triumph as compared to the introgression lines.

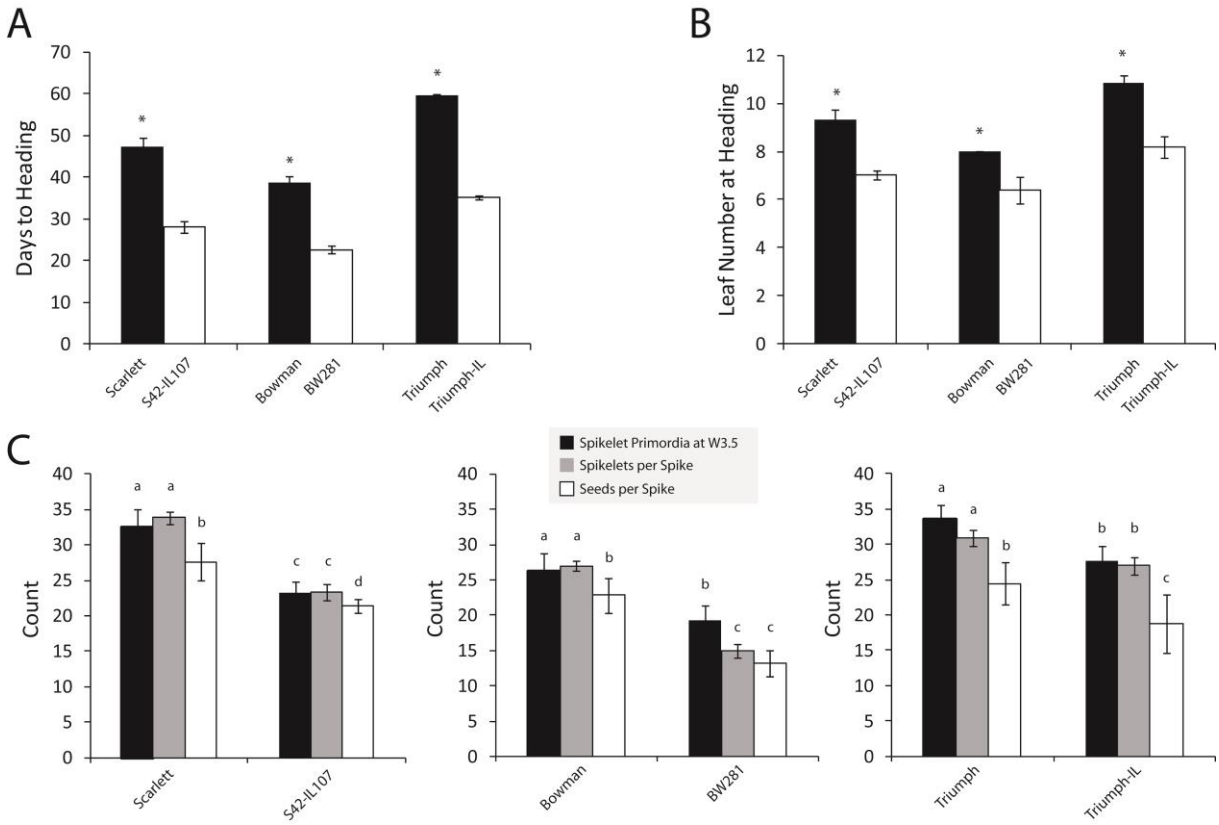

Figure 5: Development related phenotypes of Scarlett/S42-IL107, Bowman/BW281 and Triumph/Triumph-IL
(A) Main shoot related phenotypes recorded at the time of heading: **(A)** heading date, **(B)** leaf number. **(C)** Phenotypes of the main shoot spike recorded at stamen primordium stage (W3.5, spikelet primordia per inflorescence) or at plant maturity (spikelets per spike, seeds per spike). Bars represent means ± standard deviation over 5-15 plants. Significant differences ($p<0.05$) between spring barleys and derived *Ppd-H1* introgression lines and between spike related phenotypes are indicated as asterisks and small letters on top of the charts, respectively.

Taken together, the introgression lines showed an accelerated reproductive development under LDs, but not SDs. Under LDs, allelic variation for *Ppd-H1* had the strongest effect on inflorescence development, while under SDs the MSA transitioned to a reproductive state but did not lead to the production of fertile spikelets on the main shoot spike. The increased number of seeds per spike in plants carrying the *ppd-H1* allele (Fig. 5C), was caused by a decelerated IM maturation, and consequently IM termination, despite the reduced rate of spikelet primordia induction at the MSA. The coincidence of the number of spikelet primordia at W3.5 with the number of spikelets per spike

at plant maturity highlights the importance of the early reproductive development on determining the yield potential.

2.1.2 SD increases the yield potential during the vegetative and early reproductive phases while LD is required for spikelet development and internode elongation during the late reproductive phase

To further investigate the effects of the photoperiod during early phases of plant development on plant architecture and reproductive traits in more detail, we conducted a photoperiod shift-experiment, transferring Scarlett and S42-IL107 plants from SD to LD and vice versa at different stages of MSA development.

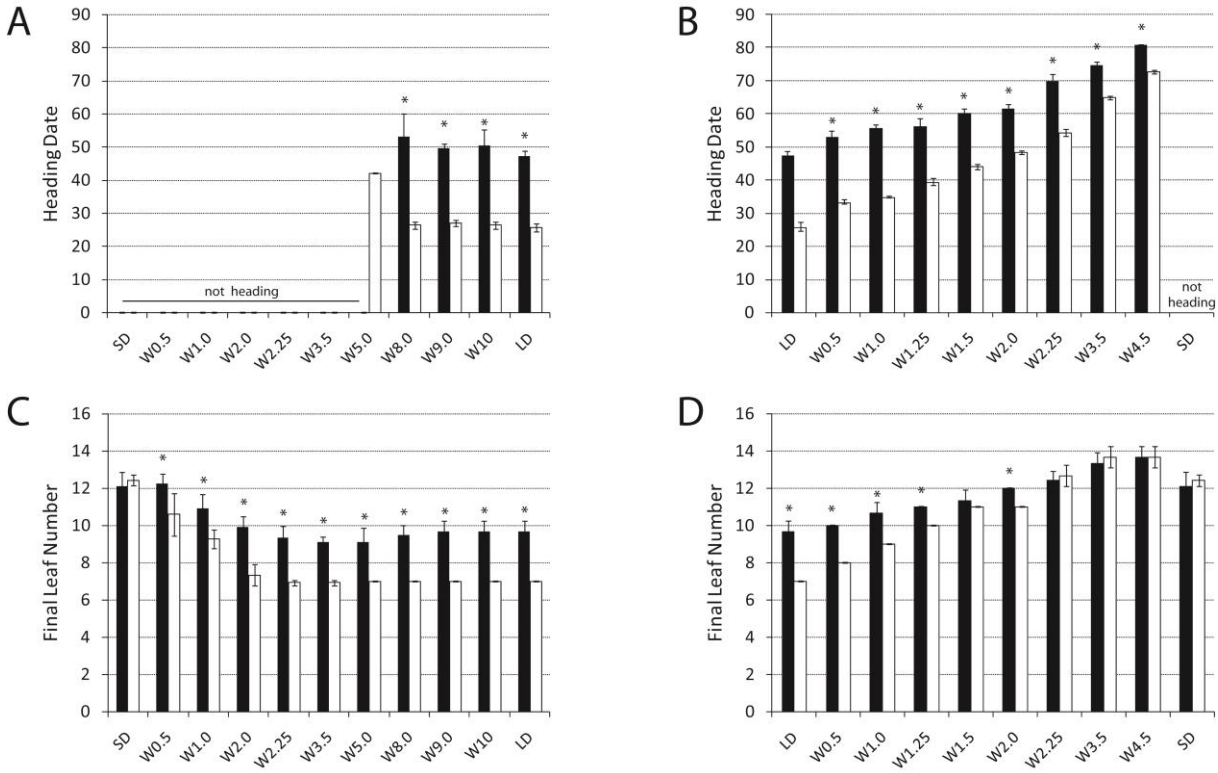

Figure 6: Effects of the photoperiod during plant development on heading date and final leaf number of Scarlett and S42-IL107

Plants of Scarlett (black) and S42-IL107 (white) were grown under short-day (SD) or long-day (LD) conditions. At different stages of MSA development (W0.5 – W10), plants were transferred from **(A, C)** LD to SD or from **(B, D)** SD to LD and remained in the respective photoperiod until plant senescence. **(A, B)** Heading date and **(C, D)** leaf number of the main shoot flag leaf were recorded for plants. Bars represent means ± standard deviation over 3 plants. Significant differences ($p<0.05$) between genotypes transferred from SD to LD and vice versa at the same developmental stage are indicated by asterisks above bar graphs.

Heading date of both genotypes was gradually delayed by short photoperiods, when plants were germinated under SD and transferred to LD conditions during early stages of MSA development (≤W4.5) (Fig. 6B). Plants responded as early as three days after germination to differences in photoperiod treatments, indicating the absence of a photoperiod insensitive, juvenile phase in barley. In agreement with the SD dependent delay of heading date, final number of leaves emerging from the main shoot gradually increased with prolonged SD treatments before shifting plants to LD, diminishing the difference of 2-3 leaves observed between genotypes under constant LD conditions (Fig. 6D). Both genotypes flowered with the same number of leaves, when plants were kept in SD until the emergence of the first spikelet primordia on the MSA, supporting that differences in the length of the vegetative phase (≤W1.5-2.25) between genotypes is reflected by the number of leaves emerged from the main shoot in barley. However, plants of both genotypes transferred to LD at W3.5 and W4.5 produced even more leaves than plants grown under SD until the end of the vegetative phase. This suggests that the number of leaves emerging from the main shoot is not a definite indication for the length of the vegetative phase, and thus does not reflect the time-point of floral transition with certainty.

When plants were shifted from LD to SD conditions, long photoperiods gradually accelerated the timing of the vegetative to reproductive transition in Scarlett and S42-IL107, as indicated by the reduced number of leaves emerging from the main shoot (Fig. 6C). The reduction in final leaf number was observed, when plants were shifted from LD to SD before the induction of the first floret primordia at the MSA (≤W2.0) and was more pronounced in S42-IL107 as compared to Scarlett, reflecting the increased photoperiod sensitivity of S42-IL107 in the presence of the photoperiod responsive *Ppd-H1* allele.

Heading was observed in Scarlett only when transferred to SD after W8.0, i.e. shortly before heading (W8.5-9.5) under constant LD conditions (Fig. 6A). S42-IL107 plants also reached the heading stage when shifted to SD conditions at W5.0 already. However, for successful seed production on the main shoot spikes, Scarlett and S42-IL107 plants required LD until W9.0 and W8.0, respectively (Fig. 7G). In coincidence with heading date and seed production, LD was required for internode elongation of shoots and spikes in both genotypes (Fig. 7A, C). Although spikes at plant maturity as well as shoot apices at any developmental stage were shorter in S42-IL107 than in Scarlett when plants were constantly grown under LD conditions (Fig. 4A, 7D), main shoot spikes were longer in S42-IL107 as compared to Scarlett, when plants were transferred to SD conditions before W8.0, i.e. the promoting effect of LD on internode elongation in spikes was retained to some extent in S42-IL107 but not in Scarlett even under SD. Despite its inhibitory effect of short photoperiods on internode elongation, SD conditions indirectly increased internode elongation of shoots and spikes, when plants were shifted to LD after a prolonged SD treatment during the vegetative phase (Fig. 7B, D). This effect was

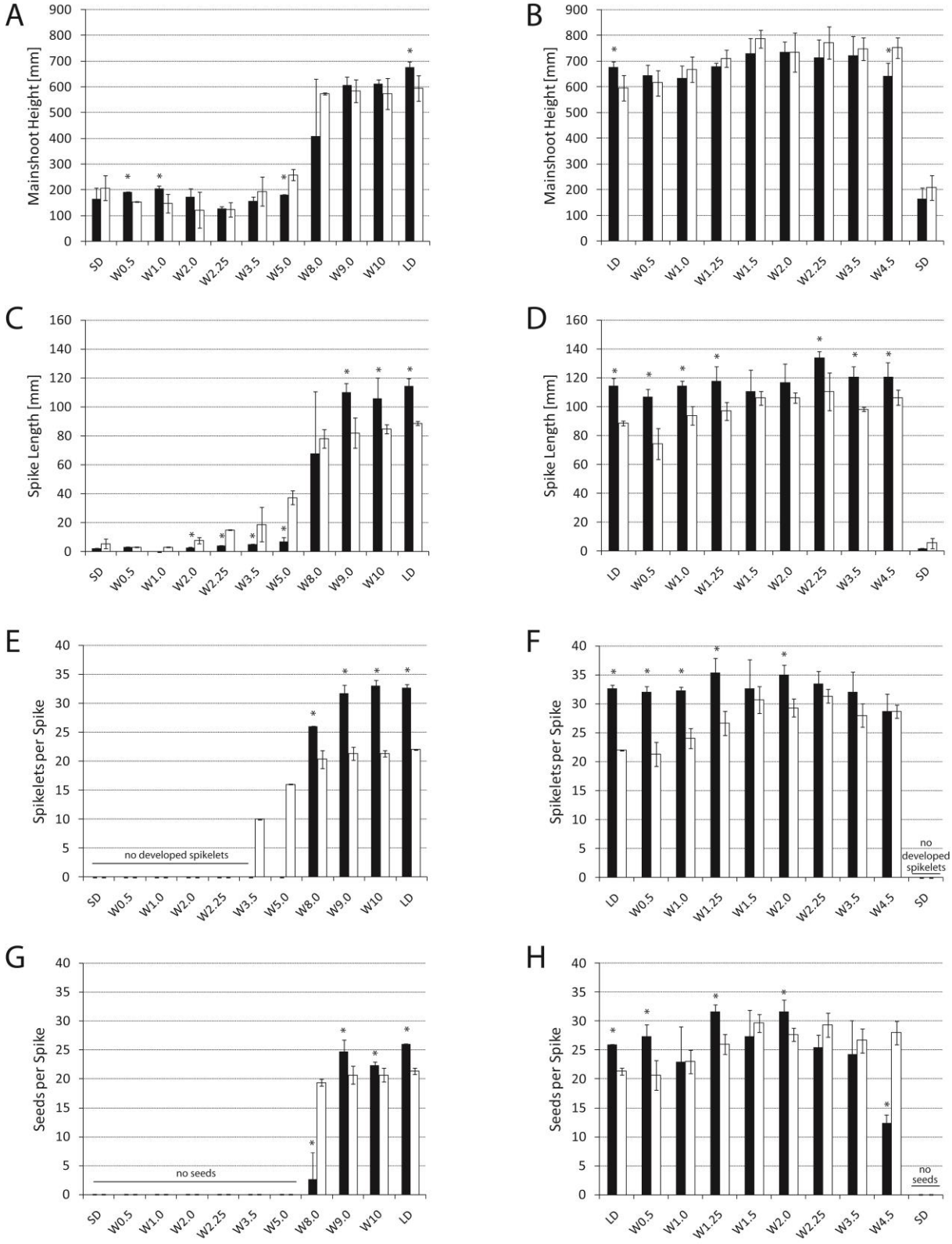

Figure 7: Effects of photoperiod during plant development on stem elongation and spike traits of Scarlett and S42-IL107
Plants of Scarlett (black) and S42-IL107 (white) were grown under short-day (SD) or long-day (LD) conditions. At different stages of MSA development (W0.5 – W10), plants were transferred from **(A, C, E, G)** LD to SD or from **(B, D, F, H)** SD to LD and remained in the respective photoperiod until plant senescence. Phenotypes of the main shoot were recorded for plants: **(A, B)** height of the main shoot, **(C, D)** spike length, **(E, F)** spikelet number per spike, **(G, H)** seed number per spike. Bars represent means ± standard deviation over 3 plants. Significant differences ($p<0.05$) between genotypes transferred from SD to LD and vice versa at the same developmental stage are indicated by asterisks above bar graphs.

observed in both genotypes, but more pronounced in S42-IL107. Similarly, the number of spikelets and seeds per spike were increased in plants, for which cultivation under LD was preceded by a period of SD during the vegetative phase (Fig. 7F, H). However, Scarlett plants shifted to LD conditions after the vegetative phase (≥W2.25) had reduced number of seeds and florets per spike, highlighting the need for long photoperiods during the reproductive phase.

Interestingly, S42-IL107 plants germinated and kept under SD until W1.25 and shifted to LD, had the same number of leaves emerging from the main shoot and the same number of seeds per spike as compared to Scarlett plants kept under constant LD (Fig. 6D, 7H). At the same time, these S42-IL107 plants still headed 8 days earlier than the respective Scarlett plants indicating a shorter reproductive phase (Fig. 6B). Taken together, this suggest that a prolonged vegetative rather than reproductive phase in Scarlett as compared to S42-IL107, when both genotypes are constantly grown under LD, leads to the observed differences in the number of seeds per spike.

In summary, long photoperiods promote MSA development during vegetative and reproductive stages in an additive manner and are crucial during the reproductive phase for internode elongation and spikelet development. SD treatments during vegetative, but not reproductive stages of plants lead to an increased number of seeds per spike. Thus, an extended vegetative phase rather than a prolonged reproductive development might account for the increased yield potential in Scarlett as compared to S42-IL107 plants.

2.2 Characterization of transcriptional changes in leaves and at the shoot apex during the vegetative and early reproductive phase

As the development of the MSA until W3.5 determined the final number of spikelets per spike, we were interested in identifying the molecular basis of variation in MSA activity and maturation until this stage. We conducted whole transcriptome expression profiling of developing shoot apices during the vegetative (W0.5-W1.0) and early reproductive phases (W2.0-W3.5) of Scarlett and S42-IL107 plants grown under LDs. Because Scarlett and S42-IL107 did not differ in development under SDs (Fig. 4), expression changes under SDs were only probed in S42-IL107. Shoot apex and leaf samples of the two genotypes and photoperiods were not harvested at the same time after germination, but at the same developmental stages. This experimental set-up enabled us to identify: a) candidate genes for the photoperiod independent regulation of shoot apex development, i.e. genes of central importance for shoot apex development *per se*, and b) candidate genes acting as part of the photoperiod and *Ppd-H1* dependent flowering pathway in leaves and apices. The latter ones are represented by intersections of differentially expressed transcripts (DETs) between photoperiods and between genotypes, i.e. transcripts co-regulated by LDs and by S42-IL107, and in the following will be termed as candidates acting down-stream of *Ppd-H1*.

2.2.1 Whole transcriptome profiles of developing shoot apices

Among the 25152 transcripts expressed in leaves or MSA samples, we identified 6602 DETs between apices at different developmental stages across photoperiods and genotypes (Fig. 8B).

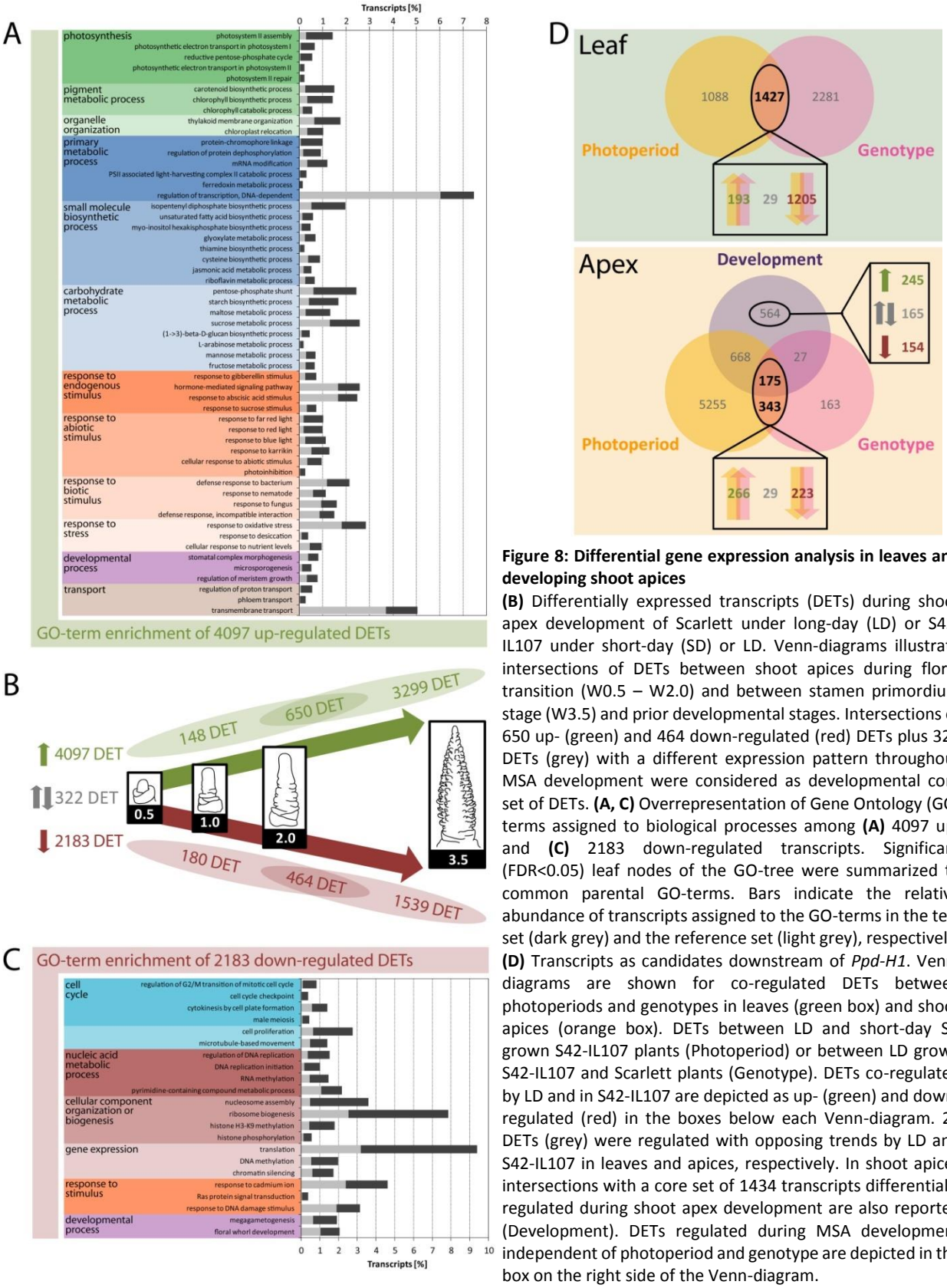

Figure 8: Differential gene expression analysis in leaves and developing shoot apices

(B) Differentially expressed transcripts (DETs) during shoot apex development of Scarlett under long-day (LD) or S42-IL107 under short-day (SD) or LD. Venn-diagrams illustrate intersections of DETs between shoot apices during floral transition (W0.5 – W2.0) and between stamen primordium stage (W3.5) and prior developmental stages. Intersections of 650 up- (green) and 464 down-regulated (red) DETs plus 320 DETs (grey) with a different expression pattern throughout MSA development were considered as developmental core set of DETs. **(A, C)** Overrepresentation of Gene Ontology (GO) terms assigned to biological processes among **(A)** 4097 up- and **(C)** 2183 down-regulated transcripts. Significant (FDR<0.05) leaf nodes of the GO-tree were summarized to common parental GO-terms. Bars indicate the relative abundance of transcripts assigned to the GO-terms in the test set (dark grey) and the reference set (light grey), respectively. **(D)** Transcripts as candidates downstream of *Ppd-H1*. Venn-diagrams are shown for co-regulated DETs between photoperiods and genotypes in leaves (green box) and shoot apices (orange box). DETs between LD and short-day SD grown S42-IL107 plants (Photoperiod) or between LD grown S42-IL107 and Scarlett plants (Genotype). DETs co-regulated by LD and in S42-IL107 are depicted as up- (green) and down-regulated (red) in the boxes below each Venn-diagram. 29 DETs (grey) were regulated with opposing trends by LD and S42-IL107 in leaves and apices, respectively. In shoot apices intersections with a core set of 1434 transcripts differentially regulated during shoot apex development are also reported (Development). DETs regulated during MSA development independent of photoperiod and genotype are depicted in the box on the right side of the Venn-diagram.

In addition, 1427 DETs in leaves and 518 DETs in apices were differentially regulated under LDs and in S42-IL107 (Fig. 8D). Taken together, we identified in total 7604 DETs, which were characterized by 31 distinct expression profiles (Fig. 9, Suppl. Fig. S1). The hierarchical structure of the 31 co-expression clusters revealed three tissue specific expression profiles (Fig. 9A, Suppl. Tab. S2), with transcripts predominantly expressed in leaves (cluster I), similarly expressed in leaves and shoot apices (cluster II) or transcripts expressed to higher levels at the shoot apex (cluster III).

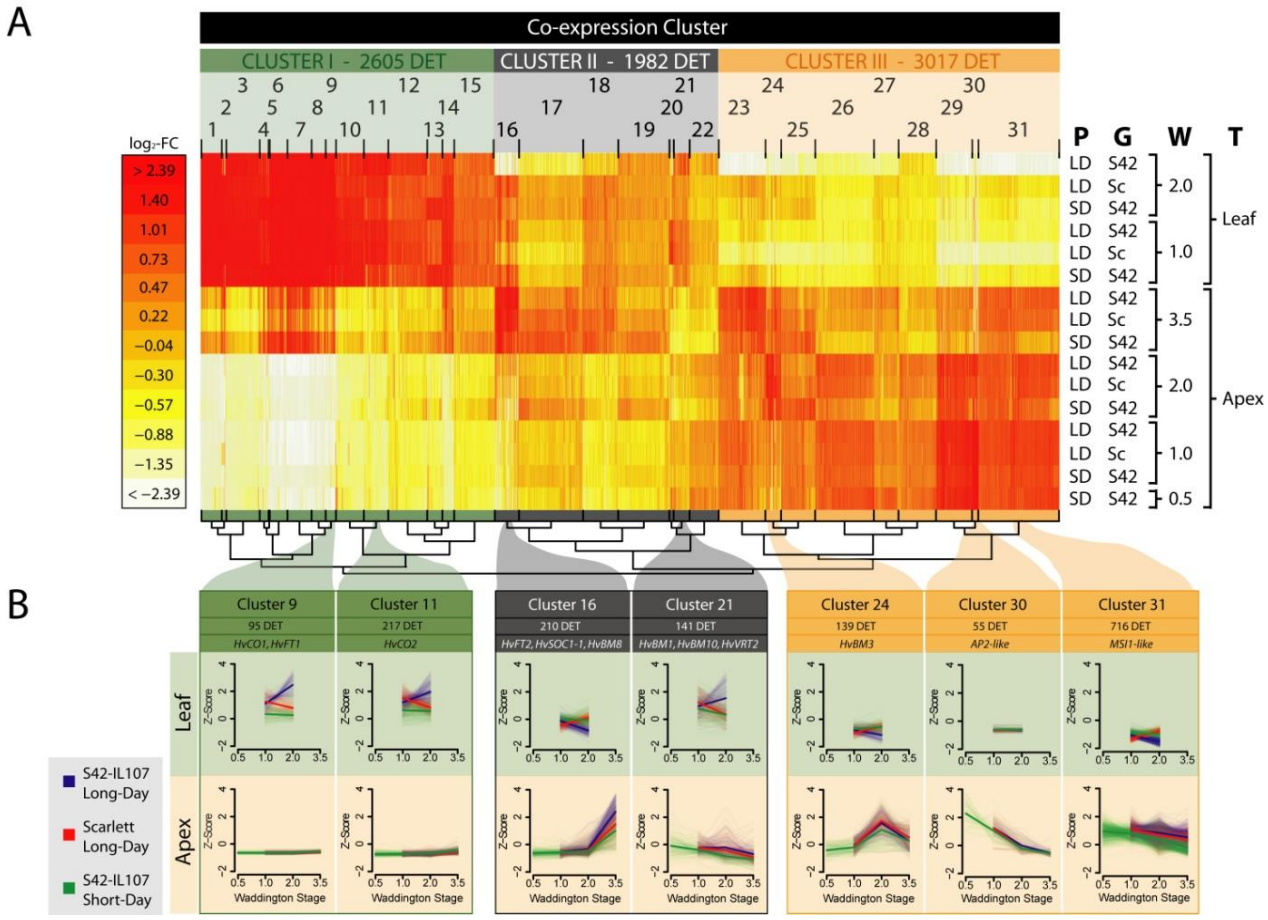

Figure 9: Model based clustering of 7604 transcripts into 31 co-expression clusters
(A) Heatmap of co-expression clusters for 7604 differentially expressed transcripts (DET). Colors represent log_2-fold changes (FC) in expression levels relative to the mean transcript abundance across the tested conditions, i.e. leaf and apex samples of Scarlett (Sc) and S42-IL107 (S42), when plants grown under short- (SD) and long-day (LD) conditions and harvested at different developmental stages (Waddington stage 0.5-3.5). P: Photoperiod; G: Genotype; W: Waddington Stage; T: Tissue. Co-expression clusters (1-31) were assigned to three higher level clusters (I-III) with distinct expression patterns between apex and leaf samples (see Suppl Tab. S2). Number and assignment of DETs to higher and lower level co-expression clusters are shown above the heatmap. Similarity of co-expression clusters is indicated in the hierarchical tree structure below the heatmap. **(B)** Selected set of co-expression clusters representative for DETs during shoot apex development and DETs co-regulated by LD and in S42-IL107. Cluster sizes and co-expressed flowering time genes are indicated above the co-expression plots. Expression levels for individual transcripts (light colors) and mean expression level across all transcripts within each cluster (bright color) were plotted. Co-expression plots depict transcript expression patterns in leaves (green) and apices (orange) as mean centered and scaled transcript levels (Z-Score).

Photosynthesis and light response related Gene Ontology (GO) terms were over-represented among leaf expressed transcripts in cluster I (Fig. 10A). Apex specific transcripts in cluster III were enriched for genes related to the regulation of the cell cycle, meristem and flower development (Fig. 10C). In all three clusters, we identified an overrepresentation of transcripts related to various transport processes (see also Fig. 10B).

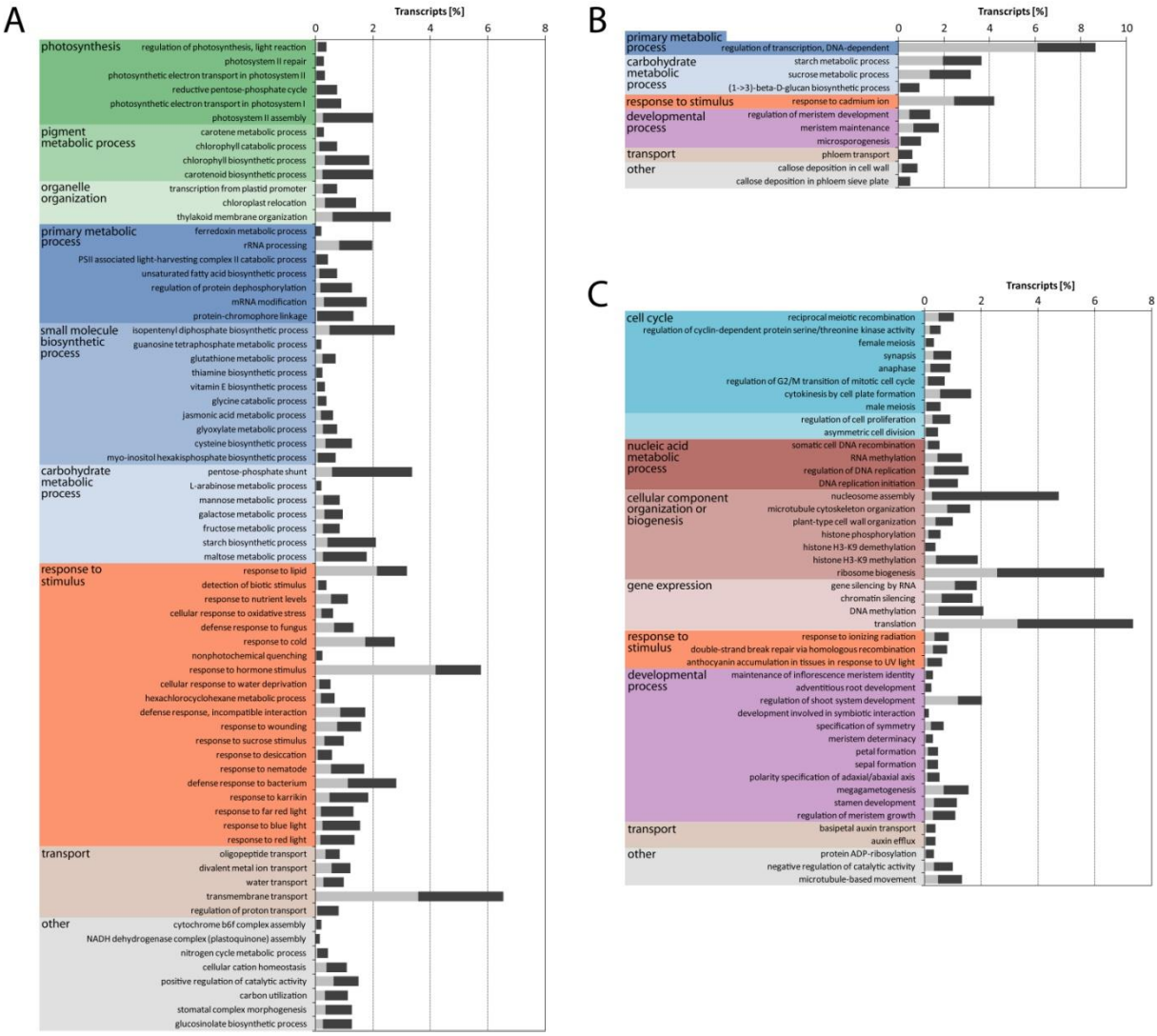

Figure 10: Overrepresentation of Gene Ontology terms among transcripts in higher level Co-expression Clusters I-III
Overrepresentation analysis of Gene Ontology terms assigned to biological processes for transcripts co-expressed within **(A)** cluster I, **(B)** cluster II and **(C)** cluster III. Clusters are representative for transcripts predominantly expressed in leaves (cluster I), shoot apices (cluster III) or equally expressed in both tissues (cluster II). Significant (FDR<0.05) leaf nodes of the GO-tree were summarized to common parental GO-terms. Bars indicate the relative abundance of transcripts assigned to the GO-terms in the test set (dark grey) and the reference set (light grey), respectively.

2.2.2 Genes differentially expressed during MSA development are involved in cell cycle control, carbohydrate metabolism, transport and meristem development

Of the 6602 DETs identified in apices, 4097 transcripts showed an up-regulation and 2183 a down-regulation during either the vegetative (W0.5-2.0) or early reproductive (W2.0-3.5) phase (Fig. 8B). 322 transcripts presented an expression pattern distinct from a consistent up- or down-regulation during early or later stages of MSA development. Among DETs regulated during MSA development, the majority of 3299 DETs were specifically induced and 1539 DETs repressed at stamen primordium stage (W2.0-3.5) and were not differentially regulated during floral transition (W0.5-W2.0).

Gene ontology (GO) term enrichment analysis revealed that transcripts involved in various metabolic processes, responses to endogenous and exogenous stimuli, developmental and transport processes were over-represented among the 4097 up-regulated transcripts (Fig. 8A). In addition, overrepresentation of photosynthesis and light response related genes was detected in the set of 3299 DETs specifically up-regulated in shoot apices at stamen primordium stage but not among DETs during floral transition (Fig. 8B, Suppl. Tab. S3 and S4). Accordingly, greening of the inflorescence was more advanced at stamen primordium stage than at double ridge stage (Fig. 4A). Whereas unsupervised clustering of all gene expression data clearly separated apex and leaf derived expression data sets (Suppl. Fig. S4C), data sets of shoot apices at the stamen primordium stage clustered at an intermediate position between leaf samples and samples of early stages of MSA development. Thus, gene expression in shoot apices at stamen primordium stage partially resembled gene expression in leaf organs.

GO-terms assigned to the regulation of the cell cycle, nucleosome assembly and histone modifications were overrepresented among the 2183 DETs down-regulated during MSA development (Fig. 8C).

Because we were interested in identifying genes causative for primary developmental changes in meristematic cells of the shoot apex throughout all tested stages of MSA development, we focused our further analyses on a core set of 1434 DETs (Fig. 8B). Transcripts in this core set were differentially regulated in the MSA during the vegetative (W0.5-2.0) and during the early reproductive (W2.0-3.5) phase. By this means we mainly excluded DETs specifically detected at stamen primordium stage, e.g. photosynthesis related transcripts, and with generally low expression levels in MSA samples as compared to leaf samples. Within the remaining core set, 650 transcripts were gradually up-regulated and 464 transcripts gradually down-regulated, while 320 DETs presented an expression pattern distinct from a consistent up- or down-regulation during MSA development (Fig. 8B). GO-enrichment analysis among the 1434 DETs highlighted genes involved in the regulation of meristem development, maintenance of inflorescence and floral meristem identity and floral meristem determinacy (Suppl. Tab. S5).

In the following, we will present a selection of identified DETs, which are either regulated during development at the shoot apex independent of the photoperiod and genotype or are expressed in a genotype and photoperiod dependent manner in leaves and apices.

2.2.3 Developmental stage specific expression *SVP*-like and homeotic genes at the shoot apex

Within the core set of 1434 DETs regulated during MSA development, 564 DETs were differentially regulated during development independent of the genotype and photoperiod (Fig. 8D). Of these, 245 DETs, represented by seven co-expression clusters (Suppl. Tab. S6), were gradually up-regulated and 154 DETs, represented by four co-expression clusters (Suppl. Tab. S7), consistently down-regulated during MSA development. 165 DETs presented developmental stage specific expression patterns distinct from gradual induction or repression during MSA development.

Table 1: Selected* transcripts up-regulated during MSA development

Transcript	Reference Set[1]	Co-expression Cluster	Barley Gene Idenifier	Arabidopsis Gene Model[2]	Arabidopsis Gene Idenifier	Description[3]
Flowering, floral organ and meristem development						
Hv.32986	Hv	16	*HvSOC1-1*	AT2G45660.1	*AtSOC1*	Supressor of overexpression of CONSTANS
Hv.12878	Hv	16	*HvKN1*	AT4G08150.1	*AtBP1*	Brevipedicellus 1
Hv.20746	Hv	16	*HvAG1*	AT4G18960.1	*AtAG*	Agamous
Hv.11508	Hv	16		AT2G41370.1	*AtBOP2*	Blade on Petiole 2
Hv.16012	Hv	16		AT3G61880.2	*AtCYP78A9*	Cytochrome P450 78A9
Hv.28414	Hv	16		AT1G53160.1	*AtSPL4*	Squamosa promoter binding protein-like 4
MLOC_13032.1	sHC	16				
MLOC_65676.1	sHC	16		AT5G59810.1	*AtSBT5.4*	Serine-type endopeptidase activity
Hv.36753	Hv	11		AT4G29100.1	*AtEPFL6*	EPF1-like 6
Hv.11726	Hv	13		AT2G27230.2	*AtLHW*	Lonesome highway
Hv.8895	Hv	17		AT5G62100.2	*AtBAG2*	BCL2-associated athanogene 2
Hv.32892	Hv	18		AT4G29900.1	*AtACA10*	Autoinhibited Ca(2+)-ATPase 10
MLOC_70653.1	sHC	24		AT4G00180.1	*AtYAB3*	Yabby 3
Homones and signalling						
Hv.2397	Hv	16		AT1G17290.1	*AtALAAT1*	Alanine aminotransferase
Hv.32781	Hv	16		AT4G11530.1	*AtCRK34*	Cysteine-rich RLK (receptor-like protein kinase) 34
Hv.15702	Hv	11		AT4G30960.1	*AtCIPK6*	CBL-interacting protein kinase 6
Hv.31377	Hv	14		AT1G48480.1	*AtRKL1*	Receptor-like kinase 1
Hv.32577	Hv	17		AT3G45860.1	*AtCRK4*	Cystein-rich RLK (receptor-like protein kinase) 4
Hv.32275	Hv	18		AT1G05010.1	*AtEFE*	Ethylene forming enzyme
Carbohydrate metabolism						
contig_35924	DNC-T	24		AT1G11720.2	*AtSS3*	Starch synthase 3
Hv.8649	Hv	24		AT2G15480.2	*AtUGT73B5*	UDP-glucosyl transferase 73B5
Hv.10624	Hv	16		AT5G13170.1	*AtSWEET15*	Senescence-associated gene 29
Others						
MLOC_36809.2	sHC	18		AT1G06490.1	*AtCALS7*	Callose synthase 7
MLOC_50471.2	sLC	18		AT3G59100.1	*AtGSL11*	Glucan synthase-like 11

*Transcripts represent the epxression profiles of 245 DETs up-regulated during MSA development indpendent of the photoperiod and genotype

[1]Set of reference transcripts:

[2]Arabidopsis gene model (Best BLASTx hit)

[3]Annotation of Arabidopsis gene model (TAIR 10)

Among the up-regulated genes we the homeotic genes *HvAG1* (*AGAMOUS-LIKE 1;* Hv.20746), *HvKN1* (*KNOTTED 1*; Hv.12878) and MLOC_13032.1, homologous to the flowering time related transcription factor *AtSPL4* (*SQUAMOSA-PROMOTER BINDING PROTEIN-LIKE 4)* in *Arabidopsis* (Table 1). These genes were induced in shoot apices upon induction of the first spikelet primordia independent of the genotype and photoperiod (Fig. 11A). Furthermore, these homeotic genes were co-expressed with *HvSOC1-1*, a barley ortholog of the floral integrator gene *AtSOC1* in *Arabidopsis* (Table 1, Fig. 9B, cluster 16). However, induction of *HvSOC1-1* at W2.0 was dependent on the photoperiod (Fig. 11A), which could be confirmed by qRT-PCR in shoot apex enriched samples of three independent sets of *Ppd-H1* introgression lines and their recurrent parents (Fig. 12B, Suppl. Fig. S2B+D).

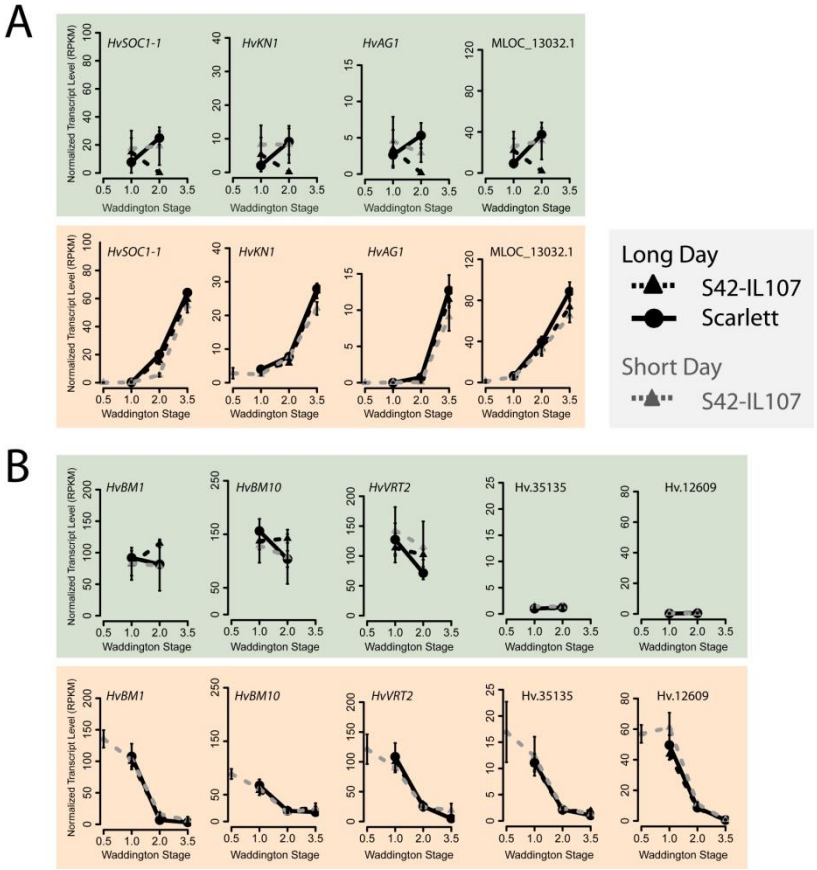

Figure 11: Transcripts expressed in a developmental stage dependent manner at the MSA
RNA-sequencing derived expression data of selected transcripts **(A)** up- or **(B)** down-regulated throughout MSA development in a developmental stage dependent manner. Transcript expression is presented for leaf (green) and shoot apex tissue (orange). Normalized expression values are reported in reads per kilo base per million (RPKM). Error bars indicate standard deviation across two to three independent RNA samples.

Among the 154 transcripts, down-regulated during MSA development we identified genes with high expression levels at the vegetative stage and a strong down-regulation upon floral transition (W2.0) (Table 2). Among those, we identified Hv.35135 and Hv.12609 as only regulated in the MSA and not detected in the leaf. Hv.35135 and Hv.12609 are homologous to *AtVRN1* (REDUCED *VERNALIZATION RESPONSE 1*) and *AtAP2* (*APETALA 2*), respectively known regulators of floral transition and flower development in *Arabidopsis* (Table 2, Fig. 9B, Fig. 11B, cluster 30) (Levy *et al.* 2002, Hong *et al.* 2010). In addition, we identified a similar expression of three MADS box transcription factors *HvVRT2*, *HvBM1* and *HvBM10*, homologous to *AtSVP* (*SHORT VEGETATIVE PHASE*) in *Arabidopsis* with high expression levels in leaves and apices (Table 2, Fig. 9B, cluster 21).

Table 2: Selected* transcripts down-regulated during MSA development

Transcript	Reference Set[1]	Co-expression Cluster	Barley Gene Idenifier	Arabidopsis Gene Model[2]	Arabidopsis Gene Idenifier	Description[3]
Flowering, floral organ and meristem development						
Hv.110	Hv	21	*HvBM1*	AT2G22540.1	*AtSVP*	Short vegetative phase
Hv.19680	Hv	21	*HvBM10*			
Hv.8782	Hv	21		AT2G30140.1	*AtUGT87A2*	UDP-Glucosyl transferase 87A2
MLOC_14596.3	sHC	29		AT1G68640.1	*AtPAN*	Perianthia
contig_10845	DNC-T	29		AT3G26120.1	*AtTEL1*	Terminal EAR1-like 1
MLOC_51836.1	sLC	29				
MLOC_56117.1	sHC	29		AT1G10120.1	*AtCIB4*	CRY2-interacting bHLH 4
Hv.35135	Hv	30		AT4G36920.2	*AtAP2*	Apetala 2
contig_22204	DNC-T	30		AT4G33280.1		AP2/B3-like transcriptional factor family protein
Hv.12609	Hv	30		AT3G18990.1	*AtVRN1*	Reduced vernalization response 1
contig_3763	DNC-T	30		AT3G23290.2	*AtLSH4*	Light sensitive hypocotyls 4
MLOC_10221.2	sHC	31		AT4G37750.1	*AtANT*	Aintegumenta
Hormones and signalling						
MLOC_52145.1	sHC	21		AT2G41510.1	*AtCKX1*	Cytokinin oxidase/dehydrogenase 1
Hv.31348	Hv	29		AT3G16500.1	*AtPAP1*	Phytochrome-associated protein 1
Hv.33734	Hv	30		AT4G35390.1	*AtAGF1*	At-hook protein of GA feedback 1
Others						
Hv.12175	Hv	29		AT3G04290.1	*AtLTL1*	Li-tolerant lipase 1
MLOC_44910.1	sHC	29		AT2G39760.1	*AtBPM3*	BTB/POZ/MATH-domains containing protein
MLOC_14316.1	sHC	29		AT4G09510.2	*AtCINV2*	Cytosolic invertase 2
contig_4243	DNC-T	30		AT1G15910.1	*AtFDM1*	Factor of DNA methylation 1
MLOC_68447.1	sLC	30		AT5G24280.1	*AtGMI1*	Gamma-irradiation and mitomycin c induced 1

*Transcripts represent the epxression profiles of 154 DETs down-regulated during MSA development indpendent of the photoperiod and genotype

[1]Set of reference transcripts:
Hv: NCBI Barley UniGenes; sHC: selected Barley High Confidence Genes; sLC: selected Barley Low Confidence Genes; DNC-T: selected *de novo* contigs

[2]Arabidopsis gene model (Best BLASTx hit)

[3]Annotation of Arabidopsis gene model (TAIR 10)

Starting from high transcript levels in vegetative shoot apices, all three *SVP*-like genes were gradually down-regulated during MSA development (Fig. 11B). *HvBM1* was completely down-regulated after floral transition coinciding with the induction of the first spikelet primordia at the shoot apex (W2.0). Reduction of *HvBM10* and *HvVRT2* transcript levels was less pronounced and complete repression of *HvVRT2* occurred at stamen primordium stage (W3.5). We independently confirmed the down-regulation of the three *SVP*-like genes during MSA development by qRT-PCR (Fig. 12B, Suppl. Fig. S2B+D). However, we did not detect a complete repression of these genes, as samples for qRT-PCR verification were only enriched for apex tissue and also comprised vegetative tissues of young leaf

primordia with presumably high transcript levels of these genes. Similarly, the photoperiod independent repression of these genes was not as clear in the apex enriched samples (qRT-PCR) as compared to the pure apex samples (RNA-sequencing).

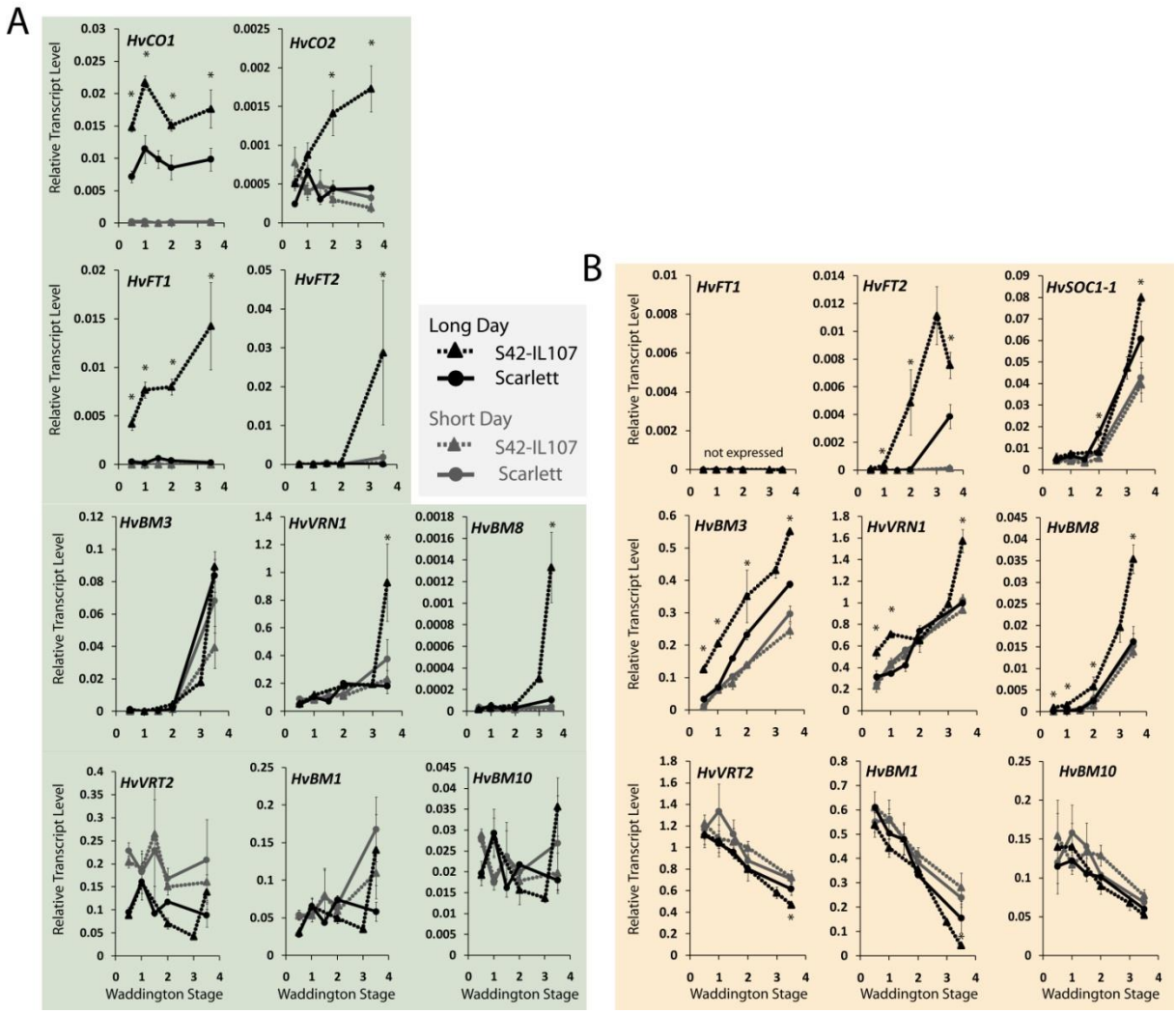

Figure 12: Validation of transcript levels in leaves and shoot apices of Scarlett and S42-IL107
Quantification of transcript levels by quantitative real time PCR (qRT-PCR) in **(A)** leaf samples and **(B)** samples enriched for shoot apex tissue at different stages of plant development. Transcript levels are demonstrated relative to the transcript abundance of *HvActin*. Error bars indicate the standard deviation over three biological replicates. Asterisks highlight significant differences ($p<0.05$) between transcript levels of S42-IL107 and Scarlett of plants at the same developmental stage grown under long photoperiods.

In summary, our analysis showed that transcripts differentially expressed at the MSA during development were enriched for genes with roles in cell cycle, carbon metabolism, transport, meristem and organ identity and development. In particular, we identified transcripts which were differentially expressed between vegetative and reproductive shoot apices independent of the photoperiod and *Ppd-H1* and thus represent valuable marker genes for the staging of the barley development.

2.2.4 Characterization of genes in leaves and at the MSA as candidates downstream of *Ppd-H1*

Allelic variation for *Ppd-H1* had strong effects on reproductive development in response to long photoperiods (Fig. 4, Fig. 5). We therefore aimed at identifying expression differences in leaves and shoot apices caused by genetic variation at *Ppd-H1*. In order to confirm the genetic effect of *Ppd-H1* on gene expression, selected candidate genes were tested in three pairs of spring barley genotypes with a mutated *ppd-H1* allele and derived lines with introgressions of the dominant *Ppd-H1* allele (Fig. 12, Suppl. Fig. S2).

2.2.4.1 *HvCO1*, *HvCO2* and *HvFT1* are co-expressed in leaves with genes related to nutrient transport and flower fertility

In leaves, we identified 1427 transcripts co-regulated between photoperiods and between genotypes at the time of floral transition (Fig. 8D), the majority of which was down-regulated under LDs and in the presence of the dominant *Ppd-H1* allele (1205 DETs), suggesting that *Ppd-H1* predominantly acts as a repressor in the leaf. GO enrichment among the down-regulated genes highlighted biological processes related to the regulation of transcription, plant growth and developmental processes (Suppl. Tab. S8).

The expression profiles of 193 transcripts up-regulated in leaves in a *Ppd-H1* dependent manner (Suppl. Tab. S9) primarily contained transcripts with high expression levels in leaves and low or no expression at the MSA (Fig. 9B, cluster 8, 9 and 11, Suppl. Fig. S1). Among those, we identified *HvCO1*, *HvFT1* (cluster 9) and *HvCO2* (cluster 11), previously described as putative downstream targets of *Ppd-H1* in barley (Turner *et al.* 2005, Faure *et al.* 2007, Campoli *et al.* 2012b). In qRT-PCR assays, the *HvFT1* expression levels in all three tested spring barley genotypes were close to the detection limit, while the presence of the photoperiod responsive *Ppd-H1* allele caused at least a ten-fold increase in H*vFT1* expression levels in leaves of the introgression lines as compared to the spring barley reference genotypes at any stage of development (Fig. 12A, Fig. 13A, Suppl. Fig. S2A+C). Interestingly, variation in *HvFT1* expression levels among spring barley genotypes correlated well with variation in MSA development, i.e. Triumph with the lowest *HvFT1* expression levels showed the strongest delay in MSA development. Similarly, transcript levels of *HvCO1* were increased under LDs in the introgression lines at the time of floral transition, but dropped in BW281 and Triumph-IL at W2.0 to the expression levels of their recurrent parents (Fig. 12A, Suppl. Fig. S2A+C). Transcript levels of *HvCO2* were 7-20 times lower than for *HvCO1*, but also up-regulated in the introgression lines grown under LDs. In contrast to *HvCO1*, *HvCO2* expression in leaves of the spring barley genotypes remained low independent of the photoperiod.

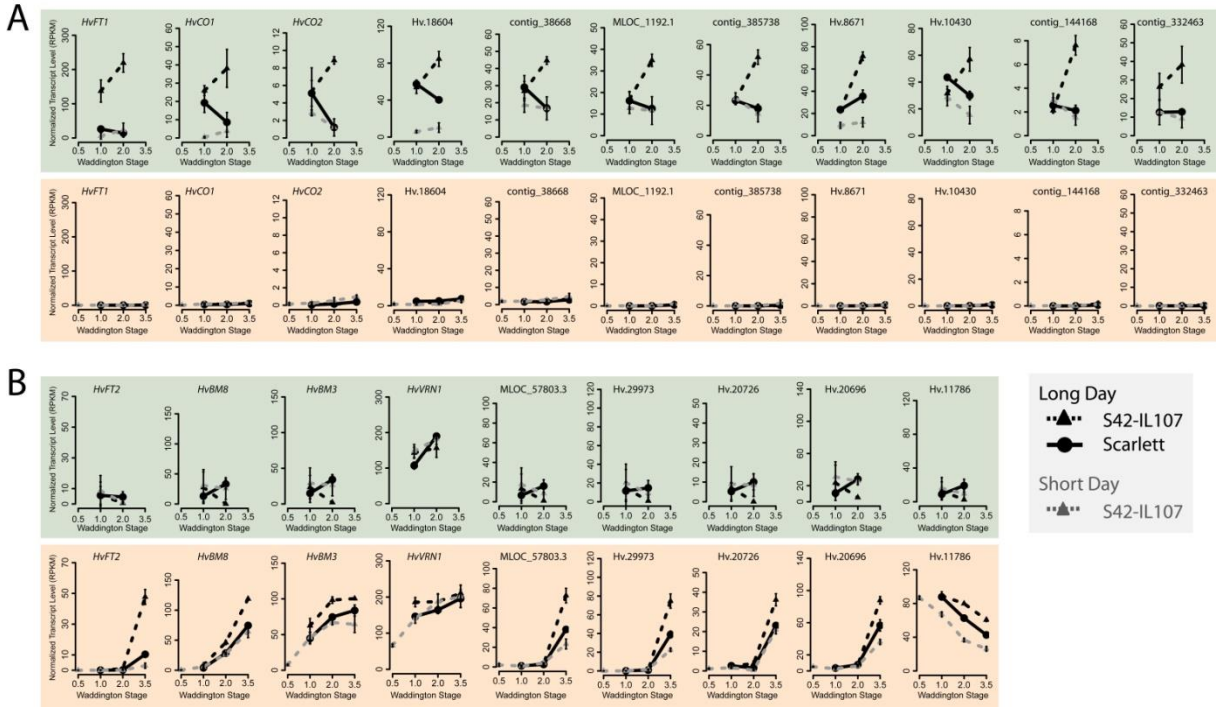

Figure 13: Expression of transcripts representing candidate genes down-stream of *Ppd-H1* in leaves and shoot apices
RNA-sequencing derived expression data of selected transcripts up-regulated in a *Ppd-H1* dependent manner in **(A)** leaves and **(B)** shoot apices. Transcript expression is presented for leaf (green) and shoot apex tissue (orange). Normalized expression values are reported in reads per kilo base per million (RPKM). Error bars indicate standard deviation across two to three independent RNA samples.

HvCO1, *HvCO2* and *HvFT1* were co-expressed with genes involved in the regulation of flowering time, disease resistance, nutrient transport and floral organ development (Table 3, Fig. 13A). Among those, we identified contig_38668, representing a barley gene homologous to the *Arabidopsis AtSPA4* (*SUPPRESSOR OF PHYA-105 1 RELATED 4*) gene, which is involved in the photoperiod dependent regulation of flowering time in *Arabidopsis* (Laubinger *et al.* 2006). Interestingly, the transcript Hv.18604, as another *CCT/B-box zinc finger* domain containing gene besides *HvCO1* and *HvCO2*, showed a *Ppd-H1* and LD dependent up-regulation in leaves upon floral transition.

Among genes involved in disease resistance, we identified the transcripts MLOC_1192.1 and contig_385738, homologous to the innate immunity receptors *AtRPM1* (*RESISTANCE TO P. SYRINGAE PV MACULICOLA 1*) and *AtFLS2* (*FLAGELLIN-SENSITIVE 2*) of *Arabidopsis*. *AtFLS2* has been linked to signaling cascades important for stem cell maintenance of the shoot apical meristem, and thus to the regulation of plant development, in addition to its function in plant defense responses (Lee *et al.* 2011). In addition, Hv.8671 and Hv.10430, encoding genes homologous to the *YELLOW STRIPE LIKE* gene *AtYSL3* and the sugar transporter *AtPMT1* (*POLYOL/MONOSACCHARIDE TRANSPORTER 1*) in *Arabidopsis*, respectively, were co-expressed with *HvCO1* and *HvFT1*. *YSL*-genes encode for metal-phytosiderophore transporters and a role has been proposed for *AtYSL3* in ensuring flower fertility (Chu *et al.* 2010). Similarly, transcripts for contig_144168 and contig_332463, homologous to the *Arabidopsis AtROXY1* and *AtMS2* (*MALE STERILITY 2*) genes, were co-regulated with *HvCO2*. In

Arabidopsis, both genes have been linked to pollen and anther development, respectively (Murmu *et al.* 2010, Chen *et al.* 2011).

Table 3: Selected* transcripts up-regulated in a *Ppd-H1* dependent manner in leaves

Transcript	Reference Set[1]	Co-expression Cluster	Barley Gene Idenifier	Arabidopsis Gene Model[2]	Arabidopsis Gene Idenifier	Description[3]
Flowering, light response						
Hv.34809	Hv	9	*HvFT1*	AT1G65480.1	*AtFT*	Flowering locus T
MLOC_6921.1	sHC	9	*HvCO1*	AT5G15850.1	*AtCOL1*	CONSTANS-like 1
Hv.29120	Hv	9		AT4G38180.1	*AtFRS5*	FAR1-related sequence 5
Hv.37168	Hv	9		AT3G04030.3	*AtMYR2*	Homeodomain-like superfamily protein
MLOC_75496.6	sHC	11	*HvCO2*	AT3G02380.1	*AtCOL2*	CONSTANS-like 2
Hv.18604	Hv	11		AT5G48250.1	*AtBBX8*	B-box type zinc finger protein with CCT domain
MLOC_51314.1	sHC	11		AT3G07500.1		Far-red impaired responsive (FAR1) family protein
contig_38668	DNC-T	11		AT1G53090.2	*AtSPA4*	SPA1-related 4
Disease resistance						
Hv.10174	Hv	9		AT5G20480.1	*AtEFR*	EF-TU receptor
MLOC_66826.2	sLC	9				
Hv.10217	Hv	9		AT2G34930.1		Disease resistance family protein / LRR family protein
Hv.30969	Hv	9		AT2G37710.1	*AtRLK*	Receptor lectin kinase
MLOC_66610.1	sHC	9		AT3G14460.1		LRR and NB-ARC domains containing disease resistance protein
contig_388521	DNC-T	9				
MLOC_1192.1	sHC	9		AT3G07040.1	*AtRPM1*	Resistance to *P. syringae* pv. *maculicola 1*
MLOC_14723.1	sLC	9		AT3G46730.1		NB-ARC domain-containing disease resistance protein
contig_385738	DNC-T	9		AT5G46330.1	*AtFLS2*	Flagellin-sensitive 2
contig_385733	DNC-T	9		AT1G47890.1	*AtRLP7*	Receptor like protein 7
Transport						
Hv.8671	Hv	9	*HvYS1*	AT5G53550.2	*AtYSL3*	YELLOW STRIPE-like 3
Hv.35529	Hv	9		AT1G05300.1	*AtZIP5*	Zinc transporter 5 precursor
Hv.10430	Hv	9		AT2G16120.1	*AtPMT1*	Polyol/monosaccharide transporter 1
MLOC_10758.2	sHC	9		AT4G13420.1	*AtHAK5*	High affinity K+ transporter 5
Hv.22725	Hv	11		AT1G15520.1	*AtPDR12*	Pleiotropic drug resistance 12
Hv.27044	Hv	11		AT1G64890.1		Major facilitator superfamily protein
Hv.19083	Hv	11		AT2G38410.1		ENTH/VHS/GAT family protein
Cell differentiation, floral organ development						
Hv.34198	Hv	9		AT1G54510.3	*AtNEK1*	NIMA-related serine/threonine kinase 1
contig_144168	DNC-T	9		AT3G11980.1	*AtMS2*	Male sterility 2
contig_332463	DNC-T	9		AT3G02000.1	*AtROXY1*	Thioredoxin superfamily protein
MLOC_6537.1	sHC	11		AT5G49660.1	*AtXIP1*	Xylem intermixed with phloem 1
MLOC_43403.1	sHC	11		AT2G03140.2		Alpha/beta-Hydrolases superfamily protein

*Transcripts represent the epxression profiles of 193 DETs up-regulated in a *Ppd-H1* dependent manner in leaves

[1]Set of reference transcripts:
Hv: NCBI Barley UniGenes; sHC: selected Barley High Confidence Genes; sLC: selected Barley Low Confidence Genes; DNC-T: selected *de novo* contigs

[2]Arabidopsis gene model (Best BLASTx hit)

[3]Annotation of Arabidopsis gene model (TAIR 10)

2.2.4.2 *HvFT2* is co-expressed with floral homeotic genes at the shoot apex

In the MSA, an intersection of 518 DETs were co-regulated between photoperiods and between the genotypes Scarlett and S42-IL107 (Fig. 8D). 266 DETs were up-regulated in a *Ppd-H1* dependent manner at the shoot apex and comprised genes involved in the regulation floral organ development, hormone synthesis and signaling, nutrient and carbohydrate metabolism, disease resistance, cell cycle regulation and nucleosome assembly (Table 4).

Interestingly, we identified *HvFT2*, a member of the barley *FLOWERING LOCUS T-LIKE* gene family, among the up-regulated DETs. qRT-PCR assays revealed that transcript levels of *HvFT2* in leaves were

Table 4: Selected* transcripts up-regulated in a *Ppd-H1* dependent manner in shoot apices

Transcript	Reference Set[1]	Co-expression Cluster	Barley Gene Idenifier	Arabidopsis Gene Model[2]	Arabidopsis Gene Idenifier	Description[3]
Flowering, floral organ and meristem development						
Hv.17528	Hv	16	*HvFT2*	AT1G65480.1	*AtFT*	Flowering locus T
Hv.169	Hv	16	*HvBM8*	AT1G69120.1	*AtAP1*	Apetala 1
Hv.4298	Hv	24	*HvBM3*			
Hv.6358	Hv	14		AT5G24860.1	*AtFPF1*	Arabidopsis flowering promoting factor 1
MLOC_44160.1	sHC	29	*HvCEN*	AT2G27550.1	*AtATC*	Centroradialis
Hv.20726	Hv	16		AT3G54340.1	*AtAP3*	Apetala 3
MLOC_57803.3	sLC	16		AT5G15800.1/2	*AtSEP1*	Sepallata 1
Hv.26912	Hv	24				
Hv.29973	Hv	16		AT1G24260.1	*AtSEP3*	Sepallata 3
Hv.20696	Hv	16		AT5G20240.1	*AtPI*	Pistillata
Hv.15352	Hv	16		AT5G65700.2	*AtBAM1*	Barely any meristem 1
MLOC_68900.1	sHC	16		AT2G26170.1	*AtMAX1*	More axillary branches 1
Hv.12185	Hv	16		AT1G69780.1	*AtHB13*	Homeobox-leucine zipper protein family
Hv.18425	Hv	11		AT2G46680.1	*AtHB7*	Homeobox domain 7
Hv.15611	Hv	15		AT2G38090.1		Dublicated homeodomain-like superfamily protein
Hormones and signalling						
Hv.21105	Hv	10	*HvGA20ox1*	AT4G25420.1	*AtGA20ox1*	Gibberellin 20-oxidase 1
Hv.23094	Hv	21		AT3G19000.1		2-oxoglutarate and Fe(II)-dependent oxygenase superfamily protein
Hv.11504	Hv	23		AT2G39540.1		Gibberellin-regulated family protein
Hv.17614	Hv	23		AT4G30610.1	*AtBRS1*	BRI1 supressor 1
Hv.3674	Hv	27		AT1G61870.1	*AtPPR336*	Pentatricopeptide repeat 336
Metabolism						
Hv.15994	Hv	14		AT1G09610.1	*AtGXM3*	Glucuronoxylan methyltransferase 3
Hv.10982	Hv	14		AT1G08650.1	*AtPPCK1*	Phosphoenolpyruvate carboxylase kinase 1
Hv.18832	Hv	14		AT2G01770.1	*AtVIT1*	Vacuolar iron transporter 1
Hv.15635	Hv	16		AT3G48360.1	*AtBT2*	BTB and TAZ domain protein 2
MLOC_62899.1	sLC	16		AT2G18950.1	*AtHPT1*	Homogentisate phytyltransferase 1
Hv.354	Hv	16		AT1G21680.1		DPP6 N-terminal domain-like protein
Hv.15809	Hv	16		AT1G22440.1		Zinc-binding alcohol dehydrogenase family protein
contig_287828	DNC-T	16		AT3G26380.1		Melibiase family protein
Hv.9784	Hv	16				
Hv.4237	Hv	21		AT4G34230.1	*AtCAD5*	Cinnamyl alcohol dehydrogenase 5
Hv.8796	Hv	21		AT1G19600.1		pfkB-like carbohydrate kinase family protein
MLOC_74713.2	sHC	21				
Hv.24746	Hv	22		AT1G62640.2	*AtKASIII*	3-ketoacyl-acyl carrier protein synthase III
Hv.3916	Hv	22		AT1G30120.1		Pyruvate dehydrogenase E1 beta
Hv.6110	Hv	22		AT1G63000.1	*AtUER1*	Nucleotide-rhamnose synthase/epimerase-reductase
Hv.16152	Hv	23		AT3G23510.1		Cyclopropane-fatty-acyl-phospholipid synthase
Hv.20490	Hv	23		AT1G19715.3		Mannose-binding lectin superfamily protein
MLOC_24654.2	sHC	23				
contig_63792	DNC-T	23				
Hv.12805	Hv	27		AT3G18080.1	*AtBGLU44*	B-S glucosidase 44
Disease resistance						
Hv.11447	Hv	16		AT3G50930.1	*AtBCS1*	Cytochrome BC1 synthesis
Hv.17743	Hv	16		AT1G19250.1	*AtFMO1*	Flavin-dependent monooxygenase 1
contig_125109	DNC-T	16		AT5G25930.1		LRR receptor-like protein kinase family protein
contig_80125	DNC-T	16				
Hv.10484	Hv	23		AT3G22400.1	*AtLOX5*	Lipoxygenase 5
Chromatin modification, nucleosome assembly						
Hv.11786	Hv	31		AT5G58230.1	*AtMSI1*	Multicopy supressor of IRA1
MLOC_71372.1	sHC	31		AT2G31270.1	*AtCDT1*	Homolog of yeast CDT1 A
Hv.15834	Hv	31		AT5G02560.1	*AtHTA12*	Histone H2A 12
MLOC_43244.1	sHC	31				
Hv.29208	Hv	23				
Hv.32211	Hv	31		AT5G22880.1	*AtH2B*	Histone B2
Hv.32725	Hv	31				
MLOC_75262.1	sLC	31				
MLOC_6467.1	sLC	23				
Hv.24307	Hv	31		AT5G59870.1	*AtHTA6*	Histone H2A 6
Hv.26391	Hv	31				
Hv.31863	Hv	31				
MLOC_37489.1	sLC	31				
Hv.22959	Hv	31		AT5G59970.1		Histone superfamily protein
Hv.26322	Hv	31				
Hv.31856	Hv	31				
Hv.32004	Hv	31				
Hv.32904	Hv	31				
MLOC_9919.1	sLC	31				
Hv.26128	Hv	23				
Hv.34411	Hv	27				

*Transcripts represent the epxression profiles of 266 DETs up-regulated in a *Ppd-H1* dependent manner in shoot apices

[1]Set of reference transcripts:
Hv: NCBI Barley UniGenes; sHC: selected Barley High Confidence Genes; sLC: selected Barley Low Confidence Genes; DNC-T: selected *de novo* contigs

[2]Arabidopsis gene model (Best BLASTx hit)

[3]Annotation of Arabidopsis gene model (TAIR 10)

only detected under LDs and in the introgression lines carrying a dominant *Ppd-H1* allele, except for Triumph-IL (Fig. 12A, Suppl. Fig. S2A+C). *HvFT2* was induced in leaves at stamen primordium stage subsequent to the expression of *HvFT1*. Expression analysis in samples enriched for shoot apex tissue confirmed the *Ppd-H1* dependent induction of *HvFT2* at the shoot apex, already before floral transition (<W2.0) in S42-IL107 and BW281 and at lemma primordium stage (W3.0) in Triumph-IL (Fig. 12B, Suppl. Fig. S2B+D). Thus, the induction of *HvFT2* in shoot apices preceded its induction in leaf tissue. In contrast to *HvFT2* expression in leaves, *HvFT2* transcripts were also detected in the shoot apices of the recurrent spring barley genotypes Scarlett and Bowman under LDs, but at later stages and lower levels than in the respective introgression lines. Expression profiles for 266 DETs, up-regulated in a *Ppd-H1* dependent manner at the shoot apex, were represented by eight co-expression clusters (Suppl. Tab. S10). *HvFT2* was co-expressed with 209 other transcripts in cluster 16 (Fig. 9B, Suppl. Tab. S10). Among those we identified transcripts for MLOC_57803.1, Hv.29973, Hv.20696 and Hv.20726, representing barley genes homologous to the *Arabidopsis* floral homeotic genes *AtSEP1* (*SEPALLATA1*), *AtSEP3*, *AtPI* (*PISTILATA*), *AtAP3* (*APETALA 3*) (Fig. 13B).

In addition to transcripts co-regulated with *HvFT2*, we identified *HvBM3*, *HvVRN1* (*HvBM5a*) and *HvBM8,* three barley homologs of the *AtAP1/AtFUL* (*APETALA 1/ FRUITFUL*) gene family of MADS-box transcription factors in *Arabidopsis* (Schmitz *et al.* 2000, Trevaskis *et al.* 2007a), to be up-regulated during MSA development in a photoperiod and *Ppd-H1* dependent manner. In general, transcript levels of *HvVRN1*, *HvBM3* and *HvBM8* gradually increased in leaves and shoot apices during pre-anthesis development (Fig. 13B). However, their induction occurred at different developmental stages and their individual expression patterns were organ specific. In leaves, transcript levels for the *AP1-/FUL*-like genes were significantly lower compared to their expression in shoot apices (Fig. 12, Suppl. Fig. S2), while this effect was less pronounced for *HvVRN1*. *HvVRN1* presented the highest expression levels among the *AP1-/FUL*-like genes in leaves and shoot apices. Induction of *HvVRN1* expression at the MSA was already observed at W0.5 in all tested genotypes and photoperiods. Interestingly, as in the RNA-sequencing data, elevated *HvVRN1* transcript levels were detected under LDs in vegetative shoot apices of BW281 and S42-IL107 (Fig. 12B, Fig. 13B, Suppl. Fig. S2B). This *Ppd-H1* dependent induction of *HvVRN1* during the vegetative phase was specific for shoot apex tissue and was not detected in leaves.

At the MSA, *HvVRN1* expression preceded the induction of *HvBM3* at W1.0 under SDs, followed by the expression of *HvBM8* at W2.0. The expression of *HvBM3* was strongly up-regulated at the MSA (W0.5) and at later developmental stages in the leaves (W3.0) under LDs and in the presence of the dominant *Ppd-H1* allele in S42-IL107 and BW281 (Fig. 12, Suppl. Fig. S2). Likewise, induction of *HvBM8* in leaves and shoot apices during MSA development was more pronounced in genotypes carrying the dominant

Ppd-H1 allele in response to LDs. In leaves of the spring barley genotypes and of plants grown under SD conditions, *HvBM8* expression remained at a low level throughout MSA development.

Among 266 DETs, up-regulated in a *Ppd-H1* dependent manner at the MSA, transcripts in cluster 31 were generally down-regulated during MSA development (Fig. 9B). Transcripts in cluster 31 were attributed to reproductive development, cell cycle, nucleosome assembly and histone modifications, as revealed by GO-enrichment analysis (Suppl. Tab. S11). For example, Hv.11786, a barley homolog of *AtMSI1* (*MULTICOPY SUPPRESSOR OF IRA1*), which is associates to the polycomb repressive complex 2 (PRC2), was up-regulated in S42-IL107 under LDs, while its expression was generally down-regulated during MSA development (Fig. 13B).

In summary, we identified sets of 1427 and 518 transcripts possibly acting as candidate genes down-stream of *Ppd-H1* in leaves and apices, respectively. In leaves, we identified a co-expression of the known flowering time regulators *HvCO1*, *HvCO2* and *HvFT1* with genes involved in nutrient transport, e.g. a metal ion-phytosiderophore transporter of the *YSL*-gene family. In shoot apices, transcripts related to the regulation of floral organ development were regulated in a *Ppd-H1* dependent manner. Interestingly, *HvFT2* was identified as a candidate down-stream of *Ppd-H1* at the MSA and the timing of its induction at the shoot apex correlated well with inflorescence development, i.e. the earlier *HvFT2* was induced during MSA development the faster the main shoot inflorescence of the respective genotype developed (Fig. 5A+12B, Suppl. Fig. S2B+D).

In addition, we identified stage and tissue specific expression patterns for the three barley *AP1-/FUL*-like MADS-box transcription factors *HvBM3*, *HvVRN1* and *HvBM8*. The successive induction of these genes during MSA development and their *Ppd-H1* dependent regulation, point to specific roles for these genes in regulating different processes during early reproductive development.

Furthermore, we identified transcripts related to chromatin and nucleosome assembly among the 266 up-regulated transcripts as candidates downstream of *Ppd-H1* at the shoot apex. This is in accordance with the faster development and presumably with a faster cell proliferation in shoot apices of plants under LDs and in the presence of the photoperiod responsive *Ppd-H1* allele.

2.2.4.3 Expression of *HvFT2* in shoot apices links *HvFT1* expression in leaves with expression of MADS-box genes at the shoot apex

To estimate the level of co-regulation between transcripts in leaves and shoot apices, we correlated their qRT-PCR derived expression profiles obtained from the three *Ppd-H1* introgression lines and their recurrent parents during shoot apex development (Fig. 14). We also aimed at identifying marker genes which are associated with spikelet number, and therefore correlated gene expression with the number of induced spikelets at the MSA at each developmental stage. In accordance with co-expression results of the RNA-sequencing data, transcript levels of *HvCO1*, *HvCO2* and *HvFT1* were positively correlated ($r > 0.66$). Interestingly, we identified a positive correlation ($r > 0.62$) between *HvFT1* expression levels

in leaves and the transcript levels of *HvFT2* in shoot apices. *HvFT2* expression levels in shoot apices were further positively correlated with *HvSOC1-1*, *HvBM3* and *HvBM8*. *HvSOC1-1* presented the highest level of connectivity among transcripts expressed in shoot apices and transcripts expressed in leaves. Its expression levels were predominantly correlated to the expression of *AP1-/FUL-like* transcripts in leaves and at the shoot apex. Furthermore, expression of *HvSOC1-1*, *HvVRN1* and *HvBM3* were positively correlated with the number of spikelet primordia formed at the shoot apex throughout development, indicating their potential contribution to the regulation of spikelet primordia induction and further development of floral organs. Although spikelet primordia were induced under SD and LD conditions, fertile flowers and seeds were only produced under LDs, which coincided with the presence of *HvFT1* expression in the leaf and *HvFT2* expression in the apex.

In further agreement with the RNA-sequencing results, transcript levels of the *SVP*-like genes *HvBM1*, *HvBM10* and *HvVRT2* were positively correlated with each other in leaves ($r > 0.65$) and in shoot apices ($r > 0.52$), respectively. In shoot apices, expression of the *SVP*-like genes negatively correlated to the transcript levels of *HvVRN1* ($r < -0.48$).

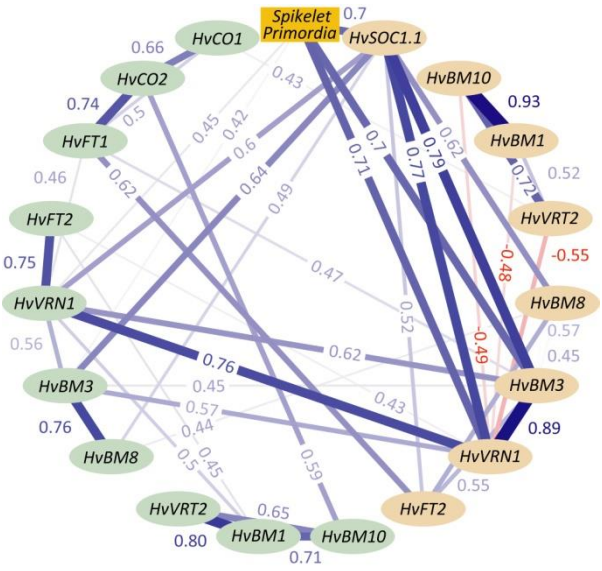

Figure 14: Correlation network for gene expression data in leaves and shoot apices
Correlation network between transcript level of flowering time genes in leaf and shoot apex samples and number of spikelet primordia emerged at the shoot apex during early stages of shoot apex development. Transcript abundance was determined by qRT-PCR in leaves (green ellipses) and shoot apex enriched tissue (orange ellipses) of Scarlett, Bowman, Triumph and their derived *Ppd-H*1 introgression lines (see also Fig. 12 and Suppl. Fig. S2). Lines connecting transcripts indicate positive correlations in blue and negative correlations in red. Only correlations with Pearson correlation coefficients R>|0.4| and FDR<0.05 were plotted.

In summary, the correlation network of qRT-PCR derived expression data of leaf and apex samples revealed that *HvFT2* possibly connects the *Ppd-H1* dependent induction of *HvFT1* in leaves with the *Ppd-H*1 dependent regulation of floral meristem identity genes such as *HvVRN1*, *HvBM3* and *HvBM8* at the shoot apex. Expression of *HvSOC1-1*, *HvVRN1* and *HvBM3* correlated positively with spikelet primordia induction, while *HvFT2* expression was in coincidence with spikelet maturation and flowering.

3 Discussion

Flowering time has a large impact on yield potential in crop plants because it 'fine-tunes' the life cycle to the target environment. The photoperiod dependent effect of *Ppd-H1* on flowering time and its adaptive value for the wide expansion of barley cultivation to diverse environments is well established (Laurie *et al.* 1994 and 1995, Jones *et al.* 2006). Here we report a more detailed analysis of the effect of allelic variation at *Ppd-H1* on individual phases of pre-anthesis development and gene expression changes in the leaf and MSA. Differences between the three tested introgression lines and their recurrent spring barley parents were only detected under LD but not under SD, indicating that the introgressed *Ppd-H1* alleles, rather than other genes within the introgressions, were causal for the observed morphological and molecular phenotypes.

3.1 Effect of the photoperiod and *Ppd-H1* on pre-anthesis development and yield component traits

3.1.1 Ppd-H1 accelerates all phases of pre-anthesis development

All phases of pre-anthesis development, but predominantly the late reproductive phase, were accelerated in the three introgression lines with the dominant *Ppd-H1* allele. This is in accordance with an increased photoperiod sensitivity of the stem elongation phase (e.g. Slafer and Rawson 1994) and with a recently reported QTL at *Ppd-H1* linked to both, the duration of the leaf and spikelet initiation phase and, more strongly, the stem elongation phase in the spring barley cross Steptoe x Morex (Borràs-Gelonch *et al.* 2012a). Interestingly, in wheat specific effects have been identified for the different homeologous copies of the *Ppd1* genes on the duration of individual pre-anthesis phases (Gonzalez *et al.* 2005, Borràs-Gelonch *et al.* 2012b). However, similar to *Ppd-H1* in barley, *Ppd-D1* was reported to affect both phases before and after the onset of stem elongation.

3.1.2 Duration of the early reproductive phase contributes to the yield potential in S42-IL107

In accordance with its effect on the duration of pre-anthesis development, variation at *Ppd-H1* affected the number of fertile spikelets per spike and seeds per spike at plant maturity. Both, the duration of spikelet initiation phase and spikelet growth during the stem elongation phase have been associated with yield potential (Kitchen and Rasmusson 1983). However, especially the pre-anthesis late reproductive phase of stem elongation has always been described as most important for yield because competition between spike and stem for limited assimilates during this phase causes the abortion of spikelet primordia (Gonzáles *et al.* 2003, Ghiglione *et al.* 2008, Gonzáles *et al.* 2011, Alqudah and

Schnurbusch 2014). Consequently, the duration of stem elongation has been associated with the number of fertile spikelets and final seeds (Miralles and Richards 2000, Gonzáles *et al.* 2003, Slafer 2003). In contrast to these findings, we show in the present study that the number of fertile spikelets and final seeds also corresponded to the number of spikelet primordia initiated before the beginning of stem elongation (W3.5) (Fig. 5C).

The introgression lines with a dominant *Ppd-H1* allele, and thus increased photoperiod response, exhibited a shorter vegetative and early reproductive phase under LD as compared to the recurrent spring barley genotypes Scarlett, Bowman and Triumph, while SD further delayed development in the genotypes independent of the *Ppd-H1* allele. Consequently, the number of spikelet primordia produced at onset of stem elongation was highest under SD in all genotypes, followed by the spring barley cultivars under LD and lowest in the introgression lines under LD. The relevance of the duration of the early reproductive phase for the final seed number was supported by results of the shift experiments, where Scarlett and S42-IL107 plants were transferred from SD to LD at different developmental stages to extent the duration of the vegetative and early reproductive phase. Shifting S42-IL107 and Scarlett plants from SD to LD during or at the end of the early reproductive phase (W2.25 and W3.5) resulted in the same number of fertile spikelets per spike between genotypes and an increased number of seeds per spike in S42-IL107 (Fig. 7F), although the late reproductive phase during stem elongation was shortened in S42-IL107 as compared to Scarlett, as indicated by the faster heading date of S42-IL107 after the transfer to LD (Fig. 6B). Thus, prolonging the vegetative and early reproductive phase independent of the duration of the late reproductive phase determined the number of fertile spikelets in S42-IL107 and was causative for the difference in final seed number observed between Scarlett and S42-IL107 when genotypes were constantly grown under LDs. This suggests that in contrast to recent studies, the duration of the vegetative and early reproductive phase might also contribute to determine the number of final seeds per spike, which in turn is associated with the number of grains/m^2 as the most important yield component in wheat grown under field conditions (e.g. Slafer and Andrade 1993, Slafer and Rawson 1994). However, the relevance of the spike initiation phase was supported by an earlier study by Kitchen and Rasmusson (1983) who showed that in barley the duration of spike initiation correlated well with leaf area, spikelet primordia number, and seed number.

3.1.3 Long photoperiods and the dominant *Ppd-H1* allele promote spikelet fertility and ensure main shoot survival

The number of fertile spikelets and seeds per spike were reduced in Scarlett as compared to S42-IL107, when both genotypes were grown under SD until the end of the early reproductive phase and subsequently transferred to LD. This indicates that a strong photoperiod response during the late

reproductive phase might be required for a fast maturation of the established spikelet primordia to ensure the production of fertile spikelets. Accordingly, the shift experiment also demonstrated that LD did not only accelerate floral transition and early reproductive development, but was also crucial for spikelet fertility in general. Scarlett and S42-IL107 grown under SD generated spikelet primordia, however, they failed to produce fertile spikelets and seeds. These were only produced when plants of both genotypes were moved to SD at or after reaching the stage W8.0, and thus just before heading (W9.0). Two recent studies have shown that application of Gibberellins (GA) under SD accelerated inflorescence development in wheat and barley, but both species failed to produce seeds under SD suggesting that in addition to GA a signal under LDs is necessary for spikelet fertility in these temperate crops (Pearce *et al.* 2013, Boden *et al.* 2014). Shading experiments in barley revealed that limitations in the supply of photoassimilates from vegetative organs to developing spikes during the stem elongation phase reduced spikelet fertility (Arisnabarreta and Miralles 2008a). Accordingly, the abortion of spikelet primordia of all genotypes grown under SD conditions and the abortion of the MSA at stages W4.0-6.0 suggests that LD might have maintained the nutrient supply or lead to a preferential distribution of assimilates to the MSA.

3.2 Transcriptional changes in leaves and shoot apices during pre-anthesis development dependent and independent of the photoperiod and *Ppd-H1*

By probing gene expression at the same developmental stage in the MSA and leaf under SD, and LD in two genotypes differing in photoperiod response, we aimed at identifying molecular changes important for the regulation of LD dependent and independent MSA development.

3.2.1 *HvFT*1 links LD and *Ppd-H1* dependent promotion of spikelet fertility to transcriptional changes in nutrient metabolic genes in leaves

In the leaf, *Ppd-H1* predominantly acted as a repressor since the majority of transcripts were down-regulated by the dominant *Ppd-H1* allele. The repressive effect of *Ppd-H1* thus corresponded to the role of the homologous pseudo response regulator genes in *Arabidopsis* which have been described as transcriptional repressors (Nakamichi *et al.* 2010). Similar to genes directly targeted by PRR7 in *Arabidopsis* (Liu *et al.* 2013), transcripts down-regulated by *Ppd-H1* in the leaves were assigned to biological processes involved in the regulation of transcription, plant growth and development.

However, we also observed the up-regulation of ca. 200 genes by *Ppd-H1* and these genes were specifically regulated in the leaf and not or little expressed in the MSA. The dominant *Ppd-H1* allele in all introgression lines caused a strong up-regulation of *HvFT1* in leaves already during the vegetative

phase and of its closest ortholog *HvFT2*, but after floral transition. Both genes encode barley orthologs of Flowering Locus T in *Arabidopsis*, which is transported as protein to the shoot apical meristem where it promotes the floral transition (Corbesier *et al.* 2007, Kikuchi *et al.* 2009). Turner *et al.* (2005) have already shown that natural variation at *Ppd-H1* affects flowering time under LDs by controlling the expression of *HvFT1* in the leaf of barley. Under LD, we also observed a *Ppd-H1* dependent up-regulation of *HvCO1* during the vegetative phase and *HvCO2* during the vegetative or reproductive phase, depending on the genotype. Both, *HvCO1* and *HvCO2*, represent the closest barley orthologs of *Arabidopsis* photoperiod response gene *CONSTANS* (Griffith *et al.* 2003). Contrastingly, previous studies in barley and wheat demonstrated that the dominant *Ppd-H1* allele in barley or increased expression of *Ppd-1a* in photoperiod insensitive wheat mutants did not lead to an increase, but rather to a decrease in the expression of CO-like genes (Campoli *et al.* 2012a, Shaw *et al.* 2013). However, Shaw *et al.* (2012) also reported that at very early developmental stages *Ppd-1a* caused an up-regulation of *TaCO1* expression, and suggested that *Ppd-1a* might specifically up-regulate *TaCO1* at early stages of development to induce *TaFT1*, which then at later stages, as a negative feedback, causes a down-regulation of *HvCO1*. This is in accordance with our results that *Ppd-H1* promotes an up-regulation of *HvCO1* at least until the end of the vegetative phase, while at later stages gene expression *HvCO1* expression levels might decrease, as seen for in Bowman/BW281 and Triumph/Triumph-IL (Fig. 12A, Suppl. Fig. S2A+C). Campoli *et al.* (2012a) have shown that *HvCO1* causes an up-regulation of *HvFT1* and promotes flowering time as in *Arabidopsis*. However, *Ppd-H1* was shown to control *HvFT1* expression also independently of *HvCO1* expression (Campoli *et al.* 2012a), suggesting that *Ppd-H1* controls *HvFT1* expression through up-regulating *HvCO1* at early stages of development and through unknown mechanism downstream of *HvCO1* expression throughout development.

HvCO1 and *HvCO2* were co-regulated with contig_38668, a transcript homologous to the *Arabidopsis AtSPA1-4* (*SUPPRESSOR OF PHYA-105 1 RELATED 4*) gene, which plays an important role in the photoperiod dependent degradation of CONSTANS protein in *Arabidopsis* (Laubinger *et al.* 2006). So far, we have very little information about the SPA gene family and their regulation in barley, however one likely ortholog has been identified from *Brachypodium* and rice, respectively (Higgins *et al.* 2010). Similar to the *Ppd-H1* and LD dependent induction of contig_38668 after the floral transition, transcript levels of *AtSPA1*, *3* and *4* were increased in adult *Arabidopsis* plants and up-regulated by light (Fittinghoff *et al.* 2006). This and the involvement of SPA genes in the regulation of responses to the photoperiod in *Arabidopsis* on the one hand, and the effect reported for SPA3 and SPA4 on elongation growth on the other hand (Laubinger *et al.* 2004), makes them interesting candidates to be studied in more detail in barley, especially since internode elongation was severely impaired in Scarlett and S42-IL107, as well as the other genotypes, under SD.

Interestingly, *HvFT1* was co-expressed with genes involved in the regulation of nutrient transport and floral organ development. These transcript included genes homologous to the sugar transporter *AtPMT1*, metal transporter *AtYSL3*, the Zinc transporter *AtZIP5* and the K+ transporter *AtHAK5*, suggesting that up-regulation of *HvFT1* was associated with an increase in nutrient and micronutrient transport. Relatively little is known about the role of nutrient and micronutrient availability on flowering time in model and crop plants. However, there is emerging evidence that carbohydrate availability and signaling play a crucial role in the regulation of vegetative and reproductive development (reviewed in Rolland *et al.* 2006), e.g. mutations in genes of key enzymes in sugar and starch metabolism such as *HEXOKINASE1* (*HXK1*) and *PHOSPHOGLUCOMUTASE1* (*PGM1*) affect various aspects of plant development, including flowering. A recent study has shown that *TREHALOSE-6-PHOSPHATE SYNTHASE 1* (*TPS1*), which catalyzes the formation of trehalose-6-phosphate (T6P) controls flowering time by up-regulating FT expression and has been suggested to function as a signaling molecule that relays information about carbohydrate availability to other signaling pathways (Wahl *et al.* 2013). In this context it is interesting to note that plants expressing *HvFT1* and nutrient transporters under LD developed fertile spikes, while under SD in the absence of *HvFT1* expression and low expression levels of transporter genes spikes stopped developing during stem elongation and became senescent. These transporter genes together with other genes, such as homologs of *Arabidopsis AtROXY1* and *AtMS2* (*MALE STERILITY 2*) co-expressed with *HvFT1*, have been associated with flower fertility in *Arabidopsis* (Chu *et al.* 2010, Murmu *et al.* 2010, Chen *et al.* 2011). Their up-regulation coincided with the improved spikelet fertility observed in plants under LD as compared to SD and in S42-IL107 with the dominant *Ppd-H1* allele as compared to Scarlett with reduced photoperiod sensitivity.

3.2.2 *HvFT2* expression acts downstream of the photoperiod pathway at the shoot apex to promote spikelet fertility

In the MSA, variation at *Ppd-H1* also controlled genes involved in the regulation of nutrient and carbohydrate metabolism and disease resistance as in the leaf and in addition to genes involved in floral organ development, hormone synthesis and signaling, cell cycle regulation and nucleosome assembly, suggesting that LD and *Ppd-H1* enhanced developmental reprogramming of the MSA.

Interestingly, *HvFT1* expression in the leaf was positively correlated with expression of *HvFT2* in the MSA, where it was expressed before floral transition in a photoperiod and *Ppd-H1* dependent manner. In accordance with this finding, the homologs of *FT2* in *Brachypodium* and wheat have recently been suggested to act downstream of *FT1*, as *FT1* and *FT2* expression levels were correlated in lines over-

expressing *FT1* under SD conditions or down-regulating *FT1* in RNAi lines (Lv et al. 2014). However, the finding, that *HvFT2* might act downstream of *HvFT1* at the shoot apex is novel to the temperate cereals. Two recent studies have shown that also in *Arabidopsis FT* is expressed in a photoperiod and CONSTANS independent manner in the inflorescences and siliques, where it is important for maintenance of inflorescence and floral meristem identity (Liu *et al.* 2014, Müller-Xing *et al.* 2014). Müller-Xing *et al.* (2014) have shown that this floral commitment requires Polycomb-group (Pc-G) proteins, which mediate epigenetic gene regulation. Pc-G proteins maintain the identity of inflorescence and floral meristems after floral induction by repressing Flowering Locus C and maintaining high levels of Flowering Locus T expression in inflorescences independently of the photoperiod (Müller-Xing *et al.* 2014). In contrast to *Arabidopsis*, *HvFT2* expression in the MSA was clearly dependent on LD and variation at *Ppd-H1* and was thus not environmental stable as in *Arabidopsis*. Barley plants shifted from LD to SD after floral transition (W2.0) produced additional leaves in our experiment. Those additional leaves were most likely derived from leaf primordia formed during the double ridge stage, which usually under inductive conditions remain as vestigial organs. A comparable phenotype of additional leaf like structures emerging from the base of the spike has also recently been reported in a Ppd1 loss of function mutant of wheat insensitive to inductive photoperiods (Shaw *et al.* 2013). Thus, the outgrowth of this leaves under non-inductive conditions or in plants insensitive to LD might thus be comparable to the floral reversion or reduced inflorescence identity observed in *Arabidopsis* Pc-G mutant lines and ft-10 mutants (Müller-Xing *et al.* 2014, Liu *et al.* 2014).

Interestingly, the transcript Hv.11786 homologous to *AtMSI1* in *Arabidopsis* was up-regulated by LD and in the introgression line S42-IL107 (Fig. 13B). In *Arabidopsis*, MSI1 protein associates with the polycomb repressive complex 2 (PRC2) and is important for photoperiodic control of flowering as it controls the expression of *AtCO*, *AtFT* and functions in the epigenetic regulation of *AtSOC1* (Bouveret *et al.* 2006, Steinbach and Henning 2014). Shift experiments showed that the transient exposure to LD caused a stable commitment to flowering in the wild type, but not in *msi1* mutant plants, suggesting that MSI1 plays a role in the epigenetic memory of inductive photoperiods and flower maintenance in the shoot apex. While in *Arabidopsis AtMSI1* has been placed upstream of the CO-FT pathway, our data suggested that expression of *AtMSI1* in the MSA of barley is controlled by photoperiod and presumably *HvFT1* as *AtMSI1* expression levels were increased by LD and in S42-IL107.

Since *HvFT2* expression correlated well with flower fertility, we were interested in identifying co-expressed genes. Genes co-regulated with *HvFT2* were homologous to the *Arabidopsis* floral homeotic genes *AtSEP*1 (*SEPALATA1*), *AtSEP3*, *AtPI* (*PISTILATA*), *AtAP3* (*APETALA 3*), which orchestrate flower organogenesis in *Arabidopsis* (review by Jack 2004 and Krizek 2005). Their counterparts have also been identified and partially characterized in cereals as recently reviewed by Murai 2013. Co-expression of

HvFT2 with the set of homeotic genes might further reflect the function of *HvFT2* in promoting floral organ development and thus contributing to flower fertility. In addition, genes involved in glycolysis and carbon transport and mobilization were co-expressed with *HvFT2* suggesting that LD and variation at *Ppd-H1* improved the nutritional status of the MSA. Early studies in *Sinapsis alba* and *Lolium temulentum* have already reported a strong mobilization of carbohydrates to the shoot apex after floral induction (Bodson *et al.* 1977, Périlleux and Bernier 1997). *FT-like* genes in barley may thus improve flower development and fertility by improving nutrient availability at the shoot apex.

3.2.3 Regulation of *SVP-like* genes and *HvSOC1-1* points to differences in the photoperiod dependent induction of flowering between barley and *Arabidopsis*

Detailed phenotyping of MSA development and spike characteristics clearly demonstrated that the duration of the early reproductive phase until W3.5 determined the number of floret primordia and spikelets. The duration of this early reproductive phase was affected by photoperiod and variation at *Ppd-H1*, but all plants transitioned to a reproductive meristem and developed until W3.5 equally under LD and SD. In addition, whereas variation at *Ppd-H1* showed large effects on inflorescence development and floral maturation, the rate of floret primordia initiation was only marginally faster in S42-IL107 as compared to Scarlett under LD. We were therefore interested in identifying molecular changes which correlated with MSA development independently of photoperiod and variation at *Ppd-H1*.

We show that *SVP-like* genes, in particular *HvBM1*, are specifically down-regulated during floral transition in the MSA under LD and SD. In *Arabidopsis*, the *Short Vegetative Phase* (*SVP*) gene encodes a MADS-box transcription factor that delays the floral transition (Hartmann *et al.*, 2000, Andrès *et al.* 2014). Mutations that disrupt *SVP* cause early flowering (Hartmann *et al.*, 2000), whereas ectopic expression of *SVP* and *SVP-like* genes results in late flowering, inhibits floral meristem identity and causes floral reversion (Brill and Watson 2004, Masiero *et al.* 2004). Similarly, ectopic over-expression of *HvBM1* and *HvBM10* in barley caused floral reversion and delayed development after the floral transition, suggesting that *SVP*-like genes also function to suppress floral meristem identity in barley (Trevaskis *et al.* 2007a, reviewed by Greenup *et al.* 2009). Trevaskis *et al.* (2007a) have found that *HvBM1*, *HvBM10* and *HvVRT2* were stably expressed in the leaves independent of the photoperiod and developmental stage, but induced upon cold temperatures. At the shoot apex the *SVP-like* genes were down-regulated during development. However, repression occurred well after floral transition. The authors concluded that in barley transcriptional repression of *SVP*-like genes is not required to promote floral transition in response to LD conditions. However, we show that transcriptional regulation of *HvBM1*, *HvBM10* and *HvVRT2* differ between MSA and leaf with a strong down-regulation of *SVP-like* genes only in the MSA upon floral transition under LD and SD. Interestingly, the time of

complete down-regulation differed between individual *SVP-like* genes: *HvBM1* was completely down-regulated at floral transition (W2.0), while complete repression of *HvVRT2* occurred at stamen primordium stage (W3.5). The differential regulation may further indicate functional diversification between the *SVP-like* genes in barley.

The differences in gene expression of *SVP-like* genes obtained from shoot apex samples of our study as compared to previous data of Trevaskis *et al.* 2007a is most likely due to differences in sample compositions used for expression analysis. Using RNA from samples enriched for apex tissue, i.e. including leaf primordia and nodal tissues (Fig. 15B), on which we conducted expression analysis by qRT-PCR, revealed a down-regulation of *SVP-like* genes during MSA development and their incomplete repression after floral transition. Additionally, analysis of these samples pointed to a photoperiod and *Ppd-H1* dependent regulation of the *SVP-like* genes in BW281 and Triumph-IL (Suppl. S2B+D). However, limiting the analysis of shoot apex pools excluding surrounding tissues (Fig. 15A), as we did for expression analysis by RNA-sequencing, revealed the complete and developmental stage specific repression of the *SVP-like* genes as early as floral transition occurred (W2.0) for *HvBM1* and later stages (W3.5) for *HvVRT2*, respectively. Thus, expression of *SVP-like* genes in and around the shoot apex seems to be spatially tightly controlled, with a photoperiod independent regulation in the shoot apex and a photoperiod dependent regulation surrounding the shoot apex.

However, this day length independent down-regulation of *SVP-like* genes specifically in the barley shoot apex seems to be in contrast to regulation of *SVP* in *Arabidopsis*. Recently, Andrès *et al.* (2014) have shown that in the early stages of the floral transition LD causes a repression of *SVP* and that this contributes to an increase in *GA20ox2* expression and synthesis of GA4 at the shoot apex. This photoperiod dependent down-regulation of *SVP* was caused by *FT* and *TSF* and their downstream target genes *SOC1* and *FUL*. We could also show that in barley variation at *Ppd-H1* and thus the levels of *HvFT1* expression controlled the expression of *GA20ox1* in the MSA at the time of floral transition (Table 4, Suppl. Fig. S3), which is in line with recent results in wheat where over-expression of an *FT* gene caused an increase in GA levels in shoot apices (Pearce *et al.* 2013). However, since *SVP-like* genes were not regulated by *FT* in barley shoot apices, *FT* might act independently of *SVP* repression to increase GA levels in shoot apices of temperate cereals. This suggests that the LD and FT dependent regulation of GA levels in the shoot apical meristem might be conserved across species, while the regulation of *SVP-like* genes differs between eudicots and monocots. However, a more detailed analysis on the spatio-temporal expression patterns of *SVP-like* genes in the MSA and in MSA surrounding tissues of barley will be needed to further support this hypothesis.

In *Arabidopsis*, SVP acts as a repressor of *SOC1* (Li *et al.* 2008), which encodes a MADS box transcription factor that is expressed in the shoot apical meristem during floral induction and is the earliest gene shown to be up-regulated by environmental cues such as day length (Samach *et al.* 2000, Lee *et al.*

2000, Borner *et al.* 2000). SOC1 binds directly within an intron of *SVP* where it might contribute to its repression during floral induction. In barley, *HvSOC1-1* and *HvBM1* show mutually exclusive temporal expression patterns at the MSA with *HvBM1* being expressed during the vegetative phase whereas *HvSOC1-1* is activated during the transition to flowering. These data demonstrate that the reciprocal repression of SVP/*SOC1* might be conserved between barley and *Arabidopsis*. In *Arabidopsis*, *SOC1* expression is induced by long photoperiods and high levels of FT expression (Lee *et al.* 2000, Samach *et al.* 2000, Yoo *et al.* 2005, Searle *et al.* 2006). This is in contrast to expression patterns of *HvSOC1-1* in the MSA of barley, where *HvSOC1-1* expression levels increased after floral transition independently of variation at *Ppd-H1*. However, it is well known that *SOC1* integrates many different flowering pathways. For example, Li *et al.* (2008) have shown that also in *Arabidopsis SOC1* mRNA increased in *svp* mutants largely independently of FT and AGL24, suggesting that removal of SVP activity may activate *SOC1* expression independently of those known *SOC1* activators. In *Arabidopsis*, *SOC1* induces the expression of *LEAFY*, a floral meristem identity gene widely conserved in monocots and dicots (Bomblies *et al.* 2003) and controls the induction of floral meristems at the shoot apex (Weigel and Nilsson 1995). *LFY* shows a weak expression in young *Arabidopsis* leaves during the vegetative phase and progressively increases as the plant approaches floral induction (Blàzquez *et al.* 1997). We found that like *HvSOC1-1*, *HvLFY* shows a rather photoperiod independent up-regulation during development (Suppl. Fig. 3). However, *HvLFY* was already strongly induced at the vegetative MSA and thus before *HvSOC1-1*. Similar to the expression of *HvLFY* at vegetative shoot apices we identified an early induction of *HvVRN1*, an *AP1/FUL-like* gene, supporting recent results in wheat which showed that *TaLFY* was up-regulated by GA and *VRN1* (Pearce *et al.* 2013). Indeed, up-regulation of *TaSOC1* and *TaLFY* were absolutely dependent on the expression of *TaVRN1* and GA, suggesting that both genes act downstream of the *FUL-like* gene *VRN1* in temperate cereals. During development, expression of *HvVRN1* was followed by the expression of two orthologous genes, *HvBM3* and *HvBM8*. Similar to the FT dependent up-regulation of *AP1* in *Arabidopsis* (Abe *et al.* 2005), all three *AP1/FUL-like* genes showed a *Ppd-H1* dependent induction at the MSA, however, their induction occurred at different stages of development. In *Arabidopsis*, *AP1* is initially expressed throughout floral meristems, and later its expression becomes restricted to sepal and petal primordia consistent with its different roles of specifying the identity of floral meristem, sepals and petals. In the present study we did not localize *AP1/FUL-like* gene expression within the MSA, but strong correlations of *HvVRN1* and *HvBM3* with the number of floret primordia formed during development until the beginning of stem elongation (W3.5), pointed to their function in regulating spikelet primordia formation in barley. Furthermore, differences in the expression levels of the three *AP1/FUL-like* genes during development suggested that *HvVRN1* was important for floral transition and acted downstream of *HvFT1* as previously proposed (Trevaskis *et al.* 2007b, Li *et al.* 2008, Pearce *et al.* 2013). The strong up-regulation of *HvBM3* and *HvBM8* in S42-

IL107 suggested that the expression of these *AP1-like* genes is also regulated by FT and LD. However, their induction in shoot apices subsequent to *HvVRN1* expression suggested a function at later stages of floral development. Accordingly, *HvVRN1*, but not *HvBM3* and *HvBM8* are regulated by vernalization (Sasani *et al.* 2009), supporting the hypothesis that these three closely related genes are functionally divergent. However, in contrast to their individual expression patterns throughout shoot apex development, Kobayashi et al. (2012) suggested a redundant role for the *AP1/FUL-like* genes *OsMADS14*, *OsMADS15* and *OsMADS18,* orthologous to *HvVRN1*, *HvBM3* and *HvBM8*, respectively, in rice in regulating the floral transition downstream of *Hd3a.*

In summary, the developmental stage dependent regulation of *SVP-like* genes independent of the photoperiod and allelic variation at *Ppd-H1* highlighted their central role in regulating early stages of shoot apex development. However, detailed analysis of their spatio-temporal expression at and around the shoot apex might help to better understand their connection also to the photoperiod dependent flowering pathway, e.g. acting through *HvSOC1-1*, downstream of *Ppd-H1/HvFT1* in barley.

3.3 Concluding Remarks

The objective of this study was to characterize the effects of the photoperiod and natural allelic variation at *Ppd-H1* on individual phases of pre-anthesis development in barley. We were aiming at the identification of transcriptional changes in leaves and shoot apices associated with the floral transition and early reproductive development.

The results confirmed the *Ppd-H1* dependent expression of *HvFT1* in the leaf of spring barley. Interestingly, a close FT-like ortholog *HvFT2* was induced by *Ppd-H1* and LD at the shoot apex. The timing of *HvFT2* induction in the MSA correlated well with the differences in the rate of shoot apex development and floret fertility. Thus, we hypothesize, that *HvFT2* might act as a central regulator of inflorescence development and is crucial for spikelet fertility in barley.

Co-regulation of *FT-like* and nutrient transport related genes with inflorescence maturation indicated that increased nutrient mobilization and transport in leaves and shoot apices might be linked to the observed spikelet fertility phenotype under LD. Thus, it would be interesting to determine the specific effects of *HvFT1* and *HvFT2* expression on nutrient levels, e.g. sugars or micronutrients like iron and zinc, in leaves and shoot apices during floral transition and inflorescences development. Future experiments should separate the effects of the photoperiod response pathway *per se* and increased availability of assimilates under LD than SD on nutrient availability and transport to the developing MSA. The shift experiments indicated that continuous exposure to LD and expression of *FT-like* genes in the leaf and the shoot apex was crucial to maintain inflorescence development. It is thus important to unravel the regulation of *HvFT2* in the MSA and to identify targets of *HvFT2* at early, but also late developmental stages to understand the effects of photoperiod on spikelet fertility. Differences in the timing of *HvFT2 e*xpression in the shoot apex (RNA-seq) as compared to shoot apex enriched samples (qRT-PCR) suggested tissue specific expression of *HvFT2* in and around the shoot apex. Future experiments should reveal the precise localization of *HvFT2* expression within the MSA to provide further information on its functional role in floral development.

Our experiments also showed that the down-regulation of *SVP-like* genes and up-regulation of *HvSOC1-1* marked the floral transition under LD and SD and thus can be used as developmental markers in barley. This is similar to *Arabidopsis*, where induction of *SOC1* in the shoot apical meristem marks the floral transition under SD and LD conditions (Borner *et al.* 2000). Interestingly, the expression of *SVP-like* genes and *HvSOC1-1* was *Ppd-H1* and thus *HvFT1* independent suggesting that floral transition in contrast to inflorescence maturation is not dependent on the expression of *FT-like* genes in barley.

In general, we report changes of the leaf and shoot apex transcriptome throughout early stages of barley development by RNA-sequencing. We believe that the generation of an improved reference for transcriptome mapping, classification of the 7604 identified DETs into 31 co-expression clusters and enriched GO-terms will be of great help for subsequent studies on early stages of pre-anthesis development in barley. We have shown that these early stages are important determinants of final number of seeds per spike. Optimizing the early reproductive development will thus greatly enhance yield potential of barley plants.

4 Materials and Methods

4.1 Plant material

In this study, we used three spring barley genotypes which carry a natural mutation in the CCT domain of *Ppd-H1* (Turner *et al.* 2005) and three derived backcross lines carrying introgressions of the dominant *Ppd-H1* allele. The spring barley genotypes were Scarlett, Bowman and Triumph and the derived introgression lines S42-IL107, BW281 and Triumph-IL, respectively. S42-IL107 and BW281 carry introgressions of the dominant *Ppd-H1* allele from wild barley (Schmalenbach *et al.* 2008, Druka *et al.* 2011). Triumph-IL is a BC4F2-selected introgression line derived from the doubled haploid (DH) population of a cross between Triumph and the winter barley Igri (Laurie *et al.* 1995) and was kindly provided by David Laurie (John Innes Centre, Norwich). The size of the introgression in S42-IL107 and BW281 was determined by high-resolution genotyping using the Barley Oligo Pool arrays (Illumina Golden Gate) (Schmalenbach *et al.* 2011, Druka *et al.* 2011). The 9 K Infinium i-Select barley array was used to genotype the Triumph-IL line.

4.1.1 Plant cultivation and phenotyping

For all experiments, plants were sown in the soil "Mini Tray" (Einheitserde®) in 96-cell growing trays. Plants were kept at 4°C for 3 days, followed by germination under SD conditions (8h, 22°Cday; 16h, 18°C night; PAR 270µM/m²s). Subsequent to germination, plants were transferred to LD conditions (16h, 22°Cday; 8h, 18°Cnight) or cultivation was continued under SDs. For the RNA-sequencing experiment, Scarlett and S42-IL107 were germinated and kept under SDs for 7 days prior to separation into LD and SD conditions.

Three representative plants per genotype and photoperiod were dissected every three to four days from germination to seed set in two independent experiments. At each time point, the developmental stage of the main shoot apex (MSA) was determined according to the quantitative scale of Waddington *et al.* (1983), in the text referred to as Waddington stage (W), reflecting the development of the most advanced floret primordium on the MSA. In addition, morphological phenotypes of the main shoot, number of emerged leaves, number of spikelet primordia were recorded for each genotype during development. Heading date (at Z49, Zadoks *et al.* 1974), and at plant maturity, number of spikelets per spike and number of grains per spike were recorded for ten plants per genotype. Minor adjustments of the Waddington scale were performed, i.e. Waddington stage 0.5 (W0.5) was assigned to shoot apices prior to the elongation of the apical dome present in transition apices at W1.0. Pictures of apices were taken with the Diskus imaging software (version 4.8.0.4562, Hilgers Technisches Büro) using a stereo microscope (model MZ FLIII, Leica) equipped with a digital camera (model KY-F70B, Leica).

Broken-line regressions were calculated for MSA development and emergence of spikelet primordia with the "segmented" package (version 0.2-9.5, Muggeo 2003, 2008) in the statistical software R (version 3.0.1, R Development Core Team, 2008). Regression models were fitted for the presence of none to four breakpoints, and the model with the highest Bayesian Information Criterion (BIC) score was selected. Slopes of the individual linear segments and their 95% confidence intervals were extracted from the broken-line regression model.

Significant genetic differences in morphological phenotypes recorded at plant maturity were identified by a Student's t-tests.

4.1.2 Photoperiod shift-experiment

Seeds of Scarlett and S42-IL107 were germinated in 96-well planting trays under SD. After germination, plants of both genotypes were transferred to 3L-sized pots and cultivation was continued under SD or LD, respectively. At eight stages of MSA development (W0.5-4.5) under SD und nine stages (W0.5-10) under LD, three plants per genotype were dissected to determine the developmental stage of the MSA prior to the transfer of another three plants from SD to LD of vice versa. Cultivation of three plants per genotype was constantly continued under either SD or LD conditions. Heading date (at Z49, Zadoks *et al.* 1974) and final leaf number of the main shoot were recorded before plant maturity for each plant. At plant maturity, height, spike length, number of spikelets and seeds per spike were recorded for the main shoot of each plant. The experiment was stopped 150 days after germination, as many plants grown under SD conditions did not flower.

4.2 Transcriptome analysis of developing barley shoot apices

4.2.1 Library preparation and sequencing

For RNA-sequencing, leaf and shoot apex tissue was harvested from main shoots of Scarlett and S42-IL107 plants grown under SD at W0.5, W1.0, W2.0 and W3.5 and under LD at W1.0, W2.0 and W3.5. Samples were harvested 2 hours before the end of the light period. MSA samples included tissues of young leaf and spikelet primordia as indicated in Figure 15A. Samples collected during the vegetative phase (W0.5 and W1.0) consisted of 25 to 30 pooled apices. At double ridge stage (W2.0) and stamen primordium stage (W3.5), 15 and 7 shoot apices were pooled, respectively. Leaf samples were harvested from a subset of seven plants, of which apex tissue was collected at the time of floral transition (W1.0, W2.0). Harvested leaf tissue was restricted to the distal part of the leaf around 2-4 cm before the leaf tip. Leaf and apex samples designated for RNA-sequencing were harvested in three replicate pools.

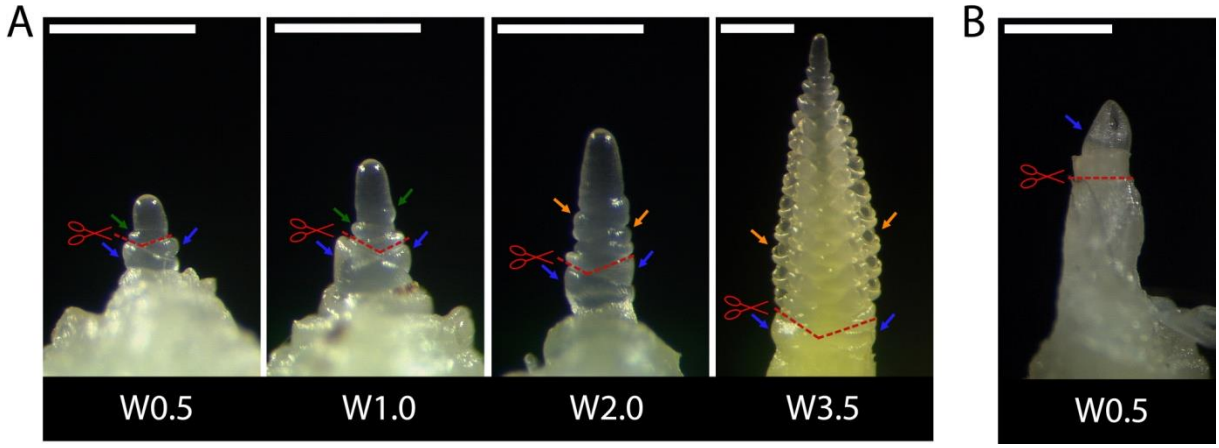

Figure 15: Representative main shoot apices dissected for RNA extraction
Total RNA was extracted from pools of isolated shoot apices including the tissue above the red dashed lines. Waddington stages (W) of harvested shoot apices are indicated below the pictures. White bars represent 500µm. **(A)** Shoot apex samples harvested for RNA-sequencing comprised dissected tissues of the apical dome, young leaf primordia (green arrows) and floret primordia (orange arrows). Older leaf primordia (blue arrows) and basal parts of the shoot apex were excluded. **(B)** Apex enriched tissue harvested for qRT-PCR analysis at different stages of development also included older leaf primordia and basal parts of the shoot apex.

For gene expression analysis by quantitative reverse transcription PCR (qRT-PCR), leaf and shoot apex tissues were harvested at four to six stages between W0.5 to W5.0 from the main shoot of all six genotypes grown under SD and LD. Each leaf and shoot apex sample comprised pooled tissues of five plants. Harvested shoot apex samples were enriched for shoot apex tissue, i.e. parts of the crown and young leaf primordia surrounding the inflorescence were also included (Fig. 15B).

Samples harvested for RNA extraction were immediately frozen in liquid nitrogen and stored at -80°C. Total RNA was extracted from ground tissue using the RNeasy® Micro Kit (Qiagen®) and TRIZOL® (Life Technologies) for RNA-sequencing and qRT-PCR, respectively. Residual DNA was removed using the DNA-*free*™ kit (Ambion®). RNA extraction and DNase treatment were performed following the manufacturers' instructions. RNA concentration and integrity were determined using the 2100 Bioanalyzer (Agilent) prior to RNA library preparation for RNA-sequencing.

cDNA-libraries were prepared according to the TruSeq™ RNA sample preparation protocol (version v2, Illumina®). Clonal sequence amplification and generation of sequence clusters were conducted on the cBot (Illumina®). Single end sequencing was performed on the HiSeq2000 (Illumina®) platform by multiplexing 12 libraries (libraries A-X, 1st set) and 24 libraries (libraries A1-AE1, 2nd set), respectively. In total, 47 libraries were sequenced, generating 672,463,624 1 x 100 bp single-end reads. Detailed information on sequencing results is presented in Suppl. Tab. S12.

Quality of the sequencing data was verified with the FastQC software (version 0.10.1, by S. Andrews) prior to further processing with the CLC Genomics workbench (version 6.0.4, CLCbio). PCR duplicates were removed from the raw sequencing data using the Duplicate Read Removal plugin of CLC. Reads

were trimmed, with an error probability limit calculated from the Phred scores of 0.05 and allowing for a maximum of two ambiguously called nucleotides per read. Reads shorter than 60bp, subsequent to the quality based trimming, were removed from the data set. After removal of PCR duplicates and quality based filtering 391,047,834 reads were retained, corresponding to an average of 59% of the raw sequencing data per library (Suppl. Fig. S4A).

4.2.2 Design of the reference sequence

To obtain a comprehensive reference sequence, we compared the mapping efficiency of the filtered reads against two sets of transcript clusters available for barley.

Recently, the International Barley Genome Sequencing Consortium (IBGSC) published the draft genome sequence of barley including the transcribed gene space assigned to a set of 26,159 annotated high-confidence genes (HC) and a set of 53,220 low-confidence genes (LC) (IBGSC, Nature 2012). Sequences of the HC and LC were downloaded from the Barley project webpage (ftp://ftpmips.helmholtz-muenchen.de/plants/barley/public_data/genes/, sequence version of March 23rd, 2012). Secondly, a cluster of 26,944 barley UniGenes (UniGene build #59 at NCBI), henceforth referred to as unigenes, was downloaded from NCBI (ftp://ftp.ncbi.nih.gov/repository/UniGene/Hordeum_vulgare/) and used for comparison.

Filtered reads of all libraries were combined and mapped against the respective reference sequences using the RNA-Seq Analysis function of CLC with default parameters. Test mappings were performed on the unigenes, HC and LC sets alone and on various combinations of those. In addition, we assembled de novo contigs using CLC *de novo* assemble tool.

To determine the most appropriate reference set for our study, we estimated the extent of sequence redundancy within the different reference sets using BLASTn. Redundancy was defined as a proportion of blast hits longer than 100bp with 97% identity. Furthermore, as an estimate for sequence redundancy, we extracted the proportion of reads with multiple mapping positions (≤10 positions) within a respective reference set. In addition to low sequence redundancy, we expected a comprehensive set of reference sequences to yield a high proportion of reads with unique mapping positions and a low percentage of reads assigned as unmapped, i.e. reads without mapping position or mapped to more than ten locations.

The unigenes were selected as a core set due to its lowest sequence redundancy and highest proportion of uniquely mapping reads as compared to the HC and LC datasets (Suppl. Fig. S4B), e.g in total we mapped 280,871,398 reads against the unigene set, of which 269,468,960 reads had unique and 11,402,438 reads had multiple mapping positions. Against transcripts of the HC dataset, we mapped 226,964,864 reads in total with unique and multiple mapping positions for 206,228,484 reads and 20,736,380 reads, respectively. Thus, other datasets were added to transcripts of the unigene set

in the following order of priority: HC, LC, *de novo* contigs. Redundancy in the combined datasets was eliminated using Minimus2 software with parameters set to 130bp overlap and 97% minimum identity. Filtering transcripts appropriately yielded 8,391 HC (sHC) and 23,232 LC (sLC) progressively added to the unigenes.

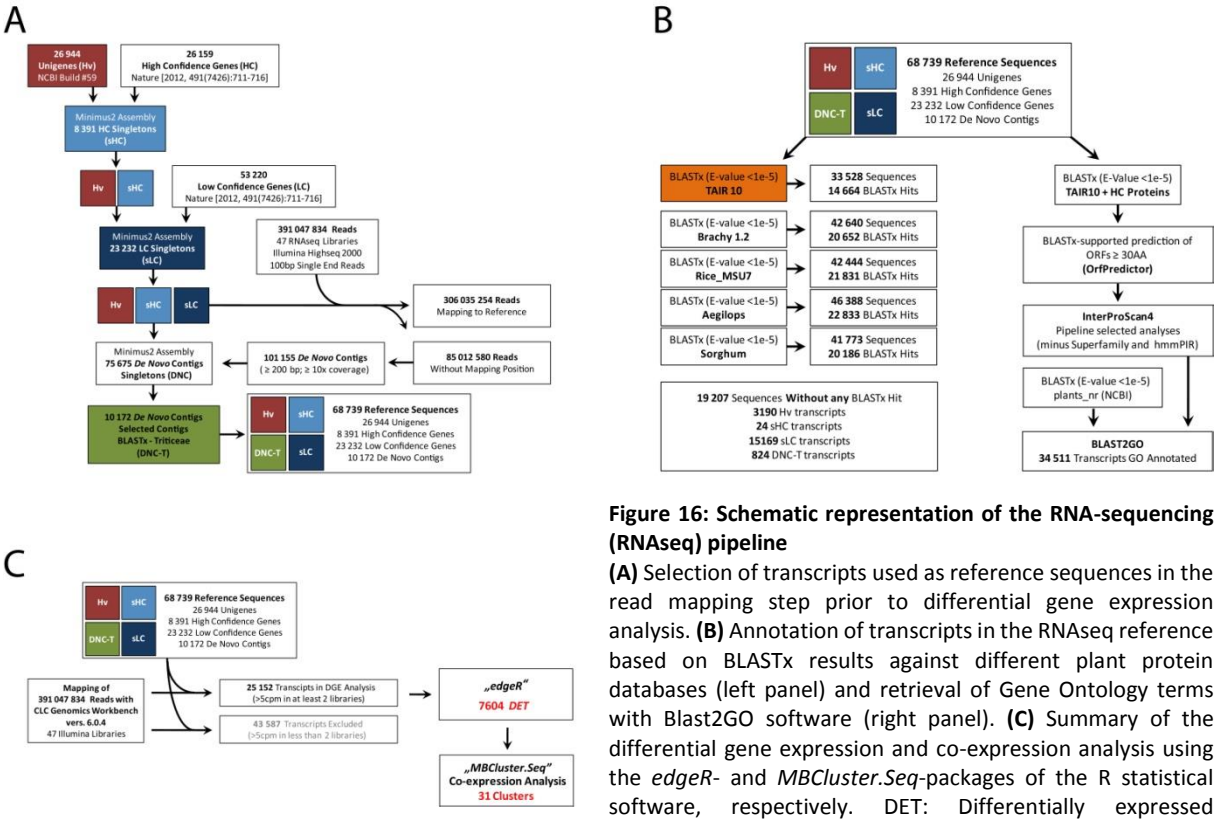

Figure 16: Schematic representation of the RNA-sequencing (RNAseq) pipeline
(A) Selection of transcripts used as reference sequences in the read mapping step prior to differential gene expression analysis. **(B)** Annotation of transcripts in the RNAseq reference based on BLASTx results against different plant protein databases (left panel) and retrieval of Gene Ontology terms with Blast2GO software (right panel). **(C)** Summary of the differential gene expression and co-expression analysis using the *edgeR*- and *MBCluster.Seq*-packages of the R statistical software, respectively. DET: Differentially expressed transcripts; Hv, Unigenes: Barley NCBI UniGene set; HC: High confidence gene set; LC: Low confidence gene set; sHC/sLC: selected subset of unique HC or LC

To allow the identification of new transcripts specific for shoot apex tissue used in our study, we used CLC *de novo* assembly tool with default parameters to construct a set of 473,651 *de novo* contigs (DNC) from 85,0125,80 reads, which did not map to a reference sequence constructed from unigenes, sHC and sLC. Contigs were filtered for a minimum length of 200bp and a 10X average coverage. A set of 10,172 DNC with BLASTx hits in the *Triticeae* family (E-value ≤ 10^{-5}), henceforth DNC-T, was selected from the 75,675 DNC identified as Minimus2 singletons. A schematic representation of the pipeline used to construct the reference sequence is presented in Fig. 16A.

In summary, a final set of 68,739 transcripts, consisting of 26,944 unigenes, 8,391 sHC, 23,232 sLC and 10,172 DNC-T, was used as a custom reference for the RNA-sequencing analysis. Using this as reference set, 80.6% (315,108,855 reads) of the quality filtered reads could be mapped in total with 74.9% (292,699,606 reads) having unique and 5.7% (22,409,249 reads) multiple mapping positions.

The reference set was annotated using BLASTx against protein databases of *Arabidopsis* (TAIR version 10), *Brachypodium* (*Brachypodium distachyon*, Project version 1.2), Rice (MSU Rice Genome Annotation Project release 7), *Aegilops* (downloaded on 8-05-2013, Jia et al 2013) and *Sorghum* (1.4, Paterson *et al.* 2009) with cut-off E-value 10^{-5}.

The open reading frames (ORF) of barley transcripts were predicted using the OrfPredictor software guided by the BLASTx results against TAIR (≥30 aa, Min *et al.* 2005). Conserved domain annotation of the translated ORFs was performed using InterProScan4 software (Hunter *et al.*, 2011). These data together with the top 20 BLASTx hits against the *Viridiplantae* sub-set of NCBI 'nr' database were used to determine gene ontology (GO) terms for the reference barley transcripts using Blast2GO pipe 2.5.0 (Consea *et al.*, 2005). An overview the reference sequence annotation pipeline is depicted in Fig. 16B.

4.2.3 Differential gene expression analysis and calculation of co-expression clusters

Quality filtered reads of each library were mapped against the reference sequence using the RNA-Seq Analysis tool of the CLC Genomics workbench with default parameters (Suppl. Tab. S12). Counts of uniquely mapped reads were extracted and used for downstream analyses. Differentially expressed transcripts (DET) were identified with the R/Bioconductor package "edgeR" (version 3.2.3, Robinson *et al.*, 2010) using the generalized linear model (GLM) with the factors genotype, photoperiod and developmental stage of the MSA. Five separate models needed to be specified because under SDs only S42-IL107 MSA and leaf samples were subjected to RNA-sequencing. For DET calling, individual contrasts were specified to extract DETs between individual developmental stages in MSA samples, between photoperiods and between genotypes in MSA and leaf samples. DETs were called at an FDR less than 10^{-4}. Additionally, DETs detected between individual developmental stages at the MSA required an absolute log2-fold-change > 1.

Prior to DEG calling transcripts with counts less than 5 cpm in at least two libraries were removed and the remaining 25,152 transcripts were considered expressed. Expression values of the filtered transcripts were correlated between individual libraries to verify quality of biological replication (Suppl. Tab. S13). One library was identified for S42-IL107 (MSA library under SD at W3.5, biological replicate 1) with correlation coefficient of $r \leq 0.86$ as compared to its biological replicates. However, transcripts with low correlations between the biological replicates in this set of libraries were also among the transcripts with highest variation between biological replicates in other library sets. Thus, we decided to keep the library with low correlation coefficient for differential gene expression analysis, as biological rather than technical reasons were causative differences in expression values in this library.

Co-expression analysis was performed on RPKM (reads per kilo base per million) normalized expression levels of 7406 DETs. To optimize the number of co-expression clusters, negative binomial models were

fitted for different numbers of co-expression clusters ranging from 5 to 120 using the R package "MBCluster.Seq" (version 1.0, Si *et al.* 2013). Convergence of the EM-algorithm for estimation of cluster centers was called in a maximum of 10^3 iterations. The final number of clusters was determined based on visual inspection of the hybrid tree supported by high average probability of clustered transcripts (Suppl. Tab. S14).

Over-representation of identified DET subsets within co-expression clusters was tested by Pearson's Chi-squared test in R (Monte Carlo simulation, 2000 replicates).

Over-representation of particular GO terms within the co-expression clusters and identified subsets of DETs was estimated against the GO-annotated reference (18,890 out of 25,152 expressed transcripts) using Fisher's exact tests implemented in the Blast2GO software (FDR < 0.05).

4.2.4 Verification of gene expression by qRT-PCR assays

DNAse-treated total RNA (1µg) was reverse-transcribed using the SuperScript™II reverse transcriptase (Life Technologies™) according to the manufacturer's instructions. Expression levels of target genes were quantified by qRT-PCR. Reactions included 1µl of cDNA, 1U of GoTaq® Flexi DNA Polymerase (Promega), 0.2 mM deoxynucleotide triphosphate (dNTP), 2.5 mM $MgCl_2$, 0.2 µM of each primer and 1 µl of EvaGreen® (Biotium). Oligonucleotide sequences for forward and reverse primers are given in Suppl. Tab. S15. qRT-PCR was performed on the Roche LightCycler® 480 System (Roche) with the following amplification conditions: 95°C (5 min), 40 cycles of 95°C (10 sec), 60°C (10 sec) and 72°C (10 sec). No template controls were included in each 384-well plate and dissociation curve analysis was performed at the end of each run to ensure specificity of single reactions. Initial concentrations of each gene were calculated from titration curves using the LightCylcer® 480 software (Roche, version 1.5.0).

HvActin, *HvGAPDH* and *HvUbiquitin* showed stable expression across tissues, developmental stages and photoperiods in the RNA-sequencing experiments and *HvActin* was chosen for relative quantification of the target gene expression levels in the qRT-PCR assays. qRT-PCR data for each target gene are presented as average expression levels over three biological replicates, with two technical replicates per reaction, relative to the expression levels of the *HvActin* reference gene.

5 Bibliography

Abe, M., Kobayashi, Y., Yamamoto, S., Daimon, Y., Yamaguchi, A., Ikeda, Y., Ichinoki, H., Notaguchi, M., Goto, K., and Araki, T. (2005). FD, a bZIP protein mediating signals from the floral pathway integrator FT at the shoot apex. Science **309,** 1052-1056.

Alqudah, A.M., and Schnurbusch, T. (2014). Awn primordium to tipping is the most decisive developmental phase for spikelet survival in barley. Functional Plant Biology **41,** 424-436.

Andrés, F., Porri, A., Torti, S., Mateos, J., Romera-Branchat, M., Garcia-Martinez, J.L., Fornara, F., Gregis, V., Kater, M.M., and Coupland, G. (2014). SHORT VEGETATIVE PHASE reduces gibberellin biosynthesis at the *Arabidopsis* shoot apex to regulate the floral transition. Proc Natl Acad Sci U S A **111,** E2760-2769.

Arisnabarreta, S.n., and Miralles, D.J. (2008a). Radiation effects on potential number of grains per spike and biomass partitioning in two- and six-rowed near isogenic barley lines. Field Crops Research **107,** 203-210.

Baum, M., Grando, S., Backes, G., Jahoor, A., Sabbagh, A., and Ceccarelli, S. (2003). QTLs for agronomic traits in the Mediterranean environment identified in recombinant inbred lines of the cross 'Arta' x *H. spontaneum* 41-1. Theor Appl Genet **107,** 1215-1225.

Beales, J., Turner, A., Griffiths, S., Snape, J.W., and Laurie, D.A. (2007). A pseudo-response regulator is misexpressed in the photoperiod insensitive *Ppd-D1a* mutant of wheat (*Triticum aestivum* L.). Theor Appl Genet **115,** 721-733.

Bezant, J., Laurie, D., Pratchett, N., Chojecki, J., and Kearsey, M. (1996). Marker regression mapping of QTL controlling flowering time and plant height in a spring barley (*Hordeum vulgare* L.) cross. Heredity **77,** 64-73.

Blázquez, M.A., Soowal, L.N., Lee, I., and Weigel, D. (1997). *LEAFY* expression and flower initiation in *Arabidopsis*. Development **124,** 3835-3844.

Boden, S.A., Weiss, D., Ross, J.J., Davies, N.W., Trevaskis, B., Chandler, P.M., and Swain, S.M. (2014). *EARLY FLOWERING3* Regulates Flowering in Spring Barley by Mediating Gibberellin Production and *FLOWERING LOCUS T* Expression. The Plant Cell Online.

Bodson, M. (1977). Changes in the carbohydrate content of the leaf and the apical bud of *Sinapis* during transition to flowering. Planta **135,** 19-23.

Bomblies, K., Wang, R.L., Ambrose, B.A., Schmidt, R.J., Meeley, R.B., and Doebley, J. (2003). Duplicate *FLORICAULA/LEAFY* homologs *zfl1* and *zfl2* control inflorescence architecture and flower patterning in maize. Development **130,** 2385-2395.

Borlaug, N.E. (1983). Contributions of Conventional Plant Breeding to Food Production. Science **219,** 689-693.

Borner, R., Kampmann, G., Chandler, J., Gleissner, R., Wisman, E., Apel, K., and Melzer, S. (2000). A MADS domain gene involved in the transition to flowering in *Arabidopsis*. Plant J **24,** 591-599.

Borrás-Gelonch, G., Slafer, G.A., Casas, A.M., van Eeuwijk, F., and Romagosa, I. (2010). Genetic control of pre-heading phases and other traits related to development in a double-haploid barley (*Hordeum vulgare* L.) population. Field Crops Research **119,** 36-47.

Borrás-Gelonch, G., Denti, M., B Thomas, W., and Romagosa, I. (2012a). Genetic control of pre-heading phases in the Steptoe x Morex barley population under different conditions of photoperiod and temperature. Euphytica **183,** 303-321.

Borrás-Gelonch, G., Rebetzke, G.J., Richards, R.A., and Romagosa, I. (2012b). Genetic control of duration of pre-anthesis phases in wheat (*Triticum aestivum* L.) and relationships to leaf appearance, tillering, and dry matter accumulation. Journal of Experimental Botany **63,** 69-89.

Borrás-Gelonch, G. (2013). Doctoral thesis: Differences in the control of pre-heading phases in barley and wheat, and relationships with agronomic traits (Lleida: Universitat de Lleida).

Bouveret, R., Schonrock, N., Gruissem, W., and Hennig, L. (2006). Regulation of flowering time by *Arabidopsis* MSI1. Development **133,** 1693-1702.

Boyd, W.J.R., Li, C.D., Grime, C.R., Cakir, M., Potipibool, S., Kaveeta, L., Men, S., Kamali, M.R.J., Barr, A.R., Moody, D.B., Lance, R.C.M., Logue, S.J., Raman, H., and Read, B.J. (2003). Conventional and molecular genetic analysis of factors contributing to variation in the timing of heading among spring barley (*Hordeum vulgare* L.) genotypes grown over a mild winter growing season. Australian Journal of Agricultural Research **54,** 1277-1301.

Brill, E.M., and Watson, J.M. (2004). Ectopic expression of a *Eucalyptus grandis SVP* orthologue alters the flowering time of *Arabidopsis thaliana*. Functional Plant Biology **31,** 217-224.

Campoli, C., Drosse, B., Searle, I., Coupland, G., and von Korff, M. (2012a). Functional characterisation of *HvCO1*, the barley (*Hordeum vulgare*) flowering time ortholog of *CONSTANS*. Plant J **69,** 868-880.

Campoli, C., Shtaya, M., Davis, S.J., and von Korff, M. (2012b). Expression conservation within the circadian clock of a monocot: natural variation at barley *Ppd-H1* affects circadian expression of flowering time genes, but not clock orthologs. BMC Plant Biol **12,** 97.

Casao, M.C., Igartua, E., Karsai, I., Lasa, J.M., Gracia, M.P., and Casas, A.M. (2011a). Expression analysis of vernalization and day-length response genes in barley (*Hordeum vulgare* L.) indicates that *VRNH2* is a repressor of *PPDH2* (*HvFT3*) under long days. J Exp Bot **62,** 1939-1949.

Casao, M.C., Karsai, I., Igartua, E., Gracia, M.P., Veisz, O., and Casas, A. (2011b). Adaptation of barley to mild winters: A role for *PPDH2*. BMC Plant Biology **11,** 164.

Chen, A., Baumann, U., Fincher, G.B., and Collins, N.C. (2009). Flt-2L, a locus in barley controlling flowering time, spike density, and plant height. Funct Integr Genomics **9,** 243-254.

Chen, Y., Carver, B.F., Wang, S., Zhang, F., and Yan, L. (2009). Genetic loci associated with stem elongation and winter dormancy release in wheat. Theor Appl Genet **118,** 881-889.

Chen, W., Yu, X.H., Zhang, K., Shi, J., De Oliveira, S., Schreiber, L., Shanklin, J., and Zhang, D. (2011). *Male Sterile2* encodes a plastid-localized fatty acyl carrier protein reductase required for pollen exine development in *Arabidopsis*. Plant Physiol **157,** 842-853.

Chen, A., and Dubcovsky, J. (2012). Wheat TILLING Mutants Show That the Vernalization Gene *VRN1* Down-Regulates the Flowering Repressor *VRN2* in Leaves but Is Not Essential for Flowering. PLoS Genet **8,** e1003134.

Chu, H.H., Chiecko, J., Punshon, T., Lanzirotti, A., Lahner, B., Salt, D.E., and Walker, E.L. (2010). Successful reproduction requires the function of *Arabidopsis Yellow Stripe-Like1* and *Yellow Stripe-Like3* metal-nicotianamine transporters in both vegetative and reproductive structures. Plant Physiol **154,** 197-210.

Cockram, J., Jones, H., Leigh, F.J., O'Sullivan, D., Powell, W., Laurie, D.A., and Greenland, A.J. (2007). Control of flowering time in temperate cereals: genes, domestication, and sustainable productivity. J Exp Bot **58,** 1231-1244.

Cockram, J., Howells, R.M., and O'Sullivan, D.M. (2010). Segmental chromosomal duplications harbouring group IV *CONSTANS-like* genes in cereals. Genome **53,** 231-240.

Comadran, J., Kilian, B., Russell, J., Ramsay, L., Stein, N., Ganal, M., Shaw, P., Bayer, M., Thomas, W., Marshall, D., Hedley, P., Tondelli, A., Pecchioni, N., Francia, E., Korzun, V., Walther, A., and Waugh, R. (2012). Natural variation in a homolog of Antirrhinum *CENTRORADIALIS* contributed to spring growth habit and environmental adaptation in cultivated barley. Nat Genet **44,** 1388-1392.

Conesa, A., Götz, S., García-Gómez, J.M., Terol, J., Talón, M., and Robles, M. (2005). Blast2GO: a universal tool for annotation, visualization and analysis in functional genomics research. Bioinformatics **21,** 3674-3676.

Corbesier, L., Vincent, C., Jang, S., Fornara, F., Fan, Q., Searle, I., Giakountis, A., Farrona, S., Gissot, L., Turnbull, C., and Coupland, G. (2007). FT protein movement contributes to long-distance signaling in floral induction of *Arabidopsis*. Science **316,** 1030-1033.

Cuesta-Marcos, A., Igartua, E., Ciudad, F., Codesal, P., Russell, J., Molina-Cano, J.L., Moralejo, M., Szücs, P., Gracia, M.a., Lasa, J.M., and Casas, A. (2008a). Heading date QTL in a spring x winter barley cross evaluated in Mediterranean environments. Molecular Breeding **21,** 455-471.

Cuesta-Marcos, A., Casas, A., Yahiaoui, S., Gracia, M.P., Lasa, J.M., and Igartua, E. (2008b). Joint analysis for heading date QTL in small interconnected barley populations. Molecular Breeding **21,** 383-399.

Diaz, A., Zikhali, M., Turner, A.S., Isaac, P., and Laurie, D.A. (2012). Copy number variation affecting the *Photoperiod-B1* and *Vernalization-A1* genes is associated with altered flowering time in wheat (*Triticum aestivum*). PLoS One **7,** e33234.

Distelfeld, A., Li, C., and Dubcovsky, J. (2009). Regulation of flowering in temperate cereals. Curr Opin Plant Biol **12,** 178-184.

Distelfeld, A., and Dubcovsky, J. (2010). Characterization of the maintained vegetative phase deletions from diploid wheat and their effect on *VRN2* and *FT* transcript levels. Molecular Genetics and Genomics **283,** 223-232.

Dixon, L.E., Knox, K., Kozma-Bognar, L., Southern, M.M., Pokhilko, A., and Millar, A.J. (2011). Temporal repression of core circadian genes is mediated through *EARLY FLOWERING 3* in *Arabidopsis*. Curr Biol **21,** 120-125.

Druka, A., Franckowiak, J., Lundqvist, U., Bonar, N., Alexander, J., Houston, K., Radovic, S., Shahinnia, F., Vendramin, V., Morgante, M., Stein, N., and Waugh, R. (2011). Genetic Dissection of Barley Morphology and Development. Plant Physiology **155,** 617-627.

Dunford, R.P., Griffiths, S., Christodoulou, V., and Laurie, D.A. (2005). Characterisation of a barley (*Hordeum vulgare* L.) homologue of the *Arabidopsis* flowering time regulator *GIGANTEA*. Theor Appl Genet **110,** 925-931.

Ehrenreich, I.M., Hanzawa, Y., Chou, L., Roe, J.L., Kover, P.X., and Purugganan, M.D. (2009). Candidate Gene Association Mapping of *Arabidopsis* Flowering Time. Genetics **183,** 325-335.

Eleuch, L., Jilal, A., Grando, S., Ceccarelli, S., Von Korff Schmising, M., Tsujimoto, H., Hajer, A., Daaloul, A., and Baum, M. (2008). Genetic Diversity and Association Analysis for Salinity Tolerance, Heading Date and Plant Height of Barley Germplasm Using Simple Sequence Repeat Markers. Journal of Integrative Plant Biology **50,** 1004-1014.

Ellis, R.H., Roberts, E.H., Summerfield, R.J., and Cooper, J.P. (1988). Environmental Control of Flowering in Barley (*Hordeum vulgare* L.). II. Rate of Developement as a Function of Temperature and Photoperiod and its Modification by Low-temperature Vernalization. Annals of Botany **62,** 145-158.

Enomoto, N. (1929). On the physiological difference between the spring and winter types in wheat and barley. J. Imp. Agric. Exp. Stat. **1,** 107-138.

FAO (2014). FAOSTAT 2014, data of 2013; FAO (Food and Agriculture Organization of the United Nations); http://faostat3.fao.org/faostat-gateway/go/to/compare/Q/QC/E; August 24th, 2014.

Faure, S., Higgins, J., Turner, A., and Laurie, D.A. (2007). The *FLOWERING LOCUS T-like* gene family in barley (*Hordeum vulgare*). Genetics **176,** 599-609.

Faure, S., Turner, A.S., Gruszka, D., Christodoulou, V., Davis, S.J., von Korff, M., and Laurie, D.A. (2012). Mutation at the circadian clock gene *EARLY MATURITY 8* adapts domesticated barley (*Hordeum vulgare*) to short growing seasons. Proceedings of the National Academy of Sciences.

Fittinghoff, K., Laubinger, S., Nixdorf, M., Fackendahl, P., Baumgardt, R.L., Batschauer, A., and Hoecker, U. (2006). Functional and expression analysis of *Arabidopsis SPA* genes during seedling photomorphogenesis and adult growth. Plant J **47,** 577-590.

Fowler, S., Lee, K., Onouchi, H., Samach, A., Richardson, K., Morris, B., Coupland, G., and Putterill, J. (1999). *GIGANTEA*: a circadian clock-controlled gene that regulates photoperiodic flowering in *Arabidopsis* and encodes a protein with several possible membrane-spanning domains. EMBO J **18,** 4679-4688.

Garcıa del Moral, L.F., Miralles, D.J., and Slafer, G.A. (2002). Initiation and appearance of vegetative and reproductive structures throughout barley development. (New York: Food Products Press).

Ghiglione, H.O., Gonzalez, F.G., Serrago, R., Maldonado, S.B., Chilcott, C., Cura, J.A., Miralles, D.J., Zhu, T., and Casal, J.J. (2008). Autophagy regulated by day length determines the number of fertile florets in wheat. Plant J **55,** 1010-1024.

González, F.G., Slafer, G.A., and Miralles, D.J. (2002). Vernalization and photoperiod responses in wheat pre-flowering reproductive phases. Field Crops Research **74,** 183-195.

González, F.G., Slafer, G.A., and Miralles, D.J. (2003). Floret development and spike growth as affected by photoperiod during stem elongation in wheat. Field Crops Research **81,** 29-38.

González, F., Slafer, G., and Miralles, D. (2005). Pre-anthesis development and number of fertile florets in wheat as affected by photoperiod sensitivity genes *Ppd-D1* and *Ppd-B1*. Euphytica **146,** 253-269.

González, F.G., Miralles, D.J., and Slafer, G.A. (2011). Wheat floret survival as related to pre-anthesis spike growth. Journal of Experimental Botany.

Greenup, A., Peacock, W.J., Dennis, E.S., and Trevaskis, B. (2009). The molecular biology of seasonal flowering-responses in *Arabidopsis* and the cereals. Ann Bot **103,** 1165-1172.

Griffiths, F.E.W., Lyndon, R.F., and Bennett, M.D. (1985). The Effects of Vernalization on the Growth of the Wheat Shoot Apex. Annals of Botany **56,** 501-511.

Griffiths, S., Dunford, R.P., Coupland, G., and Laurie, D.A. (2003). The evolution of *CONSTANS-like* gene families in barley, rice, and *Arabidopsis*. Plant Physiol **131,** 1855-1867.

Hartmann, U., Hohmann, S., Nettesheim, K., Wisman, E., Saedler, H., and Huijser, P. (2000). Molecular cloning of *SVP*: a negative regulator of the floral transition in *Arabidopsis*. Plant J **21,** 351-360.

Hayama, R., Yokoi, S., Tamaki, S., Yano, M., and Shimamoto, K. (2003). Adaptation of photoperiodic control pathways produces short-day flowering in rice. Nature **422,** 719-722.

Hemming, M.N., Peacock, W.J., Dennis, E.S., and Trevaskis, B. (2008). Low-temperature and daylength cues are integrated to regulate *FLOWERING LOCUS T* in barley. Plant Physiol **147,** 355-366.

Hemming, M.N., Fieg, S., Peacock, W.J., Dennis, E.S., and Trevaskis, B. (2009). Regions associated with repression of the barley (*Hordeum vulgare*) *VERNALIZATION1* gene are not required for cold induction. Mol Genet Genomics **282,** 107-117.

Herrero, E., Kolmos, E., Bujdoso, N., Yuan, Y., Wang, M., Berns, M.C., Uhlworm, H., Coupland, G., Saini, R., Jaskolski, M., Webb, A., Goncalves, J., and Davis, S.J. (2012). EARLY FLOWERING4 recruitment of EARLY FLOWERING3 in the nucleus sustains the *Arabidopsis* circadian clock. Plant Cell **24,** 428-443.

Higgins, J.A., Bailey, P.C., and Laurie, D.A. (2010). Comparative genomics of flowering time pathways using *Brachypodium distachyon* as a model for the temperate grasses. PLoS One **5,** e10065.

Hong, S.-Y., Lee, S., Seo, P., Yang, M.-S., and Park, C.-M. (2010). Identification and molecular characterization of a *Brachypodium distachyon GIGANTEA* gene: functional conservation in monocot and dicot plants. Plant Molecular Biology **72,** 485-497.

Huang, W., Perez-Garcia, P., Pokhilko, A., Millar, A.J., Antoshechkin, I., Riechmann, J.L., and Mas, P. (2012). Mapping the core of the *Arabidopsis* circadian clock defines the network structure of the oscillator. Science **336,** 75-79.

Hunter, S., Jones, P., Mitchell, A., Apweiler, R., Attwood, T.K., Bateman, A., Bernard, T., Binns, D., Bork, P., Burge, S., de Castro, E., Coggill, P., Corbett, M., Das, U., Daugherty, L., Duquenne, L., Finn, R.D., Fraser, M., Gough, J., Haft, D., Hulo, N., Kahn, D., Kelly, E., Letunic, I., Lonsdale, D., Lopez, R., Madera, M., Maslen, J., McAnulla, C., McDowall, J., McMenamin, C., Mi, H., Mutowo-Muellenet, P., Mulder, N., Natale, D., Orengo, C., Pesseat, S., Punta, M., Quinn, A.F., Rivoire, C., Sangrador-Vegas, A., Selengut, J.D., Sigrist, C.J.A., Scheremetjew, M., Tate, J., Thimmajanarthanan, M., Thomas, P.D., Wu, C.H., Yeats, C., and Yong, S.-Y. (2011). InterPro in 2011: new developments in the family and domain prediction database. Nucleic Acids Research **40,** D306-D312.

IBGSC. (2012). International Barley Genome Sequencing Consortium. A physical, genetic and functional sequence assembly of the barley genome. Nature **491,** 711-716.

Ivandic, V., Hackett, C.A., Nevo, E., Keith, R., Thomas, W.T., and Forster, B.P. (2002). Analysis of simple sequence repeats (SSRs) in wild barley from the Fertile Crescent: associations with ecology, geography and flowering time. Plant Mol Biol **48,** 511-527.

Jack, T. (2004). Molecular and genetic mechanisms of floral control. Plant Cell **16 Suppl,** S1-17.

Jang, S., Marchal, V., Panigrahi, K.C., Wenkel, S., Soppe, W., Deng, X.W., Valverde, F., and Coupland, G. (2008). *Arabidopsis* COP1 shapes the temporal pattern of CO accumulation conferring a photoperiodic flowering response. EMBO J **27,** 1277-1288.

Jia, J., Zhao, S., Kong, X., Li, Y., Zhao, G., He, W., Appels, R., Pfeifer, M., Tao, Y., Zhang, X., Jing, R., Zhang, C., Ma, Y., Gao, L., Gao, C., Spannagl, M., Mayer, K.F.X., Li, D., Pan, S., Zheng, F., Hu, Q., Xia, X., Li, J., Liang, Q., Chen, J., Wicker, T., Gou, C., Kuang, H., He, G., Luo, Y., Keller, B., Xia, Q., Lu, P., Wang, J., Zou, H., Zhang, R., Xu, J., Gao, J., Middleton, C., Quan, Z., Liu, G., Wang, J., Yang, H., Liu, X., He, Z., Mao, L., and Wang, J. (2013). *Aegilops tauschii* draft genome sequence reveals a gene repertoire for wheat adaptation. Nature **496,** 91-95.

Jia, Q., Zhang, J., Westcott, S., Zhang, X.-Q., Bellgard, M., Lance, R., and Li, C. (2009). GA-20 oxidase as a candidate for the semidwarf gene *sdw1/denso* in barley. Functional & Integrative Genomics **9,** 255-262.

Jones, H., Leigh, F.J., Mackay, I., Bower, M.A., Smith, L.M., Charles, M.P., Jones, G., Jones, M.K., Brown, T.A., and Powell, W. (2008). Population-based resequencing reveals that the flowering time adaptation of cultivated barley originated east of the Fertile Crescent. Mol Biol Evol **25,** 2211-2219.

Kikuchi, R., Kawahigashi, H., Ando, T., Tonooka, T., and Handa, H. (2009). Molecular and functional characterization of PEBP genes in barley reveal the diversification of their roles in flowering. Plant Physiol **149,** 1341-1353.

Kikuchi, R., Kawahigashi, H., Oshima, M., Ando, T., and Handa, H. (2011). The differential expression of *HvCO9*, a member of the *CONSTANS-like* gene family, contributes to the control of flowering under short-day conditions in barley. Journal of Experimental Botany.

Kitchen, B.M., and Rasmusson, D.C. (1983). Duration and inheritance of leaf initiation, spike initiation and spike growth in barley. Crop Science **23,** 939-943.

Krieger, U., Lippman, Z.B., and Zamir, D. (2010). The flowering gene *SINGLE FLOWER TRUSS* drives heterosis for yield in tomato. Nat Genet **42,** 459-463.

Krizek, B.A., and Fletcher, J.C. (2005). Molecular mechanisms of flower development: an armchair guide. Nat Rev Genet **6,** 688-698.

Laubinger, S., Fittinghoff, K., and Hoecker, U. (2004). The SPA quartet: a family of WD-repeat proteins with a central role in suppression of photomorphogenesis in *Arabidopsis*. Plant Cell **16,** 2293-2306.

Laubinger, S., Marchal, V., Le Gourrierec, J., Wenkel, S., Adrian, J., Jang, S., Kulajta, C., Braun, H., Coupland, G., and Hoecker, U. (2006). *Arabidopsis* SPA proteins regulate photoperiodic flowering and interact with the floral inducer CONSTANS to regulate its stability. Development **133,** 3213-3222.

Laurie, D.A., Pratchett, N., Bezant, J.H., and Snape, J.W. (1994). Genetic analysis of a photoperiod response gene on the short arm of chromosome 2(2H) of *Hordeum vulgare* (barley). Heredity **72,** 619-627.

Laurie, D.A., Pratchett, N., Snape, J.W., and Bezant, J.H. (1995). RFLP mapping of five major genes and eight quantitative trait loci controlling flowering time in a winter x spring barley (*Hordeum vulgare* L.) cross. Genome **38,** 575-585.

Law, C.N. (1987). The genetic control of day-length response in wheat. In Manipulation of flowering, J.G. Atherton, ed (London: Butterworth), pp. 225-240.

Law, C.N., and Worland, A.J. (1997). Genetic analysis of some flowering time and adaptive traits in wheat. New Phytologist **137,** 19-28.

Lee, H., Suh, S.S., Park, E., Cho, E., Ahn, J.H., Kim, S.G., Lee, J.S., Kwon, Y.M., and Lee, I. (2000). The AGAMOUS-LIKE 20 MADS domain protein integrates floral inductive pathways in *Arabidopsis*. Genes Dev **14,** 2366-2376.

Lee, H., Chah, O.-K., and Sheen, J. (2011). Stem-cell-triggered immunity through CLV3p-FLS2 signalling. Nature **473,** 376-379.

Levy, Y.Y., Mesnage, S.p., Mylne, J.S., Gendall, A.R., and Dean, C. (2002). Multiple Roles of *Arabidopsis VRN1* in Vernalization and Flowering Time Control. Science **297,** 243-246.

Lewis, S., Faricelli, M.E., Appendino, M.L., Valarik, M., and Dubcovsky, J. (2008). The chromosome region including the earliness per se locus Eps-Am1 affects the duration of early developmental phases and spikelet number in diploid wheat. J Exp Bot **59,** 3595-3607.

Li, C., and Dubcovsky, J. (2008). Wheat FT protein regulates *VRN1* transcription through interactions with FDL2. Plant J **55,** 543-554.

Liu, T., Carlsson, J., Takeuchi, T., Newton, L., and Farre, E.M. (2013). Direct regulation of abiotic responses by the *Arabidopsis* circadian clock component *PRR7*. Plant J **76,** 101-114.

Liu, L., Farrona, S., Klemme, S., and Turck, F.K. (2014). Post-fertilization expression of FLOWERING LOCUS T suppresses reproductive reversion. Front Plant Sci **5,** 164.

Lundqvist, U. (2009). Eighty years of Scandinavian barley mutation genetics and breeding. In Induced plant mutations in the genomics era. Proceedings of an International Joint FAO/IAEA Symposium, Q.Y. Shu, ed, pp. 39-43.

Lv, B., Nitcher, R., Han, X., Wang, S., Ni, F., Li, K., Pearce, S., Wu, J., Dubcovsky, J., and Fu, D. (2014). Characterization of *FLOWERING LOCUS T1* (*FT1*) Gene in *Brachypodium* and Wheat. PLoS One **9,** e94171.

Marquez-Cedillo, L.A., Hayes, P.M., Kleinhofs, A., Legge, W.G., Rossnagel, B.G., Sato, K., Ullrich, S.E., and Wesenberg, D.M. (2001). QTL analysis of agronomic traits in barley based on the doubled haploid progeny of two elite North American varieties representing different germplasm groups. Theoretical and Applied Genetics **103,** 625-637.

Masiero, S., Li, M.A., Will, I., Hartmann, U., Saedler, H., Huijser, P., Schwarz-Sommer, Z., and Sommer, H. (2004). *INCOMPOSITA*: a MADS-box gene controlling prophyll development and floral meristem identity in *Antirrhinum*. Development **131,** 5981-5990.

Min, X.J., Butler, G., Storms, R., and Tsang, A. (2005). OrfPredictor: predicting protein-coding regions in EST-derived sequences. Nucleic Acids Research **33,** W677-W680.

Miralles, D.J., and Richards, R.A. (2000). Responses of Leaf and Tiller Emergence and Primordium Initiation in Wheat and Barley to Interchanged Photoperiod. Annals of Botany **85,** 655-663.

Muggeo, V.M.R. (2003). Estimating regression models with unkown break-points. Statistics in Medicine **22,** 3055-3071.

Muggeo, V.M.R. (2008). segmented: an R package to fit regression models with broken-line relationships. R News **8,** 20-25.

Muñoz-Amatriaín, M., Moscou, M.J., Bhat, P.R., Svensson, J.T., Bartos, J., Suchánková, P., Simková, H., Endo, T.R., Fenton, R.D., Lonardi, S., Castillo, A.M., Chao, S., Cistué, L., Cuesta-Marcos, A., Forrest, K.L., Hayden, M.J., Hayes, P.M., Horsley, R.D., Makoto, K., Moody, D., Sato, K., Vallés, M.P., Wulff, B.B.H., Muehlbauer, G.J., Dolezel, J., and Close*, T.J. (2011). An Improved Consensus Linkage Map of Barley Based on Flow-Sorted Chromosomes and Single Nucleotide Polymorphism Markers. Plant Gen. **4,** 238-249.

Müller-Xing, R., Clarenz, O., Pokorny, L., Goodrich, J., and Schubert, D. (2014). Polycomb-Group Proteins and FLOWERING LOCUS T Maintain Commitment to Flowering in *Arabidopsis thaliana*. Plant Cell **26,** 2457-2471.

Murai, K. (2013). Homeotic Genes and the ABCDE Model for Floral Organ Formation in Wheat. Plants **2,** 379-395.

Murmu, J., Bush, M.J., DeLong, C., Li, S., Xu, M., Khan, M., Malcolmson, C., Fobert, P.R., Zachgo, S., and Hepworth, S.R. (2010). *Arabidopsis* basic leucine-zipper transcription factors TGA9 and TGA10 interact with floral glutaredoxins ROXY1 and ROXY2 and are redundantly required for anther development. Plant Physiol **154,** 1492-1504.

Nakamichi, N., Kiba, T., Henriques, R., Mizuno, T., Chua, N.H., and Sakakibara, H. (2010). PSEUDO-RESPONSE REGULATORS 9, 7, and 5 are transcriptional repressors in the *Arabidopsis* circadian clock. Plant Cell **22,** 594-605.

Paterson, A.H., Bowers, J.E., Bruggmann, R., Dubchak, I., Grimwood, J., Gundlach, H., Haberer, G., Hellsten, U., Mitros, T., Poliakov, A., Schmutz, J., Spannagl, M., Tang, H., Wang, X., Wicker, T., Bharti, A.K., Chapman, J., Feltus, F.A., Gowik, U., Grigoriev, I.V., Lyons, E., Maher, C.A., Martis, M., Narechania, A., Otillar, R.P., Penning, B.W., Salamov, A.A., Wang, Y., Zhang, L., Carpita, N.C., Freeling, M., Gingle, A.R., Hash, C.T., Keller, B., Klein, P., Kresovich, S., McCann, M.C., Ming, R., Peterson, D.G., Mehboob ur, R., Ware, D., Westhoff, P., Mayer, K.F.X., Messing, J., and Rokhsar, D.S. (2009). The *Sorghum bicolor* genome and the diversification of grasses. Nature **457,** 551-556.

Pearce, S., Vanzetti, L.S., and Dubcovsky, J. (2013). Exogenous gibberellins induce wheat spike development under short days only in the presence of *VERNALIZATION1*. Plant Physiol **163,** 1433-1445.

Périlleux, C., and Bernier, G. (1997). Leaf carbohydrate status in *Lolium temulentum* during the induction of flowering. New Phytologist **135,** 59-66.

Pillen, K., Zacharias, A., and Léon, J. (2003). Advanced backcross QTL analysis in barley (*Hordeum vulgare* L.). Theor Appl Genet **107,** 340-352.

Pillen, K., Zacharias, A., and Léon, J. (2004). Comparative AB-QTL analysis in barley using a single exotic donor of *Hordeum vulgare ssp. spontaneum*. Theoretical and Applied Genetics **108,** 1591-1601.

Pokhilko, A., Fernandez, A.P., Edwards, K.D., Southern, M.M., Halliday, K.J., and Millar, A.J. (2012). The clock gene circuit in *Arabidopsis* includes a repressilator with additional feedback loops. Mol Syst Biol **8,** 574.

Quail, P.H. (2002). Photosensory perception and signalling in plant cells: new paradigms? Curr Opin Cell Biol **14,** 180-188.

R Development Core Team (2008). R: A language and environment for statistical computing. R Foundation for Statistical Computing. (Vienna, Austria).

Reynolds, M., Foulkes, M.J., Slafer, G.A., Berry, P., Parry, M.A., Snape, J.W., and Angus, W.J. (2009). Raising yield potential in wheat. J Exp Bot **60,** 1899-1918.

Roberts, E.H., Summerfield, R.J., Cooper, J.P., and Ellis, R.H. (1988). Environmental Control of Flowering in Barley (*Hordeum vulgare* L.). I. Photoperiod Limits to Long-day Responses, Photoperiod-insensitive Phases and Effects of Low-temperature and Short-day Vernalization. Annals of Botany **62,** 127-144.

Robinson, M.D., McCarthy, D.J., and Smyth, G.K. (2010). edgeR: a Bioconductor package for differential expression analysis of digital gene expression data. Bioinformatics **26,** 139-140.

Rolland, F., Baena-Gonzalez, E., and Sheen, J. (2006). SUGAR SENSING AND SIGNALING IN PLANTS: Conserved and Novel Mechanisms. Annual Review of Plant Biology **57,** 675-709.

Saisho, D., Ishii, M., Hori, K., and Sato, K. (2011). Natural variation of barley vernalization requirements: implication of quantitative variation of winter growth habit as an adaptive trait in East Asia. Plant Cell Physiol **52,** 775-784.

Salome, P.A., Bomblies, K., Laitinen, R.A., Yant, L., Mott, R., and Weigel, D. (2011). Genetic architecture of flowering-time variation in *Arabidopsis thaliana*. Genetics **188,** 421-433.

Samach, A., Onouchi, H., Gold, S.E., Ditta, G.S., Schwarz-Sommer, Z., Yanofsky, M.F., and Coupland, G. (2000). Distinct roles of CONSTANS target genes in reproductive development of *Arabidopsis.* Science **288,** 1613-1616.

Sameri, M., Pourkheirandish, M., Chen, G., Tonooka, T., and Komatsuda, T. (2011). Detection of photoperiod responsive and non-responsive flowering time QTL in barley. Breeding Science **61,** 183-188.

Sasani, S., Hemming, M.N., Oliver, S.N., Greenup, A., Tavakkol-Afshari, R., Mahfoozi, S., Poustini, K., Sharifi, H.-R., Dennis, E.S., Peacock, W.J., and Trevaskis, B. (2009). The influence of vernalization and daylength on expression of flowering-time genes in the shoot apex and leaves of barley (*Hordeum vulgare*). Journal of Experimental Botany.

Schmalenbach, I., March, T.J., Bringezu, T., Waugh, R., and Pillen, K. (2011). High-Resolution Genotyping of Wild Barley Introgression Lines and Fine-Mapping of the Threshability Locus thresh-1 Using the Illumina GoldenGate Assay. G3: Genes, Genomes, Genetics **1,** 187-196.

Schmitz, J.r., Franzen, R., Ngyuen, T., Garcia-Maroto, F., Pozzi, C., Salamini, F., and Rohde, W. (2000). Cloning, mapping and expression analysis of barley MADS-box genes. Plant Molecular Biology **42,** 899-913.

Searle, I., He, Y., Turck, F., Vincent, C., Fornara, F., Kröber, S., Amasino, R.A., and Coupland, G. (2006). The transcription factor FLC confers a flowering response to vernalization by repressing meristem competence and systemic signaling in *Arabidopsis*. Genes & Development **20,** 898-912.

Shaw, L.M., Turner, A.S., and Laurie, D.A. (2012). The impact of photoperiod insensitive *Ppd-1a* mutations on the photoperiod pathway across the three genomes of hexaploid wheat (*Triticum aestivum*). Plant J **71,** 71-84.

Shaw, L.M., Turner, A.S., Herry, L., Griffiths, S., and Laurie, D.A. (2013). Mutant Alleles of *Photoperiod-1* in Wheat (*Triticum aestivum* L.) That Confer a Late Flowering Phenotype in Long Days. PLoS One **8,** e79459.

Shimada, S., Ogawa, T., Kitagawa, S., Suzuki, T., Ikari, C., Shitsukawa, N., Abe, T., Kawahigashi, H., Kikuchi, R., Handa, H., and Murai, K. (2009). A genetic network of flowering-time genes in wheat leaves, in which an *APETALA1/FRUITFULL-like* gene, *VRN1*, is upstream of *FLOWERING LOCUS T*. Plant J **58,** 668-681.

Shitsukawa, N., Ikari, C., Shimada, S., Kitagawa, S., Sakamoto, K., Saito, H., Ryuto, H., Fukunishi, N., Abe, T., Takumi, S., Nasuda, S., and Murai, K. (2007). The einkorn wheat (*Triticum monococcum*) mutant, *maintained vegetative phase*, is caused by a deletion in the *VRN1* gene. Genes & Genetic Systems **82,** 167-170.

Si, Y., Liu, P., Li, P., and Brutnell, T.P. (2013). Model-Based Clustering for RNA-Seq Data. Bioinformatics.

Slafer, G.A., and Andrade, F.H. (1993). Physiological attributes related to the generation of grain yield in bread wheat cultivars released at different eras. Field Crops Research **31,** 351-367.

Slafer, G.A., and Rawson, H.M. (1994). Sensitivity of Wheat Phasic Development to Major Environmental Factors: a Re-Examination of Some Assumptions Made by Physiologists and Modellers. Functional Plant Biology **21,** 393-426.

Slafer, G.A., Abeledo, L.G., Miralles, D.J., Gonzalez, F.G., and Whitechurch, E.M. (2001). Photoperiod sensitivity during stem elongation as an avenue to raise potential yield in wheat. Euphytica **119,** 191-197.

Slafer, G.A. (2003). Genetic basis of yield as viewed from a crop physiologist's perspective. Annals of Applied Biology **142,** 117-128.

Steinbach, Y., and Hennig, L. (2014). *Arabidopsis* MSI1 functions in photoperiodic flowering time control. Front Plant Sci **5,** 77.

Stracke, S., and Börner, A. (1998). Molecular mapping of the photoperiod response gene *ea7* in barley. Theoretical and Applied Genetics **97,** 797-800.

Szücs, P., Karsai, I., von Zitzewitz, J., Mészáros, K., Cooper, L.L.D., Gu, Y.Q., Chen, T.H.H., Hayes, P.M., and Skinner, J.S. (2006). Positional relationships between photoperiod response QTL and photoreceptor and vernalization genes in barley. Theoretical and Applied Genetics **112,** 1277-1285.

Takata, N., Saito, S., Saito, C.T., and Uemura, M. (2010). Phylogenetic footprint of the plant clock system in angiosperms: evolutionary processes of pseudo-response regulators. BMC Evol Biol **10,** 126.

Tamaki, S., Matsuo, S., Wong, H.L., Yokoi, S., and Shimamoto, K. (2007). Hd3a Protein Is a Mobile Flowering Signal in Rice. Science **316,** 1033-1036.

Teulat, B., Merah, O., Souyris, I., and This, D. (2001). QTLs for agronomic traits from a Mediterranean barley progeny grown in several environments. Theoretical and Applied Genetics **103,** 774-787.

Trevaskis, B., Tadege, M., Hemming, M.N., Peacock, W.J., Dennis, E.S., and Sheldon, C. (2007a). *Short vegetative phase-like* MADS-box genes inhibit floral meristem identity in barley. Plant Physiol **143,** 225-235.

Trevaskis, B., Hemming, M.N., Dennis, E.S., and Peacock, W.J. (2007b). The molecular basis of vernalization-induced flowering in cereals. Trends Plant Sci **12,** 352-357.

Turck, F., Fornara, F., and Coupland, G. (2008). Regulation and identity of florigen: FLOWERING LOCUS T moves center stage. Annu Rev Plant Biol **59,** 573-594.

Turner, A., Beales, J., Faure, S.b., Dunford, R.P., and Laurie, D.A. (2005). The Pseudo-Response Regulator *Ppd-H1* Provides Adaptation to Photoperiod in Barley. Science **310,** 1031-1034.

von Korff, M., Wang, H., Leon, J., and Pillen, K. (2006). AB-QTL analysis in spring barley: II. Detection of favourable exotic alleles for agronomic traits introgressed from wild barley (*H. vulgare ssp. spontaneum*). Theor Appl Genet **112,** 1221-1231.

von Korff, M., Grando, S., Del Greco, A., This, D., Baum, M., and Ceccarelli, S. (2008). Quantitative trait loci associated with adaptation to Mediterranean dryland conditions in barley. Theor Appl Genet **117,** 653-669.

von Korff, M., Léon, J., and Pillen, K. (2010). Detection of epistatic interactions between exotic alleles introgressed from wild barley (*H. vulgare ssp. spontaneum*). Theoretical and Applied Genetics **121,** 1455-1464.

Waddington, S.R., Cartwright, P.M., and Wall, P.C. (1983). A Quantitative Scale of Spike Initial and Pistil Development in Barley and Wheat. Annals of Botany **51,** 119-130.

Wahl, V., Ponnu, J., Schlereth, A., Arrivault, S., Langenecker, T., Franke, A., Feil, R., Lunn, J.E., Stitt, M., and Schmid, M. (2013). Regulation of flowering by trehalose-6-phosphate signaling in *Arabidopsis thaliana*. Science **339,** 704-707.

Wang, G., Schmalenbach, I., von Korff, M., Léon, J., Kilian, B., Rode, J., and Pillen, K. (2010). Association of barley photoperiod and vernalization genes with QTLs for flowering time and agronomic traits in a BC2DH population and a set of wild barley introgression lines. Theor Appl Genet **120,** 1559-1574.

Weltzien, E. (1988). Evaluation of Barley (*Hordeum vulgare* L.) Landrace Populations Originating from Different Growing Regions in the Near East*. Plant Breeding **101,** 95-106.

Weltzien, E. (1989). Differentiation among barley landrace populations from the Near East. Euphytica **43,** 29-39.

Weigel, D., and Nilsson, O. (1995). A developmental switch sufficient for flower initiation in diverse plants. Nature **377,** 495-500.

Whitechurch, E.M., Slafer, G.A., and Miralles, D.J. (2007). Variability in the Duration of Stem Elongation in Wheat Genotypes and Sensitivity to Photoperiod and Vernalization. Journal of Agronomy and Crop Science **193,** 131-137.

Wilhelm, E.P., Turner, A.S., and Laurie, D.A. (2009). Photoperiod insensitive Ppd-A1a mutations in tetraploid wheat (*Triticum durum* Desf.). Theor Appl Genet **118,** 285-294.

Worland, T., and Snape, J.W. (2001). Genetic basis of worldwide wheat varietal improvement. In The world wheat book: a history of wheat breeding, A.P. Bonjean and W.J. Angus, eds (Paris: Lavoisier Publishing), pp. 59-100.

Xue, W., Xing, Y., Weng, X., Zhao, Y., Tang, W., Wang, L., Zhou, H., Yu, S., Xu, C., Li, X., and Zhang, Q. (2008). Natural variation in *Ghd7* is an important regulator of heading date and yield potential in rice. Nat Genet **40,** 761-767.

Yan, L., Loukoianov, A., Tranquilli, G., Helguera, M., Fahima, T., and Dubcovsky, J. (2003). Positional cloning of the wheat vernalization gene *VRN1*. Proc Natl Acad Sci U S A **100,** 6263-6268.

Yan, L., Loukoianov, A., Blechl, A., Tranquilli, G., Ramakrishna, W., SanMiguel, P., Bennetzen, J.L., Echenique, V., and Dubcovsky, J. (2004). The Wheat *VRN2* Gene Is a Flowering Repressor Down-Regulated by Vernalization. Science **303,** 1640-1644.

Yan, L., Fu, D., Li, C., Blechl, A., Tranquilli, G., Bonafede, M., Sanchez, A., Valarik, M., Yasuda, S., and Dubcovsky, J. (2006). The wheat and barley vernalization gene *VRN3* is an orthologue of *FT*. Proc Natl Acad Sci U S A **103,** 19581-19586.

Yasuda, S., Hayashi, J., and Moriya, I. (1993). Genetic constitution for spring growth habit and some other characters in barley cultivars in the Mediterranean coastal regions. Euphytica **70,** 77-83.

Yoo, S.K., Chung, K.S., Kim, J., Lee, J.H., Hong, S.M., Yoo, S.J., Yoo, S.Y., Lee, J.S., and Ahn, J.H. (2005). CONSTANS Activates SUPPRESSOR OF OVEREXPRESSION OF CONSTANS 1 through FLOWERING LOCUS T to Promote Flowering in *Arabidopsis*. Plant Physiology **139,** 770-778.

Zadoks, J.C., Chang, T.T., and Konzak, C.F. (1974). A decimal code for the growth stages of cereals. Weed Research **14,** 415-421.

Zakhrabekova, S., Gough, S.P., Braumann, I., Muller, A.H., Lundqvist, J., Ahmann, K., Dockter, C., Matyszczak, I., Kurowska, M., Druka, A., Waugh, R., Graner, A., Stein, N., Steuernagel, B., Lundqvist, U., and Hansson, M. (2012). Induced mutations in circadian clock regulator *Mat-a* facilitated short-season adaptation and range extension in cultivated barley. Proc Natl Acad Sci U S A **109,** 4326-4331.

6 Abbreviations

Abbreviation		Explanation
#	-	number
%	-	percent
®	-	registered trademark
°C	-	degree Celcius
µM	-	micro mol / micro mol per liter
1-7H	-	barley chromosomes 1-7
95%-CI	-	95% confidence interval
aa	-	amino acid
AG1	-	*AGAMOUS 1*
An	-	anthesis
AnP	-	anther primordium stage
AP1 / 2 / 3	-	*APETALA 1 / 2 / 3*
At / Arabidopsis	-	*Arabidopsis thaliana*
AtVRN1	-	*REDUCED VERNALIZATION RESPONSE 1*
AwP	-	awn primordium stage
BIC	-	Bayesian Information Criterion
BLAST	-	Basic local alignment search tool
BLASTn	-	BLASTs with nucleotide query against a nucleotide database
BLASTx	-	BLASTs with nucleotide query against a translated nucleotide database
BM1 / BM3 / BM5a / BM8 / BM10	-	*Barley MADS box 1 / 3 / 5a / 8 / 10*
bp	-	base pair
Brachypodium	-	*Brachypodium distachyon*
CAB	-	*CHLOROPHYLL-A,B BINDING*
CAL	-	*CAULIFLOWER*
CCA1	-	*CIRCADIAN CLOCK ASSOCIATED1*
CCT-domain	-	*CONSTANS, CO-like* , and *TOC1* -domain
cDNA	-	copy DNA
CEN	-	*CENTRORADIALIS*
cm	-	centimeter
CO	-	*CONSTANS*
CO1 / 2 / 9	-	*CONSTANS-like 1 / 2 / 9*
COP1	-	*CONSTITUTIVE PHOTOMORPHOGENIC 1*
Cry1 / 2	-	CRYPTOCHROME 1 / 2
DAG	-	days after germination
DET	-	differentially expressed transcript
DH	-	doubled haploid
DNA	-	deoxyribonucleic acid
DNC, sDNC	-	de novo contigs and selected set used for RNA sequencing reference
DR	-	double ridge stage
eam 6 / 7 / 8	-	*early maturity 6 / 7 / 8*
EC	-	Evening Complex
ELF3 / 4	-	*EARLY FLOWERING 3 / 4*
EM	-	Expectation-Maximization-Alogrithm
eps	-	*earliness per se*
et al.	-	"et alii", latin for "and others"
E-value	-	expectation value
FDL2	-	*FD-like 2*
FDR	-	False Discovery Rate
Fig.	-	Figure
FLS2	-	*FLAGELLIN-SENSITIVE 2*
FLT-2L	-	*FLOWERING TIME 2L*
FT	-	*FLOWERING LOCUS T*
FT1 / 2 / 3 / 4 / 5	-	*FLOWERING LOCUS T-like 1 / 2 / 3 / 4 / 5*
FUL	-	*FRUITFUL*
g	-	gramm
GA	-	gibberellin
Ga20-oxidase	-	*GIBBERELLIN 20-OXIDASE*
Ghd7	-	*GRAIN NUMBER, PLANT HEIGHT AND HEADING DATE 7*
GI	-	*GIGANTEA*
GLM	-	generalized linear model
GO	-	Gene Ontology
h	-	hour
H. spontaneum	-	*Hordeum vulgare spp. spontaneum*
HAK5	-	*HIGH AFFINITY K+ TRANSPORTER 5*
HC, sHC	-	High confidence genes (IBGSC, 2012) and a selected subset used as reference in the RNA-sequencing analysis
Hd1 / 3a	-	*HEADING DATE 1 / 3a*
HS / HL	-	short / long arm of a barley chromosome
HSA	-	Hauptsprossapex
Hv / unigenes	-	NCBI barley UniGenes
Hv / H. vulgare	-	*Hordeum vulgare*
HXK1	-	*HEXOKINASE1*
IBGSC	-	International Barley Genome Sequencing Consortium
IM	-	inflorescence meristem
KN1	-	*KNOTTED 1*
KT	-	Kurztag
l	-	liter
LC, sLC	-	Low confidence genes (IBGSC, 2012) and a selected subset used as reference in the RNA-sequencing analysis
LD	-	long-day
LFY	-	*LEAFY*
LHY	-	*LATE ELONGATED HYPOCOTYL*
log	-	logarithm
LT	-	Langtag
LUX	-	*LUX ARRYTHMO*
M	-	molar (mol/l)
m^2	-	square meter
Mha	-	*million hectars*
MS2	-	*MALE STERILITY 2*
MSA	-	main shoot apex
MSI1	-	*MULTICOPY SUPPRESSOR OF IRA1*
Mt	-	million tons
mvp	-	*maintained vegetative phase* mutant of wheat
ORF	-	open reading frame
P. syringae	-	*Pseudomonas synringae*
PCR	-	polymerase chain reaction
PGM1	-	*PHOSPHOGLUCOMUTASE1*
PhyA / B / C	-	PHYTOCHROME A / B / C
PI	-	*PISTILATA*
PMT1	-	*POLYOL/MONOSACCHARIDE TRANSPORTER 1*
PPD1, PPD-H1 / PPD-H2	-	Photoperiod 1 / 2
PPD-A1a / -B1a / -D1a	-	mutated alleles of *PHOTOPERIOD1* Homeologs in wheat
PRC2	-	POLYCOMP REPRESSIVE COMPLEX 2
PRR7 / 37	-	*PSEUDO RESPONSE REGULATOR 7 / 37*
PV	-	pathogenic variety
p-value	-	probability value
qRT-PCR	-	quantitative reverse transcription-polymerase chain reaction
QTL	-	quantitative trait locus
RAF kinase	-	*RAPIDLY ACCELERATED FIBROSARCOMA* kinase
RNA	-	ribonucleic acid
RNA-seq	-	RNA-sequencing
RNA-Seq	-	RNA-sequencing
RPKM	-	reads per kilo base per million
RPM1	-	*RESISTANCE TO P. SYRINGAE PV MACULICOLA 1*
s	-	second
SAM	-	shoot apical meristem
SD	-	short-day
SEP1 / 3	-	*SEPALLATA 1 / 3*
SFT	-	*SINGLE FLOWER TRUSS*
sHC, sLC	-	selected subsets of the HC and LC genes
SOC1	-	*SUPRESSOR OF OVEREXPRESSION OF CONSANS 1*
SOC1-1	-	*SUPRESSOR OF OVEREXPRESSION OF CONSANS 1-like 1*
SPA4	-	*SUPPRESSOR OF PHYA-105 1 RELATED 4*
SPL4	-	*SQUAMOSA-PROMOTER BINDING PROTEIN-LIKE 4*
ssp.	-	subspecies
Suppl. Fig.	-	Supplementary Figure
Suppl. Tab.	-	Supplementary Table
SVP	-	*SHORT VEGETATIVE PHASE*
Ta	-	*Triticum aestivum*
TA	-	transition apex
TFL1	-	*TERMINAL FLOWER 1*
™	-	trademark
TOC1	-	*TIMING OF CAB EXPRESSION 1*
TP	-	"tipping" stage, see Alqudah *et al.* 2014
TPS1	-	*TREHALOSE-6-PHOSPHATE SYNTHASE 1*
VA	-	vegetative apex
VRN1, VRN-H1 / VRN-H2 / VRN-H3	-	*VERNALIZATION 1 / 2 / 3*
VRT2	-	*VEGETATIVE TO REPRODUCTIVE TRANSITION 2*
W0.5 - W10.0	-	Waddington stage 0.5 - 10, see Waddington *et al.* 1983
YSL3	-	*YELLOW STRIPE LIKE 3*
Z10 - Z65	-	Zadoks stage 10 - 65, see Zadoks *et al.* 1974
ZCCT-Ha / -Hb / -Hc	-	Zinc finger-CCT domain transcription factor Ha / Hb
ZIP5	-	*ZINC TRANSPORTER 5 PRECURSOR*

7 Supplementary Information

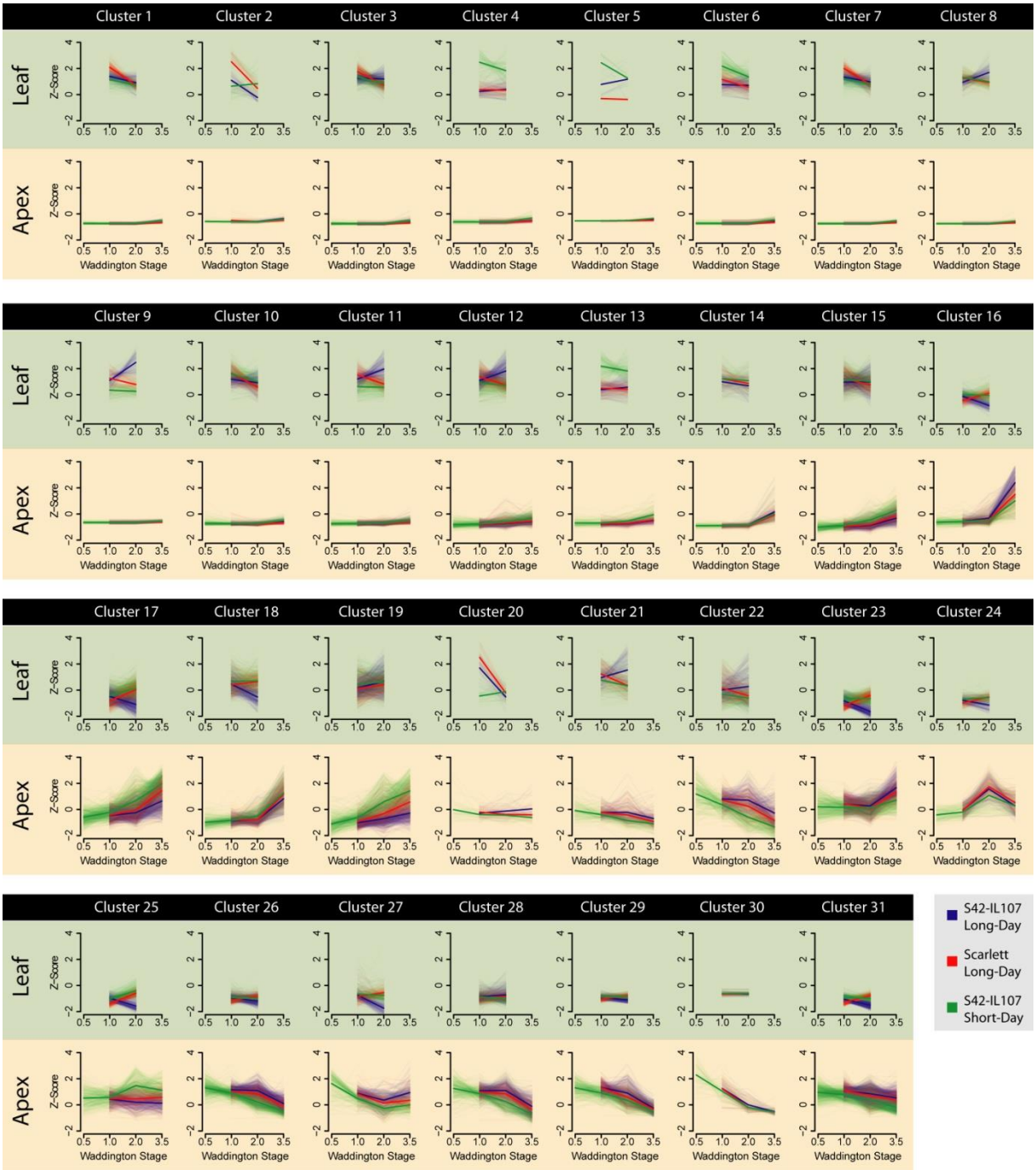

Supplementary Figure S1: Transcript expression patterns for 7604 DETs in 31 co-expression clusters
Co-expression clusters of 7604 differentially expressed transcripts (DET). Expression levels for individual transcripts (light colors) and mean expression level across all transcripts within each cluster (bright color) were plotted. Co-expression plots depict transcript expression patterns in leaves (green) and apices (orange) as mean centered and scaled transcript levels (Z-Score). Detailed statistics for each cluster are presented in Suppl. Tab. S14.

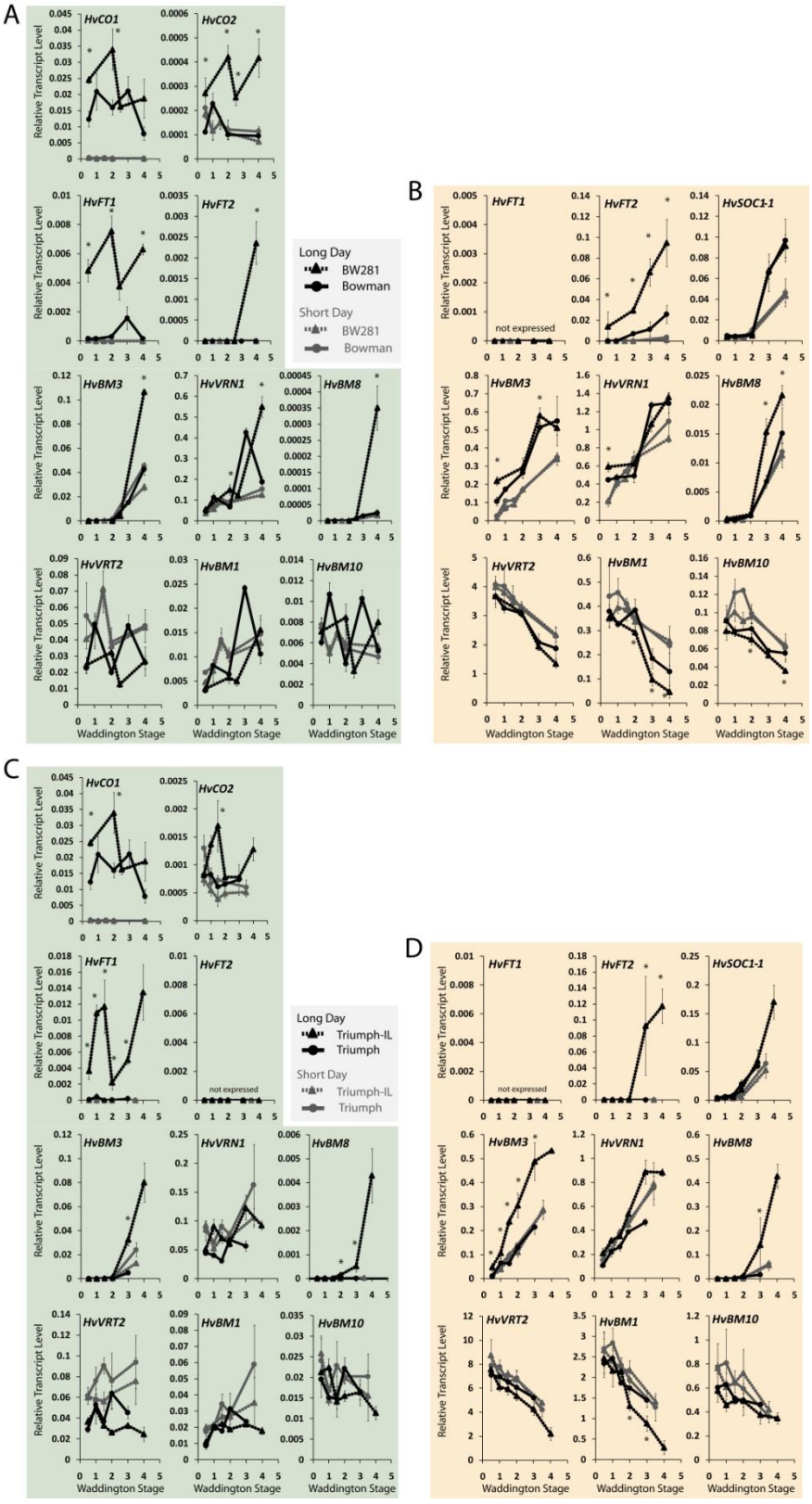

Supplementary Figure S2: Validation of transcript levels in leaves and shoot apices of Bowman, BW281, Triumph and Triumph-IL

Quantification of transcript levels by quantitative real time PCR (qRT-PCR) in leaf samples (green) and samples enriched for apex tissue (orange) at different stages of plant development. Samples were harvested from the barley genotypes **(A, B)** Bowman and BW281, as well as **(C, D)** Triumph and Triumph-IL. Transcript levels are demonstrated relative to the transcript abundance of *HvActin*. Error bars indicate the standard deviation over three biological replicates. Asterisks highlight significant differences ($p<0.05$) between transcript levels of BW281 and Bowman or Triumph-IL and Triumph, respectively, when plants were at the same developmental stage and grown under long photoperiods.

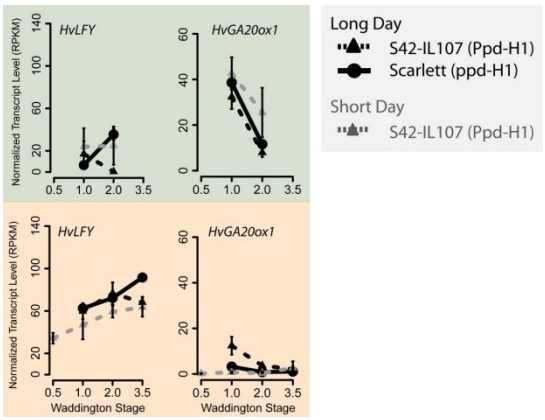

Supplementary Figure S3: Transcripts of *HvLFY* and *HvGA20ox1* expressed in leaves and at the MSA
RNA-sequencing derived expression data of *HvLFY* (MLOC_14305.1) and *HvGA20ox1* (Hv.21105). Transcript expression is presented for leaf (green) and shoot apex tissue (orange). Normalized expression values are reported in reads per kilo base per million (RPKM). Error bars indicate standard deviation across two to three independent RNA samples.

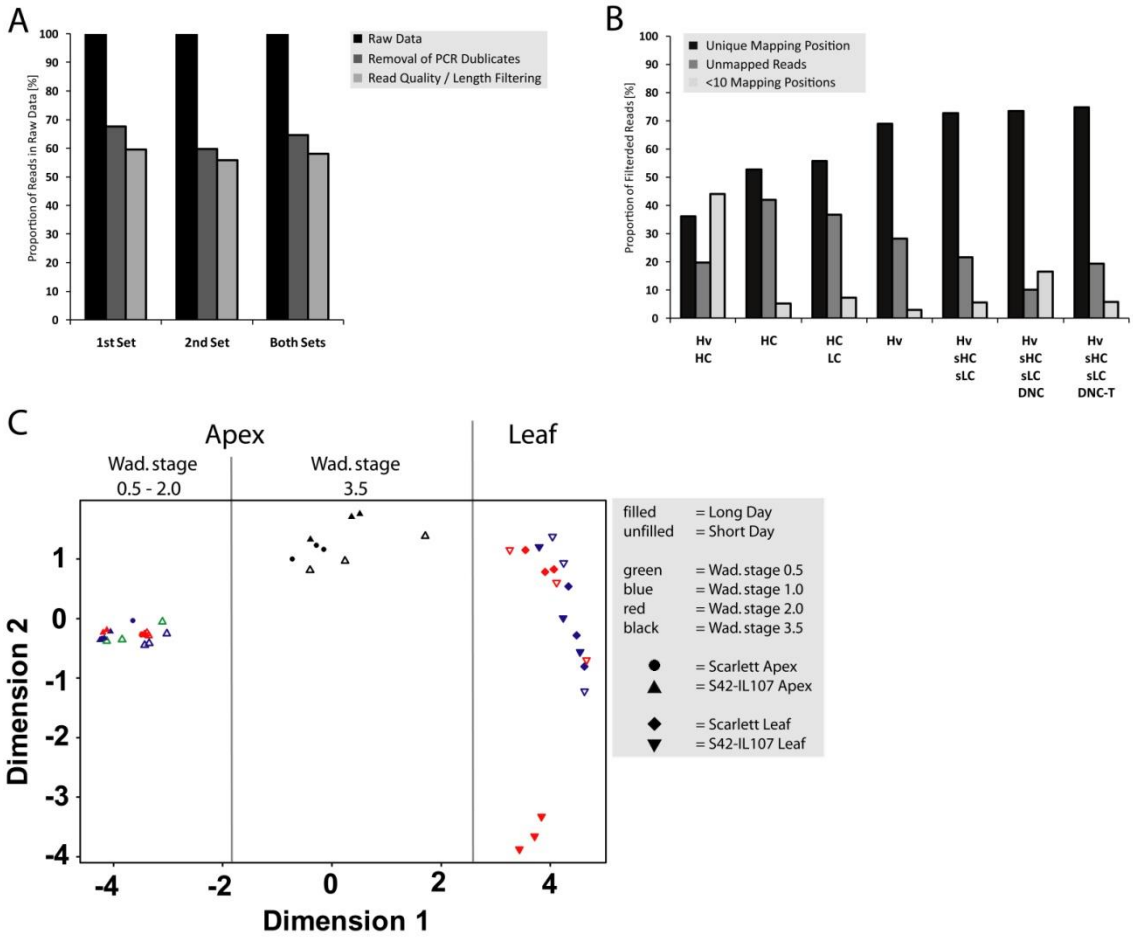

Supplementary Figure S4: Overview of RNA-sequencing statistics
(A) Quality- and length-based filtering of raw sequencing reads (100bp, single-end, Illumina), derived from two independent sequencing runs. Reads of libraries A to X (1st set) and of libraries A1-AE1 (2nd set) retained after filtering. See Suppl. Tab. S12 for detailed information on the libraries. **(B)** Statistics of mapping to reference sets of different transcript combinations. Hv: barley NCBI UniGene set; HC: high confidence gene set; LC: low confidence gene set; sHC/sLC: selected subset of unique HC or LC; DNC, d*e novo* contigs assembled from unmapped Illumina reads; DNC-T, selected *de novo* contigs with BLASTx hit in the *Triticeae*. **(C)** Unsupervised clustering of RNA samples in two dimensions by multidimensional scaling (MDS) performed with the *edgeR*-package of the R statistical software.

Supplementary Table S1: Rate of shoot apex development and induction of spikelet primordia obtained from broken-line regressions

Phenotype	Photoperiod	Genotype	Segment of Regression Line	Slope	St.Err.	Uppper 95%-CI[1]	Lower 95%-CI[1]
Shoot apex development (Fig. 4B)	Long Day	Scarlett	**segment 1**	**0.118**	0.010	**0.098**	**0.138**
			segment 2	**0.246**	0.006	**0.234**	**0.258**
			segment 3	0.057	0.019	0.019	0.094
		S42-IL017	**segment 1**	**0.207**	0.015	**0.176**	**0.237**
			segment 2	**0.440**	0.012	**0.416**	**0.463**
			segment 3	0.026	0.006	0.014	0.038
	Short Day	Scarlett	**segment 1**	**0.065**	0.001	**0.063**	**0.067**
		S42-IL017	**segment 1**	**0.063**	0.001	**0.061**	**0.066**
Induction of floret primordia (Fig. 4C)	Long Day	Scarlett	segment 1	-0.005	0.332	-0.660	0.651
			segment 2	**2.107**	0.040	**2.027**	**2.187**
			segment 3	0.098	0.069	-0.038	0.235
		S42-IL017	segment 1	-0.109	0.491	-1.081	0.863
			segment 2	**2.683**	0.087	**2.510**	**2.856**
			segment 3	-0.080	0.039	-0.158	-0.002
	Short Day	Scarlett	segment 1	0.095	0.095	-0.093	0.283
			segment 2	**1.247**	0.045	**1.158**	**1.336**
			segment 3	0.557	0.035	0.487	0.628
		S42-IL017	segment 1	0.135	0.098	-0.059	0.330
			segment 2	**1.206**	0.041	**1.125**	**1.286**
			segment 3	0.509	0.041	0.427	0.591

[1] Upper and lower 95%-Confidence Interval of the slope

Broken-line regressions performed with the 'segmented'-package in R (Muggeo et al. 2003 and 2008).

Supplementary Table S2: Average* log2-fold changes between transcripts within major co-expression clusters I-III

Tissue	Wad. Stage	Cluster I	Cluster II	Cluster III
Leaf	1.0 - 2.0	1.34	0.03	-1.07
Apex	3.5	-1.48	0.18	0.19
Apex	0.5 - 2.0	-3.10	-0.24	0.47

*Average over RPKM log2-fold changes per transcript between leaf samples at stage W1.0-2.0, apex samples at W3.5 and apex samples at W0.5-W2.0

Supplementary Table S3: GO-term enrichment for 3299 transcripts specifically up-regulated in shoot apices at stamen primordium stage

GO-ID	GO-Term[1]	FDR	GO-ID	GO-Term[1]	FDR
GO:0015979	photosynthesis	1.95E-88	GO:0044255	cellular lipid metabolic process	2.21E-04
GO:0019684	photosynthesis, light reaction	1.79E-69	GO:0006787	porphyrin-containing compound catabolic process	3.62E-04
GO:0006091	generation of precursor metabolites and energy	1.94E-35	GO:0033015	tetrapyrrole catabolic process	3.62E-04
GO:0009765	photosynthesis, light harvesting	3.62E-32	GO:0051187	cofactor catabolic process	3.62E-04
GO:0055114	oxidation-reduction process	1.67E-26	GO:0005976	polysaccharide metabolic process	3.62E-04
GO:0009767	photosynthetic electron transport chain	2.92E-23	GO:0042197	halogenated hydrocarbon metabolic process	3.85E-04
GO:0006740	NADPH regeneration	7.61E-20	GO:0042196	chlorinated hydrocarbon metabolic process	3.85E-04
GO:0006098	pentose-phosphate shunt	2.55E-19	GO:0006790	sulfur compound metabolic process	4.26E-04
GO:0006739	NADP metabolic process	1.24E-18	GO:0009416	response to light stimulus	4.60E-04
GO:0019362	pyridine nucleotide metabolic process	2.37E-18	GO:0006804	peroxidase reaction	4.80E-04
GO:0046496	nicotinamide nucleotide metabolic process	3.43E-18	GO:0009607	response to biotic stimulus	6.25E-04
GO:0042440	pigment metabolic process	4.84E-18	GO:0061024	membrane organization	6.34E-04
GO:0072524	pyridine-containing compound metabolic process	8.76E-17	GO:0019497	hexachlorocyclohexane metabolic process	6.35E-04
GO:0006733	oxidoreduction coenzyme metabolic process	4.20E-16	GO:0015996	chlorophyll catabolic process	7.37E-04
GO:0051186	cofactor metabolic process	9.48E-16	GO:0046149	pigment catabolic process	7.37E-04
GO:0019288	isopentenyl diphosphate biosynthetic process, methylerythritol 4-phosphate pathway	1.51E-15	GO:0000271	polysaccharide biosynthetic process	7.98E-04
GO:0009240	isopentenyl diphosphate biosynthetic process	2.10E-15	GO:0044264	cellular polysaccharide metabolic process	7.98E-04
GO:0046490	isopentenyl diphosphate metabolic process	2.10E-15	GO:0080167	response to karrikin	8.85E-04
GO:0019682	glyceraldehyde-3-phosphate metabolic process	2.10E-15	GO:0033559	unsaturated fatty acid metabolic process	9.63E-04
GO:0015994	chlorophyll metabolic process	2.54E-15	GO:0009410	response to xenobiotic stimulus	1.02E-03
GO:0016116	carotenoid metabolic process	4.87E-15	GO:0019637	organophosphate metabolic process	1.06E-03
GO:0016108	tetraterpenoid metabolic process	4.87E-15	GO:0051707	response to other organism	1.06E-03
GO:0018298	protein-chromophore linkage	5.75E-15	GO:0009414	response to water deprivation	1.08E-03
GO:0046148	pigment biosynthetic process	6.57E-15	GO:0006803	glutathione conjugation reaction	1.60E-03
GO:0008299	isoprenoid biosynthetic process	1.61E-14	GO:1901700	response to oxygen-containing compound	1.70E-03
GO:0016117	carotenoid biosynthetic process	2.38E-14	GO:0009658	chloroplast organization	1.78E-03
GO:0016109	tetraterpenoid biosynthetic process	2.38E-14	GO:0006979	response to oxidative stress	2.27E-03
GO:0006778	porphyrin-containing compound metabolic process	5.30E-14	GO:0033517	myo-inositol hexakisphosphate metabolic process	2.41E-03
GO:0033013	tetrapyrrole metabolic process	5.30E-14	GO:0010264	myo-inositol hexakisphosphate biosynthetic process	2.41E-03
GO:0022900	electron transport chain	7.40E-14	GO:0006767	water-soluble vitamin metabolic process	2.42E-03
GO:0006720	isoprenoid metabolic process	9.64E-14	GO:0006771	riboflavin metabolic process	2.42E-03
GO:0006090	pyruvate metabolic process	3.56E-13	GO:0042726	flavin-containing compound metabolic process	2.42E-03
GO:0010207	photosystem II assembly	1.07E-12	GO:0034637	cellular carbohydrate biosynthetic process	2.56E-03
GO:0006081	cellular aldehyde metabolic process	2.53E-12	GO:0009639	response to red or far red light	2.88E-03
GO:0000023	maltose metabolic process	2.07E-11	GO:0009415	response to water stimulus	3.06E-03
GO:0015995	chlorophyll biosynthetic process	5.89E-11	GO:0032958	inositol phosphate biosynthetic process	3.47E-03
GO:0019252	starch biosynthetic process	1.09E-10	GO:0009694	jasmonic acid metabolic process	3.56E-03
GO:0044710	single-organism metabolic process	1.42E-10	GO:0090407	organophosphate biosynthetic process	3.82E-03
GO:0005975	carbohydrate metabolic process	2.45E-10	GO:0019725	cellular homeostasis	4.35E-03
GO:0009657	plastid organization	3.63E-10	GO:0015977	carbon fixation	4.62E-03
GO:0006732	coenzyme metabolic process	3.81E-10	GO:0046487	glyoxylate metabolic process	4.62E-03
GO:0010114	response to red light	1.01E-09	GO:0044550	secondary metabolite biosynthetic process	4.67E-03
GO:0033014	tetrapyrrole biosynthetic process	1.15E-09	GO:0009628	response to abiotic stimulus	4.78E-03
GO:0010027	thylakoid membrane organization	1.57E-09	GO:0010103	stomatal complex morphogenesis	5.33E-03
GO:0009668	plastid membrane organization	1.57E-09	GO:0006364	rRNA processing	5.77E-03
GO:0006779	porphyrin-containing compound biosynthetic process	1.69E-09	GO:0006950	response to stress	6.23E-03
GO:0009773	photosynthetic electron transport in photosystem I	2.78E-09	GO:0009991	response to extracellular stimulus	6.28E-03
GO:0016556	mRNA modification	6.14E-09	GO:0019344	cysteine biosynthetic process	6.31E-03
GO:0009637	response to blue light	6.14E-09	GO:0042548	regulation of photosynthesis, light reaction	6.88E-03
GO:0016052	carbohydrate catabolic process	1.47E-08	GO:0043467	regulation of generation of precursor metabolites and energy	6.88E-03
GO:0044724	single-organism carbohydrate catabolic process	1.76E-08	GO:0009314	response to radiation	6.97E-03
GO:0044723	single-organism carbohydrate metabolic process	2.66E-08	GO:0019748	secondary metabolic process	7.14E-03
GO:0010218	response to far red light	2.66E-08	GO:0030091	protein repair	7.22E-03
GO:0035304	regulation of protein dephosphorylation	5.34E-08	GO:0009772	photosynthetic electron transport in photosystem II	7.22E-03
GO:0008152	metabolic process	5.34E-08	GO:0010206	photosystem II repair	7.22E-03
GO:0005996	monosaccharide metabolic process	5.77E-08	GO:0033692	cellular polysaccharide biosynthetic process	7.31E-03
GO:0006721	terpenoid metabolic process	6.00E-08	GO:0043647	inositol phosphate metabolic process	7.59E-03
GO:0008654	phospholipid biosynthetic process	1.02E-07	GO:0006124	ferredoxin metabolic process	7.60E-03
GO:0006007	glucose catabolic process	1.05E-07	GO:0016072	rRNA metabolic process	7.77E-03
GO:0046365	monosaccharide catabolic process	1.05E-07	GO:0009070	serine family amino acid biosynthetic process	8.11E-03
GO:0019320	hexose catabolic process	1.05E-07	GO:0006749	glutathione metabolic process	8.28E-03
GO:0019685	photosynthesis, dark reaction	1.62E-07	GO:0071496	cellular response to external stimulus	9.08E-03
GO:0010155	regulation of proton transport	1.69E-07	GO:0031668	cellular response to extracellular stimulus	9.08E-03
GO:0035303	regulation of dephosphorylation	4.78E-07	GO:0010374	stomatal complex development	9.44E-03
GO:0016114	terpenoid biosynthetic process	5.09E-07	GO:0009744	response to sucrose stimulus	9.74E-03
GO:0005984	disaccharide metabolic process	8.95E-07	GO:0034285	response to disaccharide stimulus	9.74E-03
GO:0019318	hexose metabolic process	1.34E-06	GO:0070887	cellular response to chemical stimulus	1.05E-02
GO:0016143	S-glycoside metabolic process	1.48E-06	GO:0071214	cellular response to abiotic stimulus	1.05E-02
GO:0019760	glucosinolate metabolic process	1.48E-06	GO:1901659	glycosyl compound biosynthetic process	1.38E-02
GO:0019757	glycosinolate metabolic process	1.48E-06	GO:0006534	cysteine metabolic process	1.47E-02
GO:0009311	oligosaccharide metabolic process	1.51E-06	GO:0044272	sulfur compound biosynthetic process	1.52E-02
GO:0019253	reductive pentose-phosphate cycle	1.78E-06	GO:0050896	response to stimulus	1.64E-02
GO:0006118	electron transport	2.23E-06	GO:0051640	organelle localization	1.72E-02
GO:0005982	starch metabolic process	3.13E-06	GO:0006518	peptide metabolic process	1.99E-02
GO:0051667	establishment of plastid localization	7.53E-06	GO:0006818	hydrogen transport	2.02E-02
GO:0009902	chloroplast relocation	7.53E-06	GO:0015992	proton transport	2.02E-02
GO:0051644	plastid localization	1.00E-05	GO:0009695	jasmonic acid biosynthetic process	2.08E-02
GO:0006006	glucose metabolic process	1.11E-05	GO:0006952	defense response	2.16E-02
GO:0006073	cellular glucan metabolic process	1.48E-05	GO:0046173	polyol biosynthetic process	2.37E-02
GO:0044042	glucan metabolic process	1.48E-05	GO:0055080	cation homeostasis	2.42E-02
GO:0044262	cellular carbohydrate metabolic process	1.61E-05	GO:0042631	cellular response to water deprivation	2.42E-02
GO:0009250	glucan biosynthetic process	1.74E-05	GO:0071462	cellular response to water stimulus	2.42E-02
GO:0032787	monocarboxylic acid metabolic process	1.88E-05	GO:0043269	regulation of ion transport	2.60E-02
GO:0044802	single-organism membrane organization	4.26E-05	GO:0042221	response to chemical stimulus	2.60E-02
GO:0008610	lipid biosynthetic process	4.43E-05	GO:0043155	negative regulation of photosynthesis, light reaction	2.68E-02
GO:0006766	vitamin metabolic process	5.58E-05	GO:0010205	photoinhibition	2.68E-02
GO:0051188	cofactor biosynthetic process	6.98E-05	GO:0042724	thiamine-containing compound biosynthetic process	3.17E-02
GO:0009617	response to bacterium	8.06E-05	GO:1990066	energy quenching	3.17E-02
GO:0016144	S-glycoside biosynthetic process	8.52E-05	GO:0009228	thiamine biosynthetic process	3.17E-02
GO:0019761	glucosinolate biosynthetic process	8.52E-05	GO:0010196	nonphotochemical quenching	3.17E-02
GO:0019758	glycosinolate biosynthetic process	8.52E-05	GO:0006546	glycine catabolic process	3.20E-02
GO:0006629	lipid metabolic process	1.03E-04	GO:0009071	serine family amino acid catabolic process	3.20E-02
GO:0006805	xenobiotic metabolic process	1.44E-04	GO:0009743	response to carbohydrate stimulus	3.69E-02
GO:0071466	cellular response to xenobiotic stimulus	1.44E-04	GO:0009814	defense response, incompatible interaction	4.32E-02
GO:0010109	regulation of photosynthesis	1.44E-04	GO:0006812	cation transport	4.43E-02
GO:0051656	establishment of organelle localization	1.52E-04	GO:0030003	cellular cation homeostasis	4.51E-02
GO:0010304	PSII associated light-harvesting complex II catabolic process	1.70E-04	GO:0006013	mannose metabolic process	4.52E-02
GO:0006636	unsaturated fatty acid biosynthetic process	1.71E-04	GO:0006753	nucleoside phosphate metabolic process	4.60E-02
GO:0042742	defense response to bacterium	1.93E-04	GO:0009117	nucleotide metabolic process	4.74E-02
GO:0006644	phospholipid metabolic process	2.13E-04	GO:0010258	NADH dehydrogenase complex (plastoquinone) assembly	4.74E-02
GO:0016051	carbohydrate biosynthetic process	2.18E-04			

[1] Only GO-terms assigned to biological processes are shown

Supplementary Table S4: GO-term enrichment for 798 transcripts up-regulated during floral transition (W0.5-W2.0)

GO-ID	GO-Term[1]	FDR
GO:0045449	regulation of transcription, DNA-dependent	1.34E-03
GO:0044262	cellular carbohydrate metabolic process	5.25E-03
GO:0005985	sucrose metabolic process	5.25E-03
GO:0009725	response to hormone stimulus	8.60E-03
GO:0032870	cellular response to hormone stimulus	9.46E-03
GO:0071495	cellular response to endogenous stimulus	9.46E-03
GO:0006073	cellular glucan metabolic process	9.46E-03
GO:0044042	glucan metabolic process	9.46E-03
GO:0009719	response to endogenous stimulus	9.46E-03
GO:0005976	polysaccharide metabolic process	1.10E-02
GO:0044264	cellular polysaccharide metabolic process	1.10E-02
GO:0005975	carbohydrate metabolic process	1.14E-02
GO:0033993	response to lipid	1.14E-02
GO:0009556	microsporogenesis	1.33E-02
GO:0048236	plant-type spore development	1.33E-02
GO:0005982	starch metabolic process	1.33E-02
GO:0005984	disaccharide metabolic process	2.38E-02
GO:0071396	cellular response to lipid	2.72E-02
GO:0071310	cellular response to organic substance	2.98E-02
GO:0006075	(1->3)-beta-D-glucan biosynthetic process	2.98E-02
GO:0006074	(1->3)-beta-D-glucan metabolic process	2.98E-02
GO:0009624	response to nematode	3.34E-02
GO:0009311	oligosaccharide metabolic process	3.35E-02
GO:0010233	phloem transport	3.68E-02
GO:0010232	vascular transport	3.68E-02
GO:0010033	response to organic substance	3.81E-02
GO:0006355	regulation of transcription, DNA-dependent	4.65E-02
GO:0044723	single-organism carbohydrate metabolic process	4.90E-02

[1] Only GO-terms assigned to biological processes are shown

Supplementary Table S5: GO-term enrichment for 1434 “core set” transcripts differentially expressed at the shoot apex during floral transition and at stamen primordium stage

GO-ID	GO-Term[1]	FDR	GO-ID	GO-Term[1]	FDR
GO:0045449	regulation of transcription, DNA-dependent	2.56E-08	GO:0009624	response to nematode	9.93E-03
GO:0071824	protein-DNA complex subunit organization	1.51E-05	GO:0042221	response to chemical stimulus	1.03E-02
GO:0065004	protein-DNA complex assembly	1.51E-05	GO:0005976	polysaccharide metabolic process	1.17E-02
GO:0031497	chromatin assembly	1.51E-05	GO:0005982	starch metabolic process	1.36E-02
GO:0006334	nucleosome assembly	1.54E-05	GO:0044264	cellular polysaccharide metabolic process	1.50E-02
GO:0034728	nucleosome organization	1.54E-05	GO:0009059	macromolecule biosynthetic process	1.66E-02
GO:0006323	DNA packaging	5.63E-05	GO:0034645	cellular macromolecule biosynthetic process	1.78E-02
GO:0006333	chromatin assembly or disassembly	1.59E-04	GO:0071704	organic substance metabolic process	1.99E-02
GO:0071103	DNA conformation change	8.83E-04	GO:0009058	biosynthetic process	2.00E-02
GO:0005985	sucrose metabolic process	1.27E-03	GO:0010582	floral meristem determinacy	2.01E-02
GO:0009725	response to hormone stimulus	1.29E-03	GO:0005984	disaccharide metabolic process	2.03E-02
GO:0009719	response to endogenous stimulus	1.29E-03	GO:0044249	cellular biosynthetic process	2.46E-02
GO:2001141	regulation of RNA biosynthetic process	3.22E-03	GO:0048509	regulation of meristem development	2.62E-02
GO:0043086	negative regulation of catalytic activity	3.88E-03	GO:0033993	response to lipid	3.19E-02
GO:0006073	cellular glucan metabolic process	3.95E-03	GO:0010073	meristem maintenance	3.19E-02
GO:0044042	glucan metabolic process	3.95E-03	GO:0010556	regulation of macromolecule biosynthetic process	3.19E-02
GO:0010022	meristem determinacy	3.95E-03	GO:2000112	regulation of cellular macromolecule biosynthetic process	3.19E-02
GO:0010077	maintenance of inflorescence meristem identity	6.69E-03	GO:0019219	regulation of nucleobase-containing compound metabolic process	3.52E-02
GO:0044262	cellular carbohydrate metabolic process	6.69E-03	GO:0032870	cellular response to hormone stimulus	3.68E-02
GO:0006355	regulation of transcription, DNA-dependent	6.69E-03	GO:0071495	cellular response to endogenous stimulus	3.68E-02
GO:0008152	metabolic process	8.82E-03	GO:0010033	response to organic substance	3.82E-02
GO:0042254	ribosome biogenesis	8.82E-03	GO:0009311	oligosaccharide metabolic process	3.82E-02
GO:1901576	organic substance biosynthetic process	8.82E-03	GO:1901700	response to oxygen-containing compound	3.82E-02
GO:0044092	negative regulation of molecular function	8.82E-03	GO:0031326	regulation of cellular biosynthetic process	3.82E-02
GO:0010076	maintenance of floral meristem identity	8.85E-03	GO:0051171	regulation of nitrogen compound metabolic process	3.82E-02
GO:0051252	regulation of RNA metabolic process	9.21E-03	GO:0034654	nucleobase-containing compound biosynthetic process	3.82E-02
GO:0032774	RNA biosynthetic process	9.76E-03	GO:0005975	carbohydrate metabolic process	4.12E-02
GO:0006351	transcription, DNA-dependent	9.76E-03	GO:0009889	regulation of biosynthetic process	4.20E-02
GO:0022613	ribonucleoprotein complex biogenesis	9.93E-03	GO:0071836	nectar secretion	4.20E-02
GO:0006412	translation	9.93E-03	GO:0042545	cell wall modification	4.74E-02

[1] Only GO-terms assigned to biological processes are shown

Supplementary Table S6: Co-expression clusters enriched for transcripts up-regulated during MSA development independent of the photoperiod and genotype

Cluster ID	Cluster Size	No. DEG in Cluster	Expected No. DEG in Cluster	Enrichment[1]
Cluster 24	139	23	4.48	5.14 ***
Cluster 16	210	21	6.77	3.10 ***
Cluster 17	568	34	18.30	1.86 ***
Cluster 11	217	17	6.99	2.43 **
Cluster 13	134	12	4.32	2.78 **
Cluster 14	105	10	3.38	2.96 **
Cluster 18	311	18	10.02	1.80 *
Cluster 19	454	22	14.63	1.50
Cluster 12	345	17	11.12	1.53
Cluster 15	361	17	11.63	1.46
Cluster 4	79	4	2.55	1.57
Cluster 20	38	2	1.22	1.63
Cluster 6	157	6	5.06	1.19
Cluster 23	414	14	13.34	1.05
Cluster 10	247	7	7.96	0.88
Cluster 2	40	1	1.29	0.78
Cluster 3	296	7	9.54	0.73
Cluster 1	180	4	5.80	0.69
Cluster 25	302	5	9.73	0.51
Cluster 8	125	2	4.03	0.50
Cluster 7	214	2	6.90	0.29
	SUM	**245**		

[1]Chi-squared test: *p<0.05, **p<0.01, ***p<0.001

Supplementary Table S7: Co-expression clusters enriched for transcripts down-regulated during MSA development independent of the photoperiod and genotype

Cluster ID	Cluster Size	No. DEG in Cluster	Expected No. DEG in Cluster	Enrichment[1]
Cluster 30	55	31	1.11	27.83 ***
Cluster 29	319	46	6.46	7.12 ***
Cluster 21	141	12	2.86	4.20 ***
Cluster 31	716	24	14.50	1.66 *
Cluster 26	521	16	10.55	1.52
Cluster 22	260	9	5.27	1.71
Cluster 11	217	4	4.39	0.91
Cluster 28	333	6	6.74	0.89
Cluster 27	218	3	4.42	0.68
Cluster 12	345	2	6.99	0.29
Cluster 25	302	1	6.12	0.16
	SUM	**154**		

[1]Chi-squared test: *p<0.05, **p<0.01, ***p<0.001

Supplementary Table S8: GO-term enrichment for 1427 transcripts down-regulated in leaves by long photoperiods and in S42-IL107

GO-ID	GO-Term[1]	FDR
GO:0006334	nucleosome assembly	3.08E-28
GO:0008283	cell proliferation	4.40E-08
GO:0048443	stamen development	7.22E-08
GO:0010315	auxin efflux	1.49E-05
GO:0008356	asymmetric cell division	8.55E-05
GO:0010541	acropetal auxin transport	5.99E-04
GO:0005985	sucrose metabolic process	1.15E-03
GO:0010540	basipetal auxin transport	1.87E-03
GO:0009958	positive gravitropism	1.87E-03
GO:0010073	meristem maintenance	7.31E-03
GO:0043481	anthocyanin accumulation in tissues in response to UV light	1.61E-02
GO:0051322	anaphase	3.41E-02
GO:0005982	starch metabolic process	3.63E-02
GO:0007010	cytoskeleton organization	3.72E-02
GO:0006355	regulation of transcription, DNA-dependent	3.75E-02
GO:0000911	cytokinesis by cell plate formation	4.43E-02

[1] Only GO-terms assigned to biological processes are shown

Supplementary Table S9: Co-expression clusters enriched for transcripts up-regulated in leaves by long photoperiods and in S42-IL107

Cluster ID	Cluster Size	No. DEG in Cluster	Expected No. DEG in Cluster	Enrichment[1]
Cluster 9	95	59	2.41	24.47 ***
Cluster 11	217	53	5.51	9.62 ***
Cluster 21	141	20	3.58	5.59 ***
Cluster 12	345	41	8.76	4.68 ***
Cluster 8	125	7	3.17	2.21 *
Cluster 5	10	1	0.25	3.94
Cluster 22	260	7	6.60	1.06
Cluster 3	296	2	7.51	0.27
Cluster 7	214	1	5.43	0.18
Cluster 10	247	1	6.27	0.16
Cluster 19	454	1	11.52	0.09
	SUM	**193**		

[1]Chi-squared test: *p<0.05, **p<0.01, ***p<0.001

Supplementary Table S10: Co-expression clusters enriched for transcripts up-regulated in shoot apices by long photoperiods and in S42-IL107

Cluster ID	Cluster Size	Number of DET	Expected Number of DET	Enrichment[1]
Cluster 16	210	39	7.35	5.31 ***
Cluster 21	141	17	4.93	3.45 ***
Cluster 22	260	23	9.10	2.53 ***
Cluster 31	716	43	25.05	1.72 ***
Cluster 20	38	6	1.33	4.51 **
Cluster 14	105	11	3.67	2.99 **
Cluster 23	414	26	14.48	1.80 **
Cluster 27	218	15	7.63	1.97 *
Cluster 29	319	15	11.16	1.34
Cluster 30	55	2	1.92	1.04
Cluster 11	217	7	7.59	0.92
Cluster 28	333	10	11.65	0.86
Cluster 12	345	9	12.07	0.75
Cluster 2	40	1	1.40	0.71
Cluster 26	521	12	18.23	0.66
Cluster 24	139	3	4.86	0.62
Cluster 15	361	7	12.63	0.55
Cluster 3	296	5	10.35	0.48
Cluster 10	247	4	8.64	0.46
Cluster 18	311	3	10.88	0.28
Cluster 17	568	5	19.87	0.25
Cluster 13	134	1	4.69	0.21
Cluster 1	180	1	6.30	0.16
Cluster 19	454	1	15.88	0.06
	SUM	**266**		

[1]Chi-squared test: *p<0.05, **p<0.01, ***p<0.001

Supplementary Table S11: GO-term enrichment for transcripts in co-expression cluster 31

GO-ID	GO-Term[1]	FDR	GO-ID	GO-Term[1]	FDR
GO:0006259	DNA metabolic process	1.34E-55	GO:0022403	cell cycle phase	1.587E-05
GO:0051276	chromosome organization	2.77E-45	GO:0031327	negative regulation of cellular biosynthetic process	1.708E-05
GO:0071103	DNA conformation change	1.56E-40	GO:0007127	meiosis I	1.962E-05
GO:0006325	chromatin organization	1.56E-40	GO:0009890	negative regulation of biosynthetic process	1.97E-05
GO:0031497	chromatin assembly	6.31E-36	GO:0048646	anatomical structure formation involved in morphogenesis	1.97E-05
GO:0006323	DNA packaging	2.94E-35	GO:0032259	methylation	1.978E-05
GO:0008283	cell proliferation	2.94E-35	GO:0031326	regulation of cellular biosynthetic process	2.667E-05
GO:0071824	protein-DNA complex subunit organization	5.80E-35	GO:0048731	system development	3.572E-05
GO:0065004	protein-DNA complex assembly	5.80E-35	GO:0010212	response to ionizing radiation	3.71E-05
GO:0006333	chromatin assembly or disassembly	3.83E-34	GO:0045892	negative regulation of transcription, DNA-dependent	3.735E-05
GO:0006334	nucleosome assembly	8.37E-34	GO:0051253	negative regulation of RNA metabolic process	4.035E-05
GO:0034728	nucleosome organization	8.37E-34	GO:0009889	regulation of biosynthetic process	4.42E-05
GO:0007049	cell cycle	3.86E-29	GO:0031324	negative regulation of cellular metabolic process	4.62E-05
GO:0006996	organelle organization	3.97E-27	GO:0033554	cellular response to stress	4.62E-05
GO:0090304	nucleic acid metabolic process	9.00E-25	GO:0010468	regulation of gene expression	4.62E-05
GO:0006260	DNA replication	1.64E-24	GO:0010558	negative regulation of macromolecule biosynthetic process	4.979E-05
GO:0022402	cell cycle process	4.30E-24	GO:2000113	negative regulation of cellular macromolecule biosynthetic process	4.979E-05
GO:0006261	DNA-dependent DNA replication	7.96E-20	GO:0007275	multicellular organismal development	5.032E-05
GO:0051301	cell division	3.44E-19	GO:0006310	DNA recombination	5.161E-05
GO:0016043	cellular component organization	2.02E-18	GO:0010629	negative regulation of gene expression	5.66E-05
GO:0051567	histone H3-K9 methylation	1.00E-17	GO:0032502	developmental process	6.284E-05
GO:0006139	nucleobase-containing compound metabolic process	4.86E-17	GO:0000725	recombinational repair	6.284E-05
GO:0022607	cellular component assembly	1.06E-16	GO:0000724	double-strand break repair via homologous recombination	6.284E-05
GO:0044728	DNA methylation or demethylation	2.39E-16	GO:0009987	cellular process	6.373E-05
GO:0006304	DNA modification	2.39E-16	GO:0032501	multicellular organismal process	8.467E-05
GO:0006306	DNA methylation	1.52E-15	GO:0048856	anatomical structure development	0.0001003
GO:0006305	DNA alkylation	1.52E-15	GO:0065007	biological regulation	0.0001086
GO:0051052	regulation of DNA metabolic process	1.86E-15	GO:0010332	response to gamma radiation	0.0001094
GO:0065003	macromolecular complex assembly	2.12E-15	GO:0009059	macromolecule biosynthetic process	0.0001152
GO:0000910	cytokinesis	5.41E-15	GO:0048827	phyllome development	0.0001176
GO:0043933	macromolecular complex subunit organization	6.13E-15	GO:0034645	cellular macromolecule biosynthetic process	0.0001215
GO:0034622	cellular macromolecular complex assembly	6.38E-15	GO:0010605	negative regulation of macromolecule metabolic process	0.0001332
GO:0034968	histone lysine methylation	7.43E-15	GO:0044767	single-organism developmental process	0.0001353
GO:0044763	single-organism cellular process	8.25E-15	GO:0009892	negative regulation of metabolic process	0.0001414
GO:0044699	single-organism process	1.15E-14	GO:0009791	post-embryonic development	0.0001777
GO:0007017	microtubule-based process	3.08E-14	GO:0007131	reciprocal meiotic recombination	0.0001815
GO:0006461	protein complex assembly	3.26E-14	GO:0035825	reciprocal DNA recombination	0.0001815
GO:0070271	protein complex biogenesis	3.47E-14	GO:0032508	DNA duplex unwinding	0.0003271
GO:0016570	histone modification	4.80E-14	GO:0006355	regulation of transcription, DNA-dependent	0.0003548
GO:0006270	DNA replication initiation	4.89E-14	GO:0016444	somatic cell DNA recombination	0.0004066
GO:0016571	histone methylation	7.77E-14	GO:0051252	regulation of RNA metabolic process	0.0004181
GO:0071822	protein complex subunit organization	8.80E-14	GO:0009653	anatomical structure morphogenesis	0.0004318
GO:0000278	mitotic cell cycle	1.23E-13	GO:0036211	protein modification process	0.0004335
GO:0051726	regulation of cell cycle	1.55E-13	GO:0006464	cellular protein modification process	0.0004335
GO:0016569	covalent chromatin modification	2.21E-13	GO:0032392	DNA geometric change	0.0004381
GO:0006275	regulation of DNA replication	2.35E-13	GO:0044707	single-multicellular organism process	0.0004972
GO:0006479	protein methylation	5.13E-13	GO:2001141	regulation of RNA biosynthetic process	0.0005266
GO:0008213	protein alkylation	5.13E-13	GO:0007349	cellularization	0.0006043
GO:0040029	regulation of gene expression, epigenetic	2.47E-12	GO:0048610	cellular process involved in reproduction	0.0007417
GO:0071840	cellular component organization or biogenesis	2.73E-12	GO:0042138	meiotic DNA double-strand break formation	0.0007615
GO:0046483	heterocycle metabolic process	3.24E-12	GO:0044238	primary metabolic process	0.0008281
GO:0006725	cellular aromatic compound metabolic process	3.76E-12	GO:0007059	chromosome segregation	0.0011058
GO:0016568	chromatin modification	3.92E-12	GO:0016572	histone phosphorylation	0.0011544
GO:0034641	cellular nitrogen compound metabolic process	5.96E-12	GO:0006468	protein phosphorylation	0.0017583
GO:0006974	response to DNA damage stimulus	8.76E-12	GO:0009887	organ morphogenesis	0.0018624
GO:0044260	cellular macromolecule metabolic process	1.44E-11	GO:0006346	methylation-dependent chromatin silencing	0.0018847
GO:1901360	organic cyclic compound metabolic process	1.46E-10	GO:0009886	post-embryonic morphogenesis	0.0020044
GO:0044772	mitotic cell cycle phase transition	2.29E-10	GO:0048653	anther development	0.002349
GO:0044770	cell cycle phase transition	2.29E-10	GO:0008356	asymmetric cell division	0.0024349
GO:0000086	G2/M transition of mitotic cell cycle	2.52E-10	GO:0048563	post-embryonic organ morphogenesis	0.0024834
GO:0000281	mitotic cytokinesis	4.55E-10	GO:0048444	floral organ morphogenesis	0.0024834
GO:1902410	mitotic cytokinetic process	4.55E-10	GO:0048513	organ development	0.0025398
GO:0000911	cytokinesis by cell plate formation	4.55E-10	GO:0032774	RNA biosynthetic process	0.0028949
GO:0006281	DNA repair	5.76E-10	GO:0006351	transcription, DNA-dependent	0.0028949
GO:1901990	regulation of mitotic cell cycle phase transition	8.78E-10	GO:0044237	cellular metabolic process	0.0033828
GO:1901987	regulation of cell cycle phase transition	8.78E-10	GO:0000079	regulation of cyclin-dependent protein serine/threonine kinase activity	0.0037258
GO:0032506	cytokinetic process	1.10E-09	GO:0031047	gene silencing by RNA	0.003789
GO:0043170	macromolecule metabolic process	1.10E-09	GO:0031048	chromatin silencing by small RNA	0.0044707
GO:0006807	nitrogen compound metabolic process	1.24E-09	GO:0043412	macromolecule modification	0.004508
GO:0000003	reproduction	1.49E-09	GO:0048523	negative regulation of cellular process	0.0045984
GO:0043414	macromolecule methylation	1.54E-09	GO:0048509	regulation of meristem development	0.004819
GO:0010389	regulation of G2/M transition of mitotic cell cycle	1.96E-09	GO:0048449	floral organ formation	0.0062794
GO:0007018	microtubule-based movement	6.62E-09	GO:0051225	spindle assembly	0.0066731
GO:0007010	cytoskeleton organization	8.64E-09	GO:0048645	organ formation	0.0068818
GO:0042127	regulation of cell proliferation	1.19E-08	GO:2000026	regulation of multicellular organismal development	0.0071337
GO:0019219	regulation of nucleobase-containing compound metabolic process	1.24E-08	GO:0000280	nuclear division	0.0072113
GO:0060255	regulation of macromolecule metabolic process	1.54E-08	GO:0033044	regulation of chromosome organization	0.0073622
GO:0010564	regulation of cell cycle process	1.54E-08	GO:0006471	protein ADP-ribosylation	0.0098821
GO:0000226	microtubule cytoskeleton organization	1.92E-08	GO:0071704	organic substance metabolic process	0.0110691
GO:0051171	regulation of nitrogen compound metabolic process	2.52E-08	GO:0051239	regulation of multicellular organismal process	0.0116645
GO:0006928	cellular component movement	3.35E-08	GO:0007051	spindle organization	0.012548
GO:0009908	flower development	9.03E-08	GO:0007062	sister chromatid cohesion	0.0154972
GO:0051322	anaphase	9.94E-08	GO:0010639	negative regulation of organelle organization	0.0172844
GO:0007346	regulation of mitotic cell cycle	1.45E-07	GO:0051129	negative regulation of cellular component organization	0.0172844
GO:0070192	chromosome organization involved in meiosis	1.70E-07	GO:0070925	organelle assembly	0.0178433
GO:0000279	M phase	2.54E-07	GO:0048285	organelle fission	0.0183366
GO:0006342	chromatin silencing	3.90E-07	GO:0090305	nucleic acid phosphodiester bond hydrolysis	0.0183366
GO:0045814	negative regulation of gene expression, epigenetic	3.90E-07	GO:0006268	DNA unwinding involved in DNA replication	1.84E-02
GO:0048437	floral organ development	5.46E-07	GO:0007112	male meiosis cytokinesis	2.03E-02
GO:0007129	synapsis	5.61E-07	GO:0033206	meiotic cytokinesis	2.03E-02
GO:0050794	regulation of cellular process	7.22E-07	GO:0010245	radial microtubular system formation	2.03E-02
GO:0044085	cellular component biogenesis	7.93E-07	GO:0071900	regulation of protein serine/threonine kinase activity	2.04E-02
GO:0051321	meiotic cell cycle	1.20E-06	GO:0010075	regulation of meristem growth	2.19E-02
GO:0080090	regulation of primary metabolic process	1.32E-06	GO:0048507	meristem development	2.37E-02
GO:0019222	regulation of metabolic process	1.32E-06	GO:0051026	chiasma assembly	2.71E-02
GO:0048466	androecium development	1.81E-06	GO:0034654	nucleobase-containing compound biosynthetic process	2.74E-02
GO:0048443	stamen development	1.81E-06	GO:0009558	embryo sac cellularization	2.74E-02
GO:0061458	reproductive system development	2.39E-06	GO:0035266	meristem growth	3.06E-02
GO:0048608	reproductive structure development	2.39E-06	GO:0050793	regulation of developmental process	3.16E-02
GO:0048569	post-embryonic organ development	2.91E-06	GO:0071514	genetic imprinting	3.28E-02
GO:0016458	gene silencing	3.28E-06	GO:0006349	regulation of gene expression by genetic imprinting	3.28E-02
GO:0050789	regulation of biological process	4.454E-06	GO:0048519	negative regulation of biological process	3.50E-02
GO:0031323	regulation of cellular metabolic process	5.136E-06	GO:0043247	telomere maintenance in response to DNA damage	3.57E-02
GO:0007126	meiosis	5.657E-06	GO:0048638	regulation of developmental growth	3.60E-02
GO:0048438	floral whorl development	6.028E-06	GO:0031032	actomyosin structure organization	3.81E-02
GO:0022414	reproductive process	7.364E-06	GO:0032776	DNA methylation on cytosine	3.81E-02
GO:0045934	negative regulation of nucleobase-containing compound metabolic process	7.895E-06	GO:1902407	assembly of actomyosin apparatus involved in mitotic cytokinesis	3.81E-02
GO:0051172	negative regulation of nitrogen compound metabolic process	7.895E-06	GO:0000914	phragmoplast assembly	3.81E-02
GO:0048367	shoot system development	8.66E-06	GO:0000912	assembly of actomyosin apparatus involved in cytokinesis	3.81E-02
GO:0006302	double-strand break repair	1.003E-05	GO:0010073	meristem maintenance	4.34E-02
GO:0010556	regulation of macromolecule biosynthetic process	1.372E-05	GO:0007140	male meiosis	4.70E-02
GO:2000112	regulation of cellular macromolecule biosynthetic process	1.372E-05	GO:0040008	regulation of growth	4.81E-02
GO:0003006	developmental process involved in reproduction	1.517E-05			

[1] Only GO-terms assigned to biological processes are shown

Supplementary Table S12: Overview of RNA samples and sequencing statistics

Tissue	Photoperiod	Genotype	Waddington Stage	Timepoint[1]	Library	Raw Data Read Number	Filtered Data Read Number	Total Mapped Reads	Uniquely Mapped Reads	Mapped Reads (<10 Positions)	Unmapped Reads	% Total Mapped Reads[1]	% Uniquely Mapped Reads[1]	% Mapped Reads[2] (<10 Positions)	% Unmapped Reads[1]
Apex	Short Day	**S42-IL017**	0.5	**0**	**A**	16459061	9893302	8074964	7604962	470002	1818338	81.62	76.87	4.75	18.38
Apex	Short Day	**S42-IL017**	0.5	**0**	**B**	7474058	4219953	3486797	3276316	210481	733156	82.63	77.64	4.99	17.37
Apex	Short Day	**S42-IL017**	0.5	**0**	**C**	10626845	2642659	2082591	1953507	129084	560068	78.81	73.92	4.88	21.19
Apex	Long Day	**Scarlett**	1.0	**3**	**D**	17104663	9738819	5369553	5046743	322810	4369266	55.14	51.82	3.31	44.86
Apex	Long Day	**Scarlett**	1.0	**3**	**E**	14897387	9397113	7723833	7278930	444903	1673280	82.19	77.46	4.73	17.81
Apex	Long Day	**Scarlett**	1.0	**3**	**F**	17730966	11537432	9579412	9033763	545649	1958020	83.03	78.30	4.73	16.97
Apex	Long Day	**S42-IL017**	1.0	**3**	**G**	19358313	10951141	8969982	8445259	524723	1981159	81.91	77.12	4.79	18.09
Apex	Long Day	**S42-IL017**	1.0	**3**	**H**	17092440	10071274	8000971	7537109	463862	2070303	79.44	74.84	4.61	20.56
Apex	Long Day	**S42-IL017**	1.0	**3**	**I**	16566298	9109101	7535252	7099987	435265	1573849	82.72	77.94	4.78	17.28
Apex	Long Day	**S42-IL017**	2.0	**6**	**J**	32563534	18201818	14931903	14085315	846588	3269915	82.04	77.38	4.65	17.96
Apex	Long Day	**S42-IL017**	2.0	**6**	**K**	23951610	14142385	10790186	10187863	602323	3352199	76.30	72.04	4.26	23.70
Apex	Long Day	**S42-IL017**	2.0	**6**	**(L)**	-	-	-	-	-	-	-	-	-	-
Leaf	Long Day	**S42-IL017**	2.0	**6**	**M**	17760086	9100127	7598589	6795801	802788	1501538	83.50	74.68	8.82	16.50
Leaf	Long Day	**S42-IL017**	2.0	**6**	**N**	21814456	11176202	9382236	8423041	959195	1793966	83.95	75.37	8.58	16.05
Leaf	Long Day	**S42-IL017**	2.0	**6**	**O**	20289165	11362454	9504470	8624381	880089	1857984	83.65	75.90	7.75	16.35
Apex	Long Day	**Scarlett**	2.0	**9**	**P**	14359218	9911948	8200558	7735749	464809	1711390	82.73	78.04	4.69	17.27
Apex	Long Day	**Scarlett**	2.0	**9**	**Q**	20007830	12535122	10240278	9666980	573298	2294844	81.69	77.12	4.57	18.31
Apex	Long Day	**Scarlett**	2.0	**9**	**R**	21999556	14020216	11487167	10837222	649945	2533049	81.93	77.30	4.64	18.07
Apex	Short Day	**S42-IL017**	1.0	**16**	**S**	18856390	12755506	10532000	9919814	612186	2223506	82.57	77.77	4.80	17.43
Apex	Short Day	**S42-IL017**	1.0	**16**	**T**	17899889	12181159	10004396	9428186	576210	2176763	82.13	77.40	4.73	17.87
Apex	Short Day	**S42-IL017**	1.0	**16**	**U**	13652340	9440970	7869896	7406957	462939	1571074	83.36	78.46	4.90	16.64
Apex	Short Day	**S42-IL017**	2.0	**7**	**V**	21151250	13207739	11082580	10435541	647039	2125159	83.91	79.01	4.90	16.09
Apex	Short Day	**S42-IL017**	2.0	**7**	**W**	14840256	9907029	8187503	7711492	476011	1719526	82.64	77.84	4.80	17.36
Apex	Short Day	**S42-IL017**	2.0	**7**	**X**	17692798	11220700	9302660	8762766	539894	1918040	82.91	78.09	4.81	17.09
Leaf	Long Day	**Scarlett**	1.0	**3**	**A1**	9026797	5432759	3185557	2828665	356892	2247202	58.64	52.07	6.57	41.36
Leaf	Long Day	**Scarlett**	1.0	**3**	**B1**	9895345	4829142	3239058	2876667	362391	1590084	67.07	59.57	7.50	32.93
Leaf	Long Day	**Scarlett**	1.0	**3**	**C1**	8040428	4686020	2850797	2535253	315544	1835223	60.84	54.10	6.73	39.16
Leaf	Long Day	**S42-IL107**	1.0	**3**	**D1**	9475973	5380083	3907323	3523777	383546	1472760	72.63	65.50	7.13	27.37
Leaf	Long Day	**S42-IL107**	1.0	**3**	**E1**	8876566	4646223	3713020	3314891	398129	933203	79.91	71.35	8.57	20.09
Leaf	Long Day	**S42-IL107**	1.0	**3**	**F1**	24420830	10662510	8223394	7468010	755384	2439116	77.12	70.04	7.08	22.88
Leaf	Long Day	**Scarlett**	2.0	**9**	**G1**	9299840	5336032	4592336	4157580	434756	743696	86.06	77.92	8.15	13.94
Leaf	Long Day	**Scarlett**	2.0	**9**	**H1**	7859909	4607638	3677568	3319688	357880	930070	79.81	72.05	7.77	20.19
Leaf	Long Day	**Scarlett**	2.0	**9**	**I1**	12377623	7455485	6276388	5731061	545327	1179097	84.18	76.87	7.31	15.82
Apex	Long Day	**S42-IL107**	3.5	**14**	**J1**	9050764	6141815	5143688	4799701	343987	998127	83.75	78.15	5.60	16.25
Apex	Long Day	**S42-IL107**	3.5	**14**	**K1**	9570762	6339239	5331268	4963348	367920	1007971	84.10	78.30	5.80	15.90
Apex	Long Day	**S42-IL107**	3.5	**14**	**L1**	5162724	3936287	3336398	3112804	223594	599889	84.76	79.08	5.68	15.24
Leaf	Short Day	**S42-IL107**	1.0	**16**	**M1**	10116020	5391320	4624600	4151410	473190	766720	85.78	77.00	8.78	14.22
Leaf	Short Day	**S42-IL107**	1.0	**16**	**N1**	12074847	6675503	5723413	5184815	538598	952090	85.74	77.67	8.07	14.26
Leaf	Short Day	**S42-IL107**	1.0	**16**	**O1**	9963482	6130135	5248033	4789203	458830	882102	85.61	78.13	7.48	14.39
Apex	Long Day	**Scarlett**	3.5	**20**	**P1**	9581977	6883431	5746021	5378877	367144	1137410	83.48	78.14	5.33	16.52
Apex	Long Day	**Scarlett**	3.5	**20**	**X1**	6427149	4848100	3928855	3680523	248332	919245	81.04	75.92	5.12	18.96
Apex	Long Day	**Scarlett**	3.5	**20**	**Y1**	12725456	8450127	6829176	6404370	424806	1620951	80.82	75.79	5.03	19.18
Leaf	Short Day	**S42-IL107**	2.0	**7**	**Z1**	11063884	6040842	4537274	4100767	436507	1503568	75.11	67.88	7.23	24.89
Leaf	Short Day	**S42-IL107**	2.0	**7**	**AA1**	8988461	4958127	4163623	3762488	401135	794504	83.98	75.89	8.09	16.02
Leaf	Short Day	**S42-IL107**	2.0	**7**	**AB1**	11010676	5172688	4344558	3893009	451549	828130	83.99	75.26	8.73	16.01
Apex	Short Day	**S42-IL107**	3.5	**50**	**AC1**	23918237	7202925	5797197	5368935	428262	1405728	80.48	74.54	5.95	19.52
Apex	Short Day	**S42-IL107**	3.5	**50**	**AD1**	9282564	6444967	5295853	4945492	350361	1149114	82.17	76.73	5.44	17.83
Apex	Short Day	**S42-IL107**	3.5	**50**	**AE1**	10104901	6672267	5455680	5110588	345092	1216587	81.77	76.59	5.17	18.23
				Average 1st Set		18006453	10727138	8692947	8143378	549569	2034191	80.90	75.75	5.15	19.10
				Average 2nd Set		10763134	6013486	4798795	4391747	407048	1214691	79.53	72.69	6.85	20.47
				Average		14307737	8320167	6704444	6227651	476793	1615723	80.20	74.19	6.02	19.80

[1]Days after separation of plants into short-day or long-day conditions

[2]Proportion relative to the number of filtered reads

Supplementary Table S13: Correlation analysis for quality control of biological replicates used for RNA-sequencing

Tissue	Photoperiod	Genotype	Waddington Stage	Rep1 vs. Rep2*	Rep1 vs. Rep3*	Rep2 vs. Rep3*
Apex	Short Day	S42-IL107	0.5	0.99	0.96	0.98
Apex	Short Day	S42-IL107	1	0.99	0.99	0.98
Apex	Long Day	Scarlett	1	0.95	0.94	0.99
Apex	Long Day	S42-IL107	1	0.99	0.99	0.99
Apex	Short Day	S42-IL107	2	1.00	0.99	0.99
Apex	Long Day	Scarlett	2	0.98	0.99	0.98
Apex	Long Day	S42-IL107	2	0.98	-	-
Apex	Short Day	S42-IL107	3.5	0.86	0.85	0.98
Apex	Long Day	Scarlett	3.5	0.99	0.99	0.99
Apex	Long Day	S42-IL107	3.5	0.99	0.99	0.99
Leaf	Short Day	S42-IL107	1	0.99	0.97	0.97
Leaf	Long Day	Scarlett	1	0.99	0.92	0.92
Leaf	Long Day	S42-IL107	1	0.97	0.96	0.97
Leaf	Short Day	S42-IL107	2	0.98	0.92	0.97
Leaf	Long Day	Scarlett	2	0.95	0.98	0.94
Leaf	Long Day	S42-IL107	2	0.99	0.97	0.98

*r, Pearson's correlation coefficient for RPKM expression levels of 25152 transcripts between biological replicates, $p < 10^{-8}$

Supplementary Table S14: Statistics of co-expression clustering

Cluster ID	Average Probability[1]	StDev Probablilty[1]	Cluster Size[2]
1	0.967	0.095	180
2	0.998	0.008	40
3	0.975	0.083	296
4	0.970	0.108	79
5	0.998	0.007	10
6	0.982	0.074	157
7	0.979	0.069	214
8	0.950	0.115	125
9	0.969	0.095	95
10	0.964	0.100	247
11	0.966	0.095	217
12	0.966	0.096	345
13	0.977	0.083	134
14	0.978	0.063	105
15	0.952	0.112	361
16	0.976	0.087	210
17	0.949	0.117	568
18	0.936	0.131	311
19	0.942	0.123	454
20	0.953	0.119	38
21	0.965	0.105	141
22	0.965	0.101	260
23	0.962	0.096	414
24	0.954	0.117	139
25	0.951	0.113	302
26	0.932	0.133	521
27	0.955	0.122	218
28	0.936	0.127	333
29	0.942	0.129	319
30	0.982	0.068	55
31	0.960	0.108	716
1-31	0.963	0.031	245 ± 167

[1] Average probability and standard deviation for all DETs grouping into the respective co-expression cluster

[2] Number of DETs in co-expression cluster

Supplementary Table S15: Oligonucleotide sequences used in qRT-PCR assays

Gene	Transcript in RNAseq Reference	5' -> 3' fwd - Primer Sequence	5' -> 3' rev - Primer Sequence	Reference
HvActin	Hv.23088	CGTGTTGGATTCTGGTGATG	AGCCACATATGCGAGCTTCT	Campoli et al. 2012b
HvBM3	Hv.4298	GCCGTCACCAGCACAAGCAA	CCCCATTCACCCTGTAGCAAAGA	this study
HvVRN1	Hv.23025	CTGAAGGCGAAGGTTGAGAC	TTCTCCTCCTGCAGTGACCT	Campoli et al. 2012b
HvBM8	Hv.169	CCACAGCAGCCGACACCTA	TGCCTTTGGGGGAGAAGACG	this study
HvCO1	MLOC_6921.1	CTGCTGGGGCTAGTGCTTAC	CCTTGTTGCATAACGTGTGG	Campoli et al. 2012a
HvCO2	MLOC_75496.6	AGTGGACTCTTGGCTCCTCA	CATGCTGCTGTTCTTGCATT	Campoli et al. 2012b
HvFT1	Hv.34809	GGTAGACCCAGATGCTCCAA	TCGTAGCACATCACCTCCTG	fwd primer in Campoli et al. 2012a
HvFT2	Hv.17258	TACCGAGGTTGTGTGCTACG	TCACATCCTTCTCCCGCCGG	this study
HvSOC1-1	Hv.32986	TTTGCAGCAAGTCAAAGCTG	CCTCTGATGATGCGGAGACT	this study
HvVRT2	Hv.15491	CCGATGTTGTCCCTGAAGAT	GGAACTCCCTCATGGACTCA	Campoli et al. 2012b
HvBM1	Hv.110	AGAGGAGAACGCAAGGCTAAAGG	AGTTGAAGAGTGATAATCCGAGCCTGAG	Trevaskis et al. 2007
HvBM10	Hv.19680	GCTCATCGTCTTCTCCTCCAC	CTCCTCGCCTCTCATCTGTC	Trevaskis et al. 2007

Danksagung

During the recent five years, I was accompanied by a hand full of people who supported me and my work. I would like to express my gratitude to you. Without you, this thesis would not have been possible and the time at the MPIPZ would have been a lot less enjoyable for me. Danke für Eure Unterstützung und Freundschaft. You've made my day. Thanks!

Liebe Maria, als meine Doktormutter hast du mich die letzten fünf Jahre begleitet. Du hast mir das Vertrauen geschenkt, die Zeit und den Freiraum gegeben, mich mit dem zu beschäftigen, was mich interessiert und mich stets ermutigt Neues zu lernen. Mit Deinen Ideen und Anregungen haben wir gemeinsam ein interessantes Forschungsprojekt verwirklicht. Ich danke Dir für Deine beständige Unterstützung während meiner Zeit am MPI.

Dear Professor Dr. George Coupland, I would like to thank you for the opportunity to accomplish my doctoral studies in your department. Although you may hear this sentence quite regularly, I strongly believe that the very positive working atmosphere in the Plant Developmental Biology Department depends on the way the staff is treated. Thus, thanks for the way you decided to lead your department.

Professorin Dr. Ute Höcker und Professor Dr. Ulf-Ingo Flügge, Danke für Ihre Bereitschaft das Ende meiner Doktorarbeit als Zweitprüferin und Prüfungsvorsitzender zu begleiten.

Artem, you joined the group and became a close friend. Besides your contribution to my project and work related discussions, I would like to thank you for making me addicted to coffee. Thanks for the almost daily coffee break, accompanied by discussions about politics and about whatever makes the world go round. Thanks for sharing your thoughts with me.

Jonas, wir haben Stunden damit verbracht über „R" und Statistik zu reden. Ich danke Dir für die Zeit, die Du Dir immer wieder für meine Fragen genommen hast. Danke auch für Deine sportliche Unterstützung, mich regelmäßig zum Laufen zu motivieren. Ohne Dich hätte ich womöglich 10kg zugenommen.

Aman, thanks for being a great discussion partner, for exchanging thoughts and ideas about our results and for giving me a better understanding of Islam. I enjoyed your explanations a lot.

Caren, ich danke Dir dafür, dass Du Dich so fürsorglich um meine Pflanzen im Gewächshaus gekümmert hast. Wir bräuchten definitiv mehr von Dir!

Thanks to the whole von Korff group, Chiara, Kerstin, Elisabeth, Jarod, Ermias, Cristina, Lukas, Sven, Andrea, Xiaojing, Wilma und Agatha. You all contributed to the cheerful atmosphere in our lab and made me enjoying my work at the institute even more.

Danke auch an Euch, meine Freunde Anne, Liron, Theo und Ben!

Liebe Mama, Lieber Papa, schon früh habt Ihr mich für die Naturwissenschaften begeistert und mich auf dem Weg Biologe zu werden immer unterstützt. Ich danke Euch für Eure seelische und moralische Unterstützung und das Wissen, dass immer jemand da ist, an den ich mich jederzeit wenden kann.

Besonderer Dank geht an meine Liebe Pia. Wir sind nun schon über 12 Jahre ein Paar, doch vor allem in den letzten Jahren musstest Du viel Verständnis für mich und meine Ausbildung aufbringen. Ich danke Dir für Dein Vertrauen, den Halt und die Zuversicht, die Du mir schenkst. Ich freue mich auf eine spannende Zukunft mit Dir und unserem kleinen Sohn Malte. Ich liebe Dich!

Erklärung

Ich versichere, dass ich die von mir vorgelegte Dissertation selbständig angefertigt, die benutzten Quellen und Hilfsmittel vollständig angegeben und die Stellen der Arbeit – einschließlich Tabellen, Karten und Abbildungen -, die anderen Werken im Wortlaut oder dem Sinn nach entnommen sind, in jedem Einzelfall als Entlehnung kenntlich gemacht habe; dass diese Dissertation noch keiner anderen Fakultät oder Universität zur Prüfung vorgelegt worden ist, sowie, dass ich eine solche Veröffentlichung vor Abschluss des Promotionsverfahrens nicht vornehmen werde. Die Bestimmungen dieser Promotionsordnung sind mir bekannt. Die von mir vorgelegte Dissertation ist von Jun.-Prof. Dr. Maria von Korff Schmising und Prof. Dr. George Coupland betreut worden.

Ich versichere, dass ich alle Angaben wahrheitsgemäß nach bestem Wissen und Gewissen gemacht habe und verpflichte mich, jedmögliche, die obigen Angaben betreffenden Veränderungen, dem Dekanat unverzüglich mitzuteilen.

Köln, den _____ _____

Benedikt Digel

Teilpublikationen:

Drosse, B., Campoli, C., Mulki, A., and von Korff, M. (2014). Genetic Control of Reproductive Development. In Biotechnological Approaches to Barley Improvement SE - 5, J. Kumlehn and N. Stein, eds, Biotechnology in Agriculture and Forestry. (Springer Berlin Heidelberg), pp. 81–99